Submarginal debris transport and till formation in active temperate glacier systems: the southeast Iceland type locality

David J.A. Evans[1], David H. Roberts[1], John F. Hiemstra[2], Kathryn M. Nye[1], Hanna Wright[1] and Andrew Steer[1]

1. Department of Geography, Durham University, South Road, Durham, DH1 3LE, UK
2. Department of Geography, Swansea University, Singleton Park, Swansea, SA2 8PP, UK

Abstract

Exhaustive sedimentological analysis of freshly exposed subglacial surfaces and moraines in southern Iceland provides diagnostic sedimentological signatures of: a) debris transport pathways through active temperate glacier snouts; and b) till production in subglacial traction zones dominated by deforming layers. Three till end members are recognised based on stratigraphic architecture: 1) thin and patchy tills over eroded bedrock; 2) single push moraines and complexes; and 3) overridden moraines or outwash fans. Typical till thicknesses are 0.10 - 1.40 m, with each till relating to a deformation event driven by the seasonally tuned processes of glacier sub-marginal shearing, freeze-on, squeezing and bulldozing. Clast form trends demonstrate progressive modification towards mature forms in subglacial traction zones with till being clearly differentiated from scree and glacifluvial deposits. Clast macrofabric strengths are variable, rarely matching those of laboratory shearing experiments, except where obviously lodged clasts are abundant. They also consistently record former glacier flow directions. But localized variability is introduced by bedrock protuberances, cavity infill, clast interference and freshly imported plucked clasts. Within tills, macrofabrics strengthen from lower (B horizon) to upper (A horizon) tills but at the outer edges of sub-marginally thickening till wedges or push moraines, seasonally-driven cycles of squeezing/flowage, freeze-on/melt-out and bulldozing give rise to a range of clast macrofabric strengths as well as superimposed deformation signatures. This reflects two extremes of till emplacement including the more mobile, flowing and often liquefied matrixes in push/squeeze moraines and, in contrast, the lodgement, deformation and ploughing at the thin end of sub-marginal till wedges.

Key words: Modern glacial sedimentology; Icelandic subglacial traction till; Glacial geomorphology; Push moraines

Introduction and rationale

The glacial geomorphology and sedimentology of the forelands of the piedmont glacier lobes in southern Iceland are well established as modern analogues for active temperate glacial landsystem signatures in the palaeoglaciological record (e.g. Price 1969; Eyles 1979, 1983; Boulton 1986; Russell et al. 2001, 2006; Evans & Twigg 2002; Evans 2005; Evans et al. 2009, 2016a, 2017a, b; Bennett et al. 2010; Bennett & Evans 2012; Bradwell et al. 2013; Evans & Orton 2015; Chandler et al. 2016a, b). The well preserved subglacial surfaces and latero-frontal moraines that characterize these forelands are ideal for the sampling of glacigenic debris in order to assess: a) debris transport pathways through active temperate glacier snouts; and b) the sedimentological signature of glacier bed conditions associated with subglacial deformation and other till production processes. Hence processes, specifically direct glacial sediment (till) production and emplacement, can be confidently related to form or sedimentological signatures, providing Quaternary palaeoglaciologists with diagnostic criteria with which to identify ancient tills.

A number of previous studies around the receding snouts of temperate glaciers have elucidated the patterns of debris transport pathways in glacial systems (Matthews & Petch, 1982; Benn, 1989; Evans, 1999; Spedding & Evans 2002) by using intensive sampling of clast forms along latero-frontal moraines as a surrogate for glacigenic modification of debris down-glacier flowline. This demonstrated that the moraines contain a mixture of passively and actively transported debris, the ratio of which varies according to distance down-moraine; more angular, slabby and elongate clasts, typical of passive glacial transport, at the upper ends of lateral moraines gradually give way to less angular and more blocky clasts, typical of active transport, in frontal moraines. Thereby a spatial pattern of clast form characteristics on recently deglaciated forelands has been used to infer the diminishing input of passively transported clasts from valley sides towards the glacier centre-line, where subglacially transported and abraded debris, in the form of stoss-and-lee or bullet-shaped clasts with surface wear or striae, gradually becomes more dominant (Boulton 1978). This down-glacier modification of clasts is a surrogate specifically for abrasion in the basal traction zone, a process that has been quantified by Lliboutry (1994) and MacGregor et al. (2009) to be an exponential change from angular to “fully rounded” clasts between the 400 and 4000 m points along a glacier’s centre line. However, the localized subglacial incorporation of debris that occupied the foreland prior to glacier advance can significantly increase the percentage of rounded and blocky clasts in a sample collected from frontal moraines, thereby diluting the subglacial abrasion signature with an inheritance signal, especially in areas of widespread glacifluvial deposits (e.g. Evans 2000; Evans & Twigg 2002; Lukas et al. 2013). In contrast, the quarrying of fresh blocks from bedrock protuberances that bridge the subglacial deforming layer can introduce anomalously angular material to down-glacier till deposits (Evans et al. 2016b).

This clast form signature is part of the sedimentological imprint of temperate glaciation, manifest in the various characteristics of subglacial tills, including granulometry, fabric and internal structure, which together are increasingly being employed to infer former glacier bed conditions. In the Icelandic setting, till sedimentology associated with active temperate glaciers has been reconciled with subglacial observations on deforming substrates (cf. Boulton & Hindmarsh 1987; Benn 1995) but has been, and is increasingly being related to more localized conditions associated with substrate inheritance/till overprinting (Evans 2000; Evans & Twigg 2002; Evans et al. 2016b), glacitectonic disturbance and clastic dyke intrusion (van der Meer et al. 1999; Evans & Twigg 2002; Le Heron & Etienne 2005), push moraine formation (Sharp 1984; Boulton 1986; Chandler et al. 2016a, b) and seasonal changes to sub-marginal thermal regimes

(Krüger 1993, 1994, 1996; Evans & Hiemstra 2005). From this research we now appreciate that the subglacial to sub-marginal footprints of former glacier margins, in the Icelandic setting represented by the sediment-landform imprints of the recently deglaciated Little Ice Age forelands, record an integrated signature of till production by temperate glacier processes. The architecture of this footprint has been described as a marginal-thickening wedge (Evans & Hiemstra 2005), which is represented in the landform record by push/squeeze moraines (Boulton 1986; Krüger 1993, 1994; Evans & Twigg 2002; Chandler et al. 2016a, b). This broad scale architecture has been explained by Boulton (1996) as a result of the operation of a strongly coupled ice/deforming bed interface, which leads to the production of an erosional subglacial zone beneath the accumulation area and the advection of deforming layer sediments through the ablation zone towards the glacier snout. Notwithstanding the localised influences introduced by bed roughness, a range of other processes also operate in concert with subglacial deformation beneath temperate glacier snouts to produce up-ice erosional zones and outer depositional zones a few hundred metres wide, including net adfreezing, supercooling, debris-rich ice thickening by thrusting, folding and overriding, and the concentration of subglacial fluvial sediments (cf. Boulton 1987; Alley *et al.* 1997; Evans 2018 and references therein). The outermost limit of this depositional zone is characterized by increasing sediment availability and the concomitant production of marginally thickened glacigenic sediment sequences. In terms of till production this is manifest in the gradual cessation of subglacial processes such as lodgement, ploughing and deformation, increasing volumes of melt-out debris and the initiation of ice-marginal squeezing, bulldozing and seasonal cycles of till slab freeze-on and melt release (cf. Price 1970; Krüger 1996; Evans & Twigg 2002; Evans & Hiemstra 2005; Chandler et al. 2016a, b).

Clast macrofabrics from Icelandic tills have been employed alongside textural characteristics and internal structures to formulate diagnostic sedimentological criteria for different styles of subglacial sediment deformation and lodgement (Benn 1995; Evans & Hiemstra 2005). However, these field data have been difficult to reconcile with laboratory based experiments aimed at the simulation of subglacial shearing (Evans et al. 2006; Iverson et al. 2008; Evans 2018 and references therein). Specifically, despite the development of a "steady state fabric" (S_1 eigenvalues > 0.78) at shear strains of 7-30 in laboratory experiments (Iverson et al. 2008), field sampling of Icelandic till fabrics yields relatively weak S_1 eigenvalues ranging from 0.44-0.74 even though a bed deformation origin implies that shear strains should be in excess of 100. By separating out the macrofabrics of unequivocally lodged boulders, which are predictably strong (0.77-0.81), from the more weakly aligned sub-boulder sized clasts in subglacial traction tills, Evans and Hiemstra (2005) and Evans et al. (2016b) have demonstrated that the weaker S_1 eigenvalues likely reflect perturbation of the deforming matrix and smaller clasts in the leeside pressure shadows of the boulders (cf. Kjær & Krüger 1998; Carr & Rose 2003). The study of multiple till stacks by Evans et al. (2016b) demonstrates also that superimposition of tills can result in the overprinting of deformation styles but not necessarily the strengthening of existing clast macrofabrics. A representative sample of strain indicators from modern till assemblages created at monitored glacier beds (e.g. Icelandic piedmont lobes typified by Breiðamerkurjökull;

Boulton & Hindmarsh 1987; Boulton et al. 2001) is therefore required in order to ensure a set of diagnostic field criteria for subglacial traction till identification in the ancient geological record, even though strain magnitude cannot be measured by such data (cf. Clarke 2005; Iverson et al. 2008).

Detailed above are the reasons why the sedimentology of contemporary sub-marginal till wedges, recorded either in single push moraines/till wedges (i.e. continuous annual active recession) or in till stacks (i.e. composite push moraines/till wedges of stationary snouts), is critical not only to deciphering former subglacial deformation signatures in the traction zones of active temperate glacier snouts but also assessing the role of debris modification versus inheritance by subglacial processes in such settings. Hence the aims of this study are to quantify, firstly, the impact of glacial transport pathways on debris as it moves through an active temperate glacier snout and, secondly, the depositional signature of subglacial deformation and other till production processes. From this we compile a set of diagnostic sedimentological criteria that relate till production and emplacement to process in the type area for subglacial deforming layers.

In order to assess the role of these process-form relationships, the sedimentology of seven local till sites, each representing a variant of the active temperate glacial landsystem but related to glaciers of similar size and morphology, is presented here (Figure 1). The first aim of quantifying the impact of glacial transport pathways on debris characteristics can be achieved only in settings where latero-frontal moraines exist and hence can be used as a surrogate for down-glacier modification of clasts (cf. Matthews & Petch, 1982; Benn, 1989; Evans, 1999, 2010; Spedding & Evans 2002). In only one south Iceland foreland can this be effectively executed, that of Fláajökull, and therefore this site is used exclusively to evaluate the principles of down-glacier debris modification. Since the Little Ice Age maximum, this glacier has descended over a stepped bedrock profile to terminate on a foreland composed of overridden proglacial sandur fans and composite moraines (Evans et al. 2016a; Jónsson et al. 2016). Another six forelands, each containing one or more specific till sites, are used to evaluate the second aim of quantifying and characterising the depositional signature of till production by subglacial deformation and other potential processes. So the second study location is Fjallsjökull, which descends steeply from the summit of the Öraefi stratovolcano, and during early LIA recession terminated on a series of overridden composite moraine arcs and outwash fans (Evans et al. 2009); it presently calves into a lake that occupies an overdeepening. Third, Heinabergsjökull presently occupies a partially flooded trough and hence the snout calves into a proglacial lake which represents an elongate erosional overdeepening. During the early LIA recession it terminated on a broad outwash plain but later receded behind an outwash head, which formed the steep adverse slope of a depositional overdeepening (Evans & Orton 2015). Fourth, Skalafellsjökull has retreated from its LIA maximum limit over a low relief subglacial surface characterized by push moraines and flutings and more recently over patchy thin till and roches moutonnées (Evans & Orton 2015; Chandler et al. 2016a, b); localized thickening of sediment cover occurs where the till is underlain by outwash gravels and pockets of lake sediment (Evans

2000). Fifth, Skaftafellsjökull occupies a deep valley incised into the margins of the Öraefi stratovolcano and since the LIA maximum has receded from an undulatory, low profile foreland composed of closely spaced push moraines (Evans et al. 2017a). It has only recently been associated with a proglacial lake, which occupies a shallow overdeepened foreland. Sixth, Falljökull descends steeply from the southern slopes of the Öraefi stratovolcano and its snout is presently downwasting in a flooded overdeepening (Bradwell et al. 2013; Everest et al. 2017). Excellent subglacial till exposures with lodged boulders are available on the very recently uncovered steep bedrock slopes on the eastern margin of the foreland. Finally, east Breiðamerkurjökull has recently receded from a foreland characterized by bedrock erosional forms such as whalebacks and roches moutonnées capped by patchy till, which has been injected into the crevices of the upper zones of the bedrock.

Methods

The stratigraphy and sedimentology of natural exposures on the forelands of the seven glaciers were evaluated using the standard procedures outlined in Evans and Benn (2004). This involved a multi-parameter approach in order to assess the full range of sedimentological characteristics that can be regarded as diagnostic for subglacial traction tills (sensu Evans et al. 2006; Evans 2018). Individual lithofacies are described in detail in vertical sediment logs or section sketches, which were compiled based on the identification of separate lithofacies according to bedding, texture, lithology and sedimentary structures. The lithofacies are described and classified according to the modified scheme of Eyles *et al.*, (1983; cf. Evans & Benn 2004).

Debris transport pathways in glaciers have been evaluated widely by employing clast form analysis (see Benn 2004a, 2007 for a review; Lukas et al. 2013), a technique that has proven to be very effective in identifying the spatial operation of glacial processes in debris modification (e.g. Matthews & Petch 1982; Benn 1989; Benn & Ballantyne 1994; Evans 1999, 2010). Clast form was quantified in this study using the standard methods of shape (derived from A, B and C axis measurements) and roundness (assessed using Powers charts) on samples of 50 massive basalt lithologies. Surface features such as striae were also noted and presented as percentages for each sample, because they are further diagnostic indicators of glacial abrasion (cf. Sharp 1982; Krüger 1984; Benn 2004a). Analysis of the data followed the procedures outlined in Benn (2004a, 2007) and involved: a) calculation of the C_{40} index (the percentage of clasts with a C:A axis ratio of <0.4; Benn & Ballantyne 1993); b) clast roundness, classified according to Powers (1953) and then used to calculate the RA summary index (percentage of angular and very angular clasts within a sample; Benn & Ballantyne 1993) and the RWR summary index (percentage of rounded and well-rounded clasts; Benn et al. 2004; Lukas et al. 2013); and c) mean roundness, based upon a numerical classification of Powers roundness as VA = 0 to WR = 5 (cf. Spedding & Evans 2002; Evans 2010). Co-variance plots (Benn & Ballantyne 1994) are then used to compare the clast form results with existing datasets on different glacigenic materials. Three co-variance plots are critical to this study. First, the “Type 1” co-variance plot of Lukas et al. (2013; Figure 2a) accounts for the low anisotropy basalt clast lithologies and the ice cap outlet glacier setting for our Icelandic glacigenic deposits. Second, a sub-Type 1 co-variance plot (Figure 2b) was identified for Fláajökull by Lukas et al. (2013) based upon the data presented in this paper, and was highlighted because of the wide spread of RWR values in the subglacial till samples, likely reflecting inheritance of glacifluvial materials. Third, a further variant of the Type 1 co-variance plot (Figure 2c) was identified by Evans et al. (2016b; cf. Benn 2004a) for tills that have ingested freshly plucked fragments from bedrock outcrops that protrude into or through the deforming layer. The down-glacier trends of clast form data could be analyzed only for the Fláajökull foreland due to the occurrence of continuous latero-frontal moraines at that site. Exhaustive control sampling of scree and glacifluvial deposits was also undertaken at Fláajökull and employed as control at all sites (previously used by Lukas et al. 2013 as a case study).

Clast macrofabrics were measured using 50 clasts per sample where possible; a minimum of 30 clasts was necessary in sedimentary units where clasts were more sparsely distributed and to ensure that data collection was confined to small areas and thereby reflected local variability in till properties (cf. Evans & Hiemstra 2005; Evans et al. 2016b). Macrofabric is based on the dip and azimuth (orientation) of the A-axes of clasts predominantly in the range of 30-125 mm (A-axis length) to allow comparison with other studies (Benn 1994a, b, 1995; Evans 2000; Evans & Hiemstra 2005). Note therefore that clast fabrics are based on sub-boulder size material and hence tend to underestimate the lodged component of tills according to the assessment of Evans and Hiemstra (2005) and Evans et al. (2016b). In some samples the orientation and dip of clast A/B planes was also measured in order to provide comparison with A axis data and an expanding database on A/B plane measurements (Benn 1995, 2004b; Li et al. 2006; Evans et al. 2007, 2016b). It is generally understood that clast A-axes and A/B planes will tend to rotate to parallelism with the direction of shear in a Coulomb plastic medium like till (cf. March 1932; Ildefonse & Mancktelow 1993; Hooyer & Iverson 2000) but Evans et al. (2007) proposed that within thin subglacial shear zones A/B planes will adopt a flow-parallel dip more readily than A-axes and that A-axes can align transverse to flow to display bi-modal orientations. However, ongoing assessments of till macrofabrics reveal that the different trends of A-axis and A/B plane data are more complex (Evans et al. 2016b), an aspect of till sedimentology that will be further investigated in this study.

Fabric data were plotted on spherical Gaussian weighted, contoured lower hemisphere stereonets, using Rockware™ software. Statistical analysis was undertaken using eigenvalues (S_1 - S_3), based on the degree of clustering around three orthogonal vectors (V_1 - V_3), presented in fabric shape ternary diagrams (Benn, 1994a; Figure 3a). This identifies end members as being predominantly isotropic fabrics (S_1-S_2~S_3), girdle fabrics (S_1-S_2>>S_3) or cluster fabrics (S_l>>S_2~S_3) and allows visual categorization of samples according to their isotropy and elongation. Also included in Figure 3a are envelopes of fabric shapes for lodged clasts, subglacial traction tills (Icelandic A and B horizons or upper and lower tills) and glacitectonites from both modern Icelandic settings as well as ancient glacigenic deposits. Further labelling on Figure 3a reflects the outcomes of laboratory experiments on the shearing of till-like materials by Iverson et al.

(2008). They plot the influence of initial consolidation and then increasing shear strain on clast fabric shapes, as represented by the arrows that depict changing fabric shape with increasing shear strain magnitude, from isotropic to girdle to cluster.

Strain histories were investigated further by classifying the fabric data according to five modal groups (un - unimodal, su - spread unimodal, bi- bimodal, sb - spread bimodal and mm - multimodal) and plotting these against isotropy (S_3/S_1) in a modality-isotropy plot (Hicock et al. 1996; Evans et al. 2007; Figure 3b). The envelopes on Figure 3b represent the spread of data from deposits of known origin (lodged clasts, subglacial traction till and glacitectonite) and the shaded area represents that part of the graph in which stronger modality and isotropy in subglacial traction tills or glacitectonites reflects an increasing lodgement component. Hence the graph is employed to interpret trends in cumulative strain signature in the glacitectonite-subglacial traction till continuum. Once plotted on this graph, the positions of macrofabric samples can be used to infer the cumulative relative strain immediately prior to till deposition.

Debris transport pathways: Fláajökull moraine clast form sampling and control samples

Debris transport pathways through glaciers have been quantified using clast form on latero-frontal moraine loops in a number of settings (Matthews & Petch, 1982; Benn, 1989; Evans, 1999; Spedding & Evans 2002) whereby distance down-moraine is regarded as a surrogate for glacigenic modification of debris down-glacier. Few glacier forelands on the south coast of Iceland display well developed latero-frontal moraine loops that interface with lowland tills and hence the rare example of such relationships at Fláajökull is employed here to assess the signature of glacial debris modification with distance down-glacier. This is then employed as control site for clast form analysis at the till exposures on all the forelands.

i) Description

The latero-frontal moraines of the Fláajökull foreland form a striking band of inset, arcuate push ridges, the frontal components being superimposed over glacially overridden, fluted moraine arcs (Evans et al. 2016a; Jónsson et al. 2016). Four scree and three glacifluvial control samples (Figure 4) were used alongside five subglacial till samples (see Till sedimentology sub-section below) as control data for a Fláajökull case study in Lukas et als. (2013) overview of clast forms in glacigenic settings. This identified the sub-Type 1 co-variance plot (Figure 2b) for settings with tills that have inherited glacifluvial roundness characteristics. Glacifluvial and scree samples form discrete clusters on the co-variance plots (Figure 4b) and are therefore easily differentiated by RA, RWR and average roundness indices but not by C_{40}, a characteristic of Icelandic basalt clast form data identified previously by Evans (2010).

Three sample transects were selected on the Fláajökull foreland (Figure 5), one along the eastern lateral moraine (samples L1-34), one along the Little Ice Age maximum frontal moraine (samples F1-6) and another along the mid-1990s readvance composite moraine identified by Evans and Hiemstra (2005; samples P1-13). In combination these provide two complete latero-frontal moraine transects, one for the Little Ice Age and one for the mid-1990s readvance. The eastern lateral moraine transect reveals weak down-glacier trends in all clast form criteria, compounded by a marked decrease in clast rounding and blocky clasts from around 700 to 1000 m (Figure 6a) and anomalously high RWR between 300 – 500 m. The aggregate statistics for the lateral moraine, as reflected in co-variance plots (cf. Figs. 2, 4b, 6b), reveal distinct glacifluvial to subglacial signatures, especially apparent in the sub-Type I plot (Fig. 2b), and very low RA values indicative of negligible supraglacial debris input.

The LIA frontal moraine clast form samples are tightly clustered on the covariance plots (Fig. 6c) with very low RA and low C_{40} values and are distinctly different to the glacifluvial and scree control samples (Fig. 4b). When compared to the Type I plots in Figure 2, the data envelopes clearly conform to those for subglacial materials. Additionally mean roundness is relatively high, typical of the glacifluvial control samples (Fig. 4b) and clearly more blocky (low C_{40}).

When combined as a single transect, the eastern lateral moraine and LIA frontal moraine data provide the means to assess clast form change down-glacier and towards the central flowline of the snout at the LIA maximum (i.e. along a latero-frontal moraine; Fig. 6d). Although this extension of the former down-valley transport pathway beyond the apparently anomalous oscillations of RWR and C_{40} (clast rounding and blockiness) at 300 - 1000 m creates more predictable trends, they are nonetheless statistically very weak; C_{40} generally declines, RWR increases, RA rapidly zeroes and mean roundness rapidly rises and then settles to a plateau after 1000 m. Overall these trends indicate that the frontal moraine contains material that is not appreciably modified beyond that contained within the lower lateral moraine, although a stronger set of down-flow trends would likely be apparent if the apparently anomalous oscillations did not occur along the 300 – 1000 m stretch of the lateral moraine. The graphs in Figure 6d clearly show that the oscillation is actually a positive spike in RWR and a negative spike in C_{40} at 300 – 500 m and is created by an influx of well rounded clasts.

The mid-1990s composite moraine samples are tightly clustered on the covariance plots, with the exception of one outlier, with very low RA and low C_{40} values (Fig. 6e). Like the LIA frontal moraine samples they are also distinctly different to the glacifluvial and scree control samples (Fig. 4b), even though mean roundness is again relatively high and thereby typical of blocky glacifluvial clasts. Also similar to the LIA frontal moraine samples is the clear subglacial signature when comparing the data clouds with those in the Type I plots, particularly the sub-Type I/Fláajökull control data plot, in Figure 2.

ii) Interpretation

The weak down-glacier, or more specifically down-laterofrontal moraine, clast form trends provide a strong signature of a mixed subglacial and glacifluvial clast population, as identified previously by Lukas et al. (2013). The anomalous spikes of RWR and C_{40} in the laterofrontal moraine transect (around 300 - 500 m; Figure 6d) are likely related to the concentration of a subglacial/englacial meltwater corridor on the northeast corner of the foreland, recorded by an esker complex draping an overdeepening, identified by landsystem mapping by Evans et al. (2016a). Sediment transport within this part of the glacier snout when it occupied its LIA maximum position on the mountain shoulder may have been overwhelmingly fluvial, especially if englacial drainage was bypassing the overdeepening; a similar scenario has been identified around the receding margins of Kviarjokull by Spedding and Evans (2002) and Bennett and Evans (2012).

A strong subglacial signature is apparent in both the LIA maximum moraine and the mid-1990s composite moraine samples, using both the Type I and sub-Type I covariance plots, with a C_{40} spread indicative of some fluvial inheritance and no evidence for plucking in terms of elevated RA values. These data clearly indicate that bedrock outcrops played no role in re-charging the subglacial till with large rock fragments, probably because they are blanketed with pre-advance glacifluvial outwash and older till carapaces.

Overall, the clast form data from Fláajökull reveal that the influence of supraglacial or passive debris transfer is indistinct in the signatures from both lateral and frontal moraine samples and that there is a strong inheritance of clast form either from englacial drainage sediments and/or pre-existing glacifluvial deposits. Hence there is no strong down-glacier trend in clast form modification in this piedmont lobe setting (i.e. the polynomial R^2 value on down-glacier RA trend is 0.17), in contrast to the more alpine/glaciated valley settings of some previous studies (e.g. Matthews & Petch 1982; Benn 1989; Evans 1999; Spedding & Evans 2002). Similar contrasts were identified by Evans (2010) for valley-confined and unconfined outlet lobes of the Tungnafellsjökull plateau icefield in central Iceland, wherein the greater role of passive transport was reflected in higher RA and C_{40} values and a stronger down-glacier trend in clast modification in the moraines of valley-confined snouts. For example, the polynomial R^2 values on down-glacier RA trends for valley-confined snouts at Tungnafellsjökull were 0.66 - 0.85, which contrasts with a range of 0.18 - 0.57 for unconfined snouts deriving debris predominantly from their beds.

Till sedimentology

Either single or multiple locations were identified for sedimentological investigation on the forelands of the seven glaciers. The till exposures at these sites represent the full spectrum of depositional settings including: a) multiple tills on overridden moraines at Fláajökull and Skaftafellsjökull; b) subglacial deforming layer tills emplaced over glacitectonite complexes with hydrofracture fills at Falljökull and Fjallsjökull; c) till overlying coarse-grained outwash at Heinabergsjökull; d) four sites on fluted till surfaces at Skaftafellsjökull, including potential melt-out deposits; e) a cliff section through a recessional push moraine at Skaftafellsjökull; and f) thin and patchy till veneers over striated and plucked bedrock at Breiðamerkurjökull and Skalafellsjökull.

i) Fláajökull

The glacial deposits on the Fláajökull foreland (Figures 1 & 5) have been described briefly by Evans et al. (2016a) and investigated in greater sedimentological detail by Jónsson et al. (2016), the latter proposing that the area contains drumlins composed of glacifluvial outwash cores and a carapace of either one or two subglacial traction tills of up to 2 m but generally less than 1 m thick. Both studies additionally identify overridden moraines and sawtooth moraines, and Evans et al. (2016a) recognize crevasse-squeeze ridges and possible till eskers (*sensu* Evans et al. 2010) created by the squeezing of water saturated till into longitudinal or splaying crevasses at the ice margin.

Till sedimentology was studied in a fluvially eroded cliff in the innermost overridden moraine arc on the north side of the foreland (Figure 7a). This exposure displayed three diamictons (LFs 1, 3 and 5) separated by laterally discontinuous beds of gravels (LFs 2 & 4; Figure 7b). The diamictons are massive and matrix-supported but LF3 also contains small attenuated lenses of stratified sands and fine gravels and LF5 displays very weak macroscale lamination. Clast macrofabrics range from moderately isotropic to girdle-like but consistently display weak westerly-dipping orientations for both A axes and A/B plane data. The gravels of LFs2 and 4 are massive to matrix-supported and a clast macrofabric from the top of LF2, where it is likely to have been influenced by subglacial processes, displays a westerly-dipping orientation similar to the overlying diamictons even though the A/B plane data is isotropic. Clast forms are consistent through all lithofacies sampled, with high levels of blockiness, very low angularity and average roundness values of 2.44-2.88. The percentage of clasts displaying striations range from 8-40%.

The characteristics of the diamictons of LFs 1, 3 and 5 are entirely consistent with those of subglacial traction tills reported previously from Iceland (cf. Krüger 1979; Sharp 1982; Boulton & Hindmarsh 1987; Benn 1995; Evans 2000; Evans & Twigg 2002; Evans & Hiemstra 2005; Evans et al. 2006, 2016b; Jónsson et al. 2016) with some important site-specific clast form details. Clast macrofabric shapes are similar to the range of A horizon tills but most tend towards relatively high levels of isotropy indicative of low cumulative strain (Figures 3a & 7b). Nevertheless there is a consistent indicative imposed stress direction from the west or WNW, which is consistent with surface flutings created by lobate flow of the Fláajökull snout at this location. Multiple tills separated by discontinuous beds of poorly-sorted gravels in the cores of overridden moraines such as this site can be related to the construction of composite push moraines, whereby partially superimposed sub-marginal till wedges/push moraines are locally subject to proglacial flowage and fluvial reworking to produce distal slope aprons (Sharp 1984; Evans & Hiemstra 2005). Clast forms (Figure 7b) are entirely consistent with a subglacial origin as defined by both the Benn and Ballantyne (1994) and Lukas et al. (2013) Type I covariance plots (Figure 2) and form distinct envelopes independent of the scree and glacifluvial control samples in the area (Figure 4b). However, they show no signature of local bedrock plucking when compared to the sub-Type I plot of Evans et al. (2016b; Figure 2). Some fluvial inheritance of clast form is possible but this is not particularly evident in the trend from 2.44 to 2.88 in mean roundness and 20% to 40% in striated clasts between the top of LF2 and overlying LF3. The top of LF2 has nevertheless been deformed during the emplacement of LF3, as indicated by the remarkably similar clast macrofabrics, and the attenuated stratified lenses in the Dmm are likely to be rafts of underlying material.

ii) Fjallsjökull

Multiple tills and sub-marginal till wedges/push moraines have been reported previously from the Fjallsjökull foreland by Evans and Twigg (2002) and Evans and Hiemstra (2005) respectively. Evans and Twigg (2002) recorded seven diamictons separated by discontinuous stratified units and/or clast pavements, which they interpreted as stacked subglacial traction tills emplaced by consistent NW-SE ice flow, compatible with surface fluting orientations, on the proximal slopes of a large overridden moraine. Although the emplacement of these tills had resulted in the partial erosion of till tops, vertical strengthening of intra-till clast macrofabrics did indicate that A and B horizon couplets were likely preserved in the sequence (cf. Benn 1995). Observations on modern examples of till and push moraine emplacement at the site were made by Evans and Hiemstra (2005) using the mid-1990s composite push moraine to support their sub-marginal till emplacement model; weak and steeply-dipping clast macrofabrics at the site indicated significant post-depositional modification or sub-marginal squeezing, as previously proposed for the same foreland by Price (1970).

Sedimentological analysis was undertaken on an exposure through an area of closely-spaced to partially overprinted push moraines on the east side of Fjállsarlón, one of the areas used in Price's (1970) push moraine investigations (Figure 8). Surface flutings at this site indicate former ice flow from WSW-ENE. The base of the exposure comprises more than 2 m of poorly to moderately well sorted cobble and pebble gravels with minor, discontinuous sandy gravel beds or lenses, arranged in horizontal beds (Figure 8b) and representative of sheetflows typical of the glacifluvial outwash fans (sandar) of the region. This is directly overlain by ≤0.30 m of massive and then stratified diamicton, which in turn is capped by ≤2.10 m of sand, sillt and clay rhythmites with lonestones (dropstones), indicative of glacilacustrine sedimentation. Importantly these rhythmites are cross-cut by numerous complex sub-vertical dykes, some containing laminated silts and clays orientated parallel to the dyke walls and others containing fine to medium gravels. Tributaries or branches occur at the bases of the silt/clay dykes and at the tops of the gravel dykes, the latter appearing as plumes or burst-out structures akin to those described by Rijsdijk et al. (1999). Cross-cutting reverse faults (Riedel shears) are also common in the rhythmites. The rhythmites are separated by an erosional contact from a 0.30-0.50 m thick overlying unit that ranges from a massive or pseudo-laminated, matrix-supported diamicton with attenuated basal silt/clay intraclasts rising from thrust overfolds at the left side of the exposure to heavily brecciated rhythmites at the right side. This is then overlain by up to 1 m of inter-layered and internally deformed diamictons, gravels, sands and rhythmites, some layers of which pinch-out towards the right side of the exposure making them a series of stacked WNW-tapering wedges. The sequence is capped by two matrix-supported diamictons, one of 0.10 – 0.25 m thick and densely fissile and the uppermost of 0.50 – 0.60 m thick and varying from fissile at the base to loose and friable at the top.

Clast form and fabric orientation data from the upper diamictons reveal vertically consistent signatures from sample F3 in the lower Dmm to samples F2 and then F1 in the base and middle of the capping Dmm (Figure 8b). Macrofabrics all dip westwards but are bimodal to spread bimodal and strengthen vertically. The lower Dmm (F3) displays a fabric shape similar to previously reported B horizons (Figure 3a). Within the upper Dmm, fabric F2 is typical of more clustered A horizon signatures, whereas the overlying F1 fabric is more isotropic than typical for A horizons. Clast forms display reasonably high levels of blockiness (C_{40} = 22-26%) and low angularity (14-26%) with average roundness values of 2.16-2.22 (cf. Figures 2 & 8b) and significant percentages of clasts displaying striations (42-46%).

The basal part of the east Fjallsarlon exposure records a period of significant outwash sedimentation, which was shutdown and replaced by an environment of massive to stratified diamicton production, likely ice-proximal subaqueous deposition, prior to the accumulation of more distal glacilacustrine rhythmites. Disturbance of these deposits is recorded by deformation, in the form of Riedel shear production, followed by the emplacement of clastic dykes, likely due to hydrofracture filling. Such features are common in Icelandic sub-till sediments, and fine-grained downward tapering and branching dykes with fine-grained laminae relate to downward propagating hydrofractures driven by subglacially pressurized meltwater (van der Meer et al. 1992, 2009; Le Heron & Etienne 2005). In contrast, upward branching, gravel-filled burst-out structures are produced by the vertical escape of water and sediment from pressurized aquifers (Rijsdijk et al. 1999), the ideal candidate for which at this site is the basal outwash deposit. The occurrence of shear structures and hydrofracture fills in the glacilacustrine deposits indicates that they were glacially overrun, the direct evidence for which is available in the overlying materials. The lateral changes in the overlying Dmm/Dml and brecciated rhythmites as well as its attenuated basal rafts rising from thrust overfolds are indicative of a glacitectonite (*sensu* Benn & Evans 1996) derived from the rhythmites. Similarly, the WNW-tapering wedges of inter-layered and internally deformed diamictons, gravels, sands and rhythmites are most simply explained as glacitectonic slices of pre-existing ice-proximal glacilacustrine deposits that have been excavated from lower parts of the sequence and elevated by shallow thrusting towards the ESE and stacked; hence they are classified as a glacitectonite complex (GT).

The glacitectonite complex is capped by two diamictons that display typical subglacial traction till characteristics (see Evans et al. 2006; Evans 2018 for review). For example, they are less than 0.60 m thick, matrix supported and largely fissile in structure, with fissility in the upper Dmm grading upwards into a loose friable structure (Figure 8b) typical of the structures of typical Icelandic tills (Boulton & Hindmarsh 1987; Benn 1995). The high levels of clast blockiness, low angularity and significant striations are all consistent with transport in the subglacial traction zone and have no indications of local bedrock plucking (Lukas et al. 2013; Evans et al. 2016b; Figure 2). The clast macrofabric strengths indicate a vertical weakening from a typical of B horizon (F3) through an A horizon (F2) to a relatively isotropic or weak A horizon signature, and each sample reveals a westerly orientation, consistent with both surface flutings and the tapering and dip direction of the glacitectonite wedges. Hence the diamictons appear to represent a typical Icelandic south coast till composed of A and B horizons (Boulton & Hindmarsh 1987; Benn 1995; Evans 2000; Evans & Twigg 2002).

iii) Heinabergsjökull

Previous work on the tills and associated deposits on the Heinabergsjökull and Skalafellsjökull foreland was undertaken on a river cliff located directly east of the Skalafellsjökull ice front by Evans (2000). He identified a complex vertical continuum of glacially overridden outwash and discontinuous thin tills that had been glacitectonized and increasingly homogenized up section and capped by ≤2.5 m of subglacial till with clear A and B horizon characteristics. This till (LFA 5 of Evans 2000) is strongly fissile in its basal 0.50 m, which also contains a large concentration of rounded clasts derived from the underlying gravelly deposits. The clast fabrics reveal a vertical modification from a cluster fabric typical of B-horizon tills to the slightly more isotropic and less elongate fabrics of A-horizon tills (Benn 1995), but it is apparent that the lowest fabric has been largely inherited or influenced by the clast alignments in underlying gravels; this prompted Evans (2000) to propose a hybrid glacitectonite/subglacial deformation origin for the lower part of the till.

The till stratigraphy at two further, more recently exposed, river cliffs are reported here, one located in the spillway channel from the Heinabergsjökull proglacial lake (Figure 9) and the other located on the Skalafellsjökull foreland (Figure 10a), 300 m north of the site reported by Evans (2000; see section iv below). At Heinabergsjökull, 0.50 m of matrix-supported boulder gravel and massive gravel (LF1) is overlain by 1.75 m of gravel and matrix-supported gravel (LF2) and capped by 1.25 m of massive, matrix-supported diamicton (LF3). The poorly-sorted and very coarse grained nature of LFs 1 and 2 are typical of the partially jökulhlaup-influenced glacifluvial outwash deposits at Heinabergsjökull (Þórarinsson 1939; Bennett et al. 2000; Evans & Orton 2015). Although massive and clast rich at macroscale, the diamicton contains a poorly developed clast pavement at a depth of 0.50 cm (Figure 9). An A axis clast macrofabric from around the area of the clast pavement displays a moderately strong orientation towards the northwest, which is only very weakly reflected in its A/B plane fabric. The sampling of an A axis and A/B plane clast macrofabric from the top of LF2, where it is most likely to have been influenced by subglacial processes, yielded a WNW-dipping orientation with a weak transverse element, reasonably similar to the overlying diamicton. Clast forms from both LFs 2 and 3 are characterized by high levels of blockiness and extremely low angularity, but RWR and average roundness values increase markedly from LF2 to LF3 even though striated clast totals are similar.

The LF3 diamicton at Heinabergsjökull is interpreted as a subglacial traction till based upon its massive, matrix-supported nature and clast form characteristics, in addition to its weakly developed clast pavement. Its clast macrofabric is also comparable to those of previously reported Icelandic A horizon tills (Figure 3a). The clast forms of LF3 display relatively elevated roundness values, which place them close to the subglacial-fluvial transition on the Type I covariance plots of Lukas et al. (2013; Figure 2a, b) and indicate some inheritance of forms from pre-existing fluvial materials even though 16% of the clasts are striated; lower roundness values in underlying LF2 indicates that this material was not the direct source of such inheritance.

The occurrence of clast pavements in tills has been an aspect of some debate in till sedimentology (see Evans 2018 for a review), but the general consensus is that they represent a form of lag created by the preferential removal of finer grained matrix and smaller clasts due to the downward migration of a deforming layer till (Boulton 1996; Eyles et al. 2016) likely also associated with meltwater flushing during phases of ice-bed decoupling (Boyce & Eyles 2000). The occurrence of clast pavements in Icelandic tills has been related to the development of up-ice thinning, sub-marginal till wedges by Evans and Hiemstra (2005). Clast macrofabric orientation in LF3 is also indicative of a subglacial genesis, as it records deformation imparted by stress from the northwest. The subglacial deformation associated with the emplacement of LF3 at Heinabergsjökull appears to have impacted also upon underlying LF2, as indicated by the similar clast macrofabric orientation, albeit a weaker girdle, similar to the less clustered A horizon fabrics reported previously (Figure 3a). The similarity in striated clast numbers between LFs 2 and 3 and a subglacial clast form signature in LF2 (Figure 2), strongly suggests that LF2 is ice-proximal outwash containing clasts that have undergone little modification since their release from the subglacial traction zone. The marked increase in rounding in the overlying till presumably attests to entrainment of fluvially more mature gravels from deeper in the foreland stratigraphy at a location further up-ice; therefore, any clast form inheritance in LF3 from LF2 presumably acted to dilute the rounding signature, which is somewhat counter-intuitive but a possibility nonetheless.

iv) Skalafellsjökull

Two sites were investigated at Skalafellsjökull and included the lower foreland site, located 300 m north of the cliff studied by Evans (2000; Figure 10a), and a higher elevation, glacially abraded bedrock site located along the southern margin of the glacier (Figure 10b-e) and described briefly by Evans and Orton (2015). The sites provide a significant contrast in subglacial depositional processes in that the lower foreland area was characterized by till emplacement over thick soft sediments but the abraded bedrock site consists of a thin and patchy till partially covering subglacially streamlined bedrock forms such as roches moutonnées and whalebacks.

The lower foreland site, similar to the stratigraphy reported by Evans (2000), displays multiple units of massive, matrix-supported diamicton (LFs 2-5), which overlie more than 7 m of largely crudely bedded to unbedded massive gravels and matrix-supported gravels (LF1; Figure 10a). Sampling from the middle and top of LF1 allows both a characterization of the whole lithofacies as well as internal vertical changes, especially in relation to impacts of subglacial processes on its upper zone of gradation into overlying LF2. In this respect, there are small increases in clast form criteria between lower and upper LF1 (Figure 10a). This reflects a small increase in rounding overall, a decrease in blockiness and an increase in the number of striated clasts. The Dmm of LF2 is a 1.6 m thick unit from which a lower and upper sample provide clast form and fabric characterizations. The lower sample indicates very similar clast forms to the immediately underlying part of LF1 but significant changes are visible towards the upper part of LF2. This involves a reduction in rounding, increased blockiness and a doubling of the number of striated clasts (Figure 10a). The diamictons LF3 and LF4 are highly fissile and compact in nature and are 0.7 and 0.3 m thick respectively. They are separated by a gradational boundary, with LF4 being differentiated through its more dense fissility. Clast form indicators reveal negligible change between LF3 and underlying LF2 and only reduced blockiness and striated clast numbers between LFs 3 and 4. However, average roundness falls consistently through upper LF1 to LF4 and also into LF5, reflected in a concomitant overall vertical fall in RWR values (Figure 10a). The 0.7 m thick upper diamicton of LF5 contrasts with those below in that it has a loose, crumbly structure and lacks fissility and both blockiness and striated clast numbers increase from those in underlying LF4. Clast macrofabrics reveal a change from southerly dipping to westerly dipping clasts between lower and upper LF1, although a weak W-E alignment is apparent in the spread bi-modal fabrics from the lower sediments (Figure 10a). The westerly orientation, particularly in A-axis alignments, persists through all overlying diamictons with the exception of LF2, in which multi-modal fabrics pick out only a very weak westerly-orientated girdle.

Like the basal lithofacies at Heinabergsjökull, the poorly-sorted and very coarse grained nature of LF1 at Skalafellsjökull are typical of the partially jökulhlaup-influenced glacifluvial outwash deposits on the combined foreland. The diamictons LFs2-5 display a range of characteristics typical of subglacial traction tills, including their massive to fissile matrix, their predominantly subglacial to marginally fluvial clast forms (Figure 2) and prominence of striations, in addition to their clast macrofabric orientations and strengths. Glacier-induced stress at this ice-proximal study site will always be from the west, as is recorded by surface flutings (Evans & Hiemstra 2005; Evans & Orton 2015; Chandler et al. 2016b). In contrast, a southerly or southeasterly dip to the lower LF1 macrofabric aligns with the modern drainage pathway of the Kolgrima River and hence could reflect palaeocurrents in its precursor thalweg. This orientation appears to have been modified in upper LF1 to a very weak westerly dip, with A/B planes being steepened; these patterns are similar to those in overlying LF2 and hence are interpreted as the products of glacially-induced stress when Skalafellsjökull overran the proglacial outwash to deposit the first subglacial till (LF2) in the stratigraphic sequence. The persistent westerly dipping macrofabrics, particularly in A-axis signatures, from LF2 through to LF5 indicate incremental subglacial till emplacement by Skalafellsjökull. The textural and structural appearances of LFs 3-5 potentially reflect the development of an open framework A horizon (LF5) over two superimposed B horizons (LFs 3 and 4), wherein the later westerly-imposed stress responsible for LFs 4 and 5 partially excavated and overprinted the WNW-imposed stress recorded by the LF3 fabric. Such excavation and overprinting has been proposed at other Icelandic till sections by Evans and Twigg (2002) and Evans et al. (2016b). Although directional indicators in the stereonets are acknowledged above, the clast macrofabrics overall are not particularly strong and few plot at the more clustered end of the A horizon till fabric shape envelope, with only LF3 plotting close to the B horizon envelope of previously reported Icelandic tills (Figure 3a).

The glacially abraded bedrock site is characterized by patchy tills, which were sampled in an area of thin cover over predominantly flat to gently tilted, striated bedrock (Figure 10b) and in an area of localized till thickening where flutings extend from the plucked faces of roches moutonnées, hence comprising crag-and-tail flutings (Figure 10c; cf. Hart et al. 2018). An independent assessment of local ice flow direction and its manifestation in lodgement signatures was obtained by sampling striae orientations on abraded bedrock outcrops and the macrofabrics of boulders embedded (lodged) in and protruding through the surface of the till (cf. Evans & Hiemstra 2005; Evans et al. 2016b). These data (Figure 10) reveal a strong ESE-WNW alignment and strong clast dip ($S1 = 0.89$) towards the ESE, reflecting ice flow from the SW margin of nearby Skalafellsjökull.

The thin till at the abraded bedrock site comprises ≤0.50 m of densely fissile and compact but otherwise massive, matrix-supported diamicton capped by ≤0.15 m of similar diamicton but with a loose and crumbly structure. The fissile diamicton displays a strong SE-NW cluster-type macrofabric ($S1 = 0.77$) and the upper diamicton a weak ESE-WNW alignment ($S1 = 0.53$). Clast forms are blocky with low angularity values, with C_{40} (25-10%) and RA (25.5-16.5%) decreasing and average roundness (2.0-2.3) increasing between the lower and upper diamicton. All the characteristics of the thin till exposure are indicative of classic A and B horizon deforming layer tills, specifically the vertical change from a fissile to crumbly structure and from cluster to girdle clast macrofabrics (Figure 3a & 10d) and hence a decreasing lodgement component and concomitant weakening of the ice flow directional indicators. The vertical change in clast form, essentially from subangular to more subrounded characteristics and of increasing blockiness, are instructive in that they convey greater impacts of clast wear in the A horizon (Figure 2 & 10e). This can be interpreted simply as greater transport distances for clasts in the A horizon and hence samples in the B horizon contain clasts derived from plucking of the underlying bedrock (cf. Evans et al. 2016b).

Diamictons in the crag-and-tail flutings display a similar two-tiered structure to the adjacent thin tills with the exceptions that the lower material (≤0.60 m) is less fissile and the upper (≤0.20 m) is more clast-rich. Clast macrofabrics display ESE-WNW alignments compatible with the adjacent striae and lodged clast data, with the exception of one of the upper diamicton samples, which displays clast dips towards the SSE (Figure 10c). In contrast to the thin till site, fabric strengths are the same ($S1 = 0.59$) between the horizons in one fluting but weaken vertically ($S1 = 0.54$ – 0.64) in the other (Figure 10d). Clast forms generally conform to the trends at the thin till site, with C_{40} markedly decreasing in one fluting (30-20%) and increasing slightly at the other (26-30%), RA decreasing from 44-14% and 44-38%, and average roundness increasing albeit still being predominantly subangular (Figure 10e). The characteristics of the diamictons in the crag-and-tail flutings are thereby less convincing as A and B horizon tills, although their macrofabric alignments and strengths are indicative of subglacially strained materials; vertical fabric strengthening and hence increased cumulative shear strain potentially reflects a relatively low pressure lee-side cavity infill origin for the lower tills and increased shearing in the upper tills due to their production during later cavity fill/closure and ice-bed coupling (Figure 10d).

Relatively more subangular clast roundness signatures overall, especially for the lower tills, compared to the thin till site (Figure 10e) potentially reflects the greater input of clasts freshly plucked from the roche moutonnée or crag.

v) Skaftafellsjökull

Six locations were selected for sedimentological investigation on the foreland of Skaftafellsjökull, including four sites (Sk1-4) on fluted till surfaces between recessional push moraines, one site (Sk5) on a fluted, glacially overridden moraine, and one site (Sk6) on a cliff section through a recessional push moraine (Figure 11a-e). Because site Sk6 was chosen as a representative site for the emplacement of tills at the ice-marginal or thicker end of sub-marginal till wedges/push moraines (cf. Sharp 1984; Evans & Hiemstra 2005), it is presented separately here (Figure 11f).

Sites Sk1-4 are exposures through diamictons that lie beneath fluted surfaces and overlie stratigraphically older glacifluvial outwash deposits. As the latter are not the focus of this study, they are described only briefly here based specifically on the most substantial exposures at sites Sk1 and Sk2 (Figures 11a & b) . They comprise stacked sequences of at least 3 m of interbedded cobble to granule gravels arranged in horizontal and in some places clinoform bedding or as massive and very poorly-sorted to matrix-supported units. At site Sk2 poorly-sorted units become locally diamictic and hence can be classified as stratified diamicton (Dms). Discontinuous pockets or lenses of horizontally bedded sand occur in some units. The generally poorly-sorted and very coarse grained nature of these lower gravels, sands and diamictons are typical of the partially jökulhlaup-influenced glacifluvial outwash deposits laid down on the sandur fans of southeast Iceland (Maizels 1989, 1993, 1995; Russell & Marren 1999; Marren 2005). Importantly at site Sk2, the glacifluvial deposits and stratified diamictons have been heavily deformed, presumably by glacier overriding, and hence an ice-contact, debris flow-fed fan origin is likely for at least part of the lower, diamicton-rich stratigraphic sequence.

The diamictons of site Sk1 (Figure 11a), beneath NNE-SSW aligned surface flutings, comprise a lower, 0.20 m thick Dmm with lenses of crudely horizontally bedded gravel similar to those in the underlying gravel and sand lithofacies, a middle, 0.30 m thick Dmm with a clear fissile structure, and an upper, 0.40 m thick Dmm containing a narrow fissile zone and several small, sub-vertical clastic dykes that rise from an important zone of inter-layered diamicton, sand and granule gravel. This 10-15 cm thick zone separates the upper and middle diamictons and is best described as a discontinuous and relatively thin unit of pseudo-stratified to fissile-structured diamicton with irregular lenses of sand and fine gravel (Figure 11a inset photograph). Clast forms in the middle and upper diamictons are blocky (C_{40} = 0-13.3%) and of low angularity (RA = 10-16.7%), and striated clast numbers are notable (16.6-30%) and increase vertically. Clast macrofabrics are not particularly strong but both A-axes and A/B plane data identify NE-SW and WNW-ESE alignments indicative of bi-modal distributions.

At site Sk2, the capping diamicton (Figure 11b) lies above a discontinuous clast (boulder) pavement that has been developed at the top of the underlying coarse-grained outwash deposits. It is a 1 m thick, massive to fissile, matrix-supported diamicton with a higher concentration of clasts in its lower 0.20 m and with characteristics that are remarkably consistent across the >50 m long exposure. Internally it displays strong fissility in its lower 0.50 m, which changes vertically to weak fissility between 0.50 and 0.20 m and then to massive in its upper 0.20 m where it constitutes weakly developed flutings orientated NE-SW. Clast forms in the weakly fissile and massive parts of the diamicton are relatively blocky (C_{40} = 26.6%) and of relatively low angularity (RA = 13.3-33.3%) with large numbers (23%) of striated clasts. A sample from the underlying sandy gravels reveals markedly more blocky and less angular clasts with greater numbers of striated clasts but with slightly higher average rounding, which overall demonstrates minor differences, particularly the typical glacial signatures, between outwash deposits and diamicton at this site. Clast A-axis macrofabrics reveal moderately strong alignments in the diamicton, which compare with the NE-SW alignments of surface flutings. A slight weakening is apparent between the fissile and massive samples. A clast macrofabric taken from the underlying sandy gravels for comparison reveals a girdle fabric with a preferential E-W alignment.

A particularly thick and complex stack of diamictons is exposed at site Sk3 (Figure 11c) where ten lithofacies are identified, seven of which (LFs 2, 4, 5 and 7-10) are massive to fissile and matrix-supported and ranging in thickness from 0.10 – 1.50 m, and three (LFs 1, 3 and 6) are clast-supported, massive and very gravelly in nature. The lowermost matrix-supported diamctons (LFs 2, 4, 5 and 7) are compact or indurated and fissile in appearance, with a clear dip in the planes of the fissile partings in LF2 towards the north-northeast. These diamictons are differentiated either by their grain size, structure and clast content and/or intervening clast-supported diamictons LFs 1, 3 and 6; a thin laminated silty-clay band separates LFs 4 and 5. A cobble-rich diamicton (LF 8) is locally clast-supported and is the only diamicton that lacks any form of fissile structure. The capping diamicton (LF 10) is only faintly fissile in its lower 0.10 m and is otherwise of crumbly texture and only loosely packed. Clast macrofabrics are moderately to well orientated, with consistent NE-SW alignments that are compatible with those of surface flutings.

Diamictons at site Sk4 (Figure 11d) can be subdivided according to their fissility patterns, clast densities and sizes and matrix grain size. The basal diamicton is 0.45 m thick, massive and characterized by a matrix with significant concentrations of granules to fine gravels, giving it a locally clast-supported appearance. This grades abruptly into an overlying, 0.50 m thick, matrix-supported diamicton with a weakly fissile silty-sand matrix. The section is then capped by a 0.70 m thick matrix-supported diamicton with a clear vertical change in matrix structure, from a widely spaced fissility at the base to a densely fissile and then fissile and crumbly appearance at the top. Clast A-axes macrofabrics from the 0.25 and 0.65 m levels in this diamicton display weak E-W orientations, transverse to the surface flutings.

At site Sk5, an overridden moraine adorned with NNW-SSE aligned flutings has been cliffed by proglacial meltwater to expose a complex upper lithofacies, comprising 2.25 m of clast rich, massive and matrix-supported diamicton and containing several boulder lags, overlying a stratified and clast-supported diamicton; a substantial boulder lag separates the two diamictons (Figure 11e). The upper diamicton is fissile in structure throughout, with the exception of its middle 0.50 m, where attenuated sand pods and increased concentrations of clasts occur in association with an entirely massive appearance to the matrix. Fissility is also only weakly developed in the upper 0.20 m of the diamicton. In contrast, the basal 0.30 m is characterized by dense fissility and cross-cutting faults thought to be representative of conjugate shearing. The boulder lags are effectively boundaries between different sub-units within the diamicton but do not display obviously accordant, facetted and striated tops, with the exception of one prominent cobble that contained NNW-SSE aligned surface striae. Clast A-axis macrofabrics display weak to moderate northeasterly or north-northeasterly dipping trends, with the weakest fabric strength occurring in the middle, massive and relatively clast-rich diamicton; weak girdle trends to the data, especially in samples F1 and F2 also indicate a subordinate northwesterly dip.

The push moraine cross-section at site Sk6 contains massive, matrix-supported diamicton with only localized indications of potential sub-division into sub-units, such as a discontinuous clast lag in the proximal part of the exposure (Figure 11f). A clear sub-vertical lineament also occurs immediately below the clast lag, picked out by a parting within the diamicton matrix dipping at 33˚ towards the northeast. Two small sections were chosen for analysis based upon them being representative of diamicton emplacement on the distal and proximal sides of the push moraine. Clast forms were analysed from the proximal section and revealed predominantly blocky (C_{40} = 10-33%) and sub-angular to sub-rounded (RA = 7-20%; AvR = 1.53-2.57) clasts. Clast A-axis macrofabrics collected in the upper 1.2 m of the proximal section display a consistent NE-SW orientated and predominantly NE dipping signature, with the exception of the upper sample, which has the weakest fabric strength and is essentially multi-modal despite a very weak NNW dip alignment. These fabrics can be compared with the orientations of the surface flutings which adorn the proximal moraine slope and are aligned NNE-SSW. In contrast, the lower macrofabric taken from the distal slope displays a south-southeasterly, spread-bimodal dip, whereas the upper macrofabric, like that of the proximal slope, is multi-modal.

The diamictons from all six sites at Skaftafellsjökull are now interpreted collectively as deposits potentially representative of subglacial processes across the foreland, hence clast form and clast macrofabric data are presented in aggregated form in the analytical Figures 11g and 11h respectively. The variable massive or fissile structures of the matrix-supported diamictons, especially where fissility increases towards the base of units, is typical of subglacial traction tills and has been clearly related to the development of A and B horizons in deforming layers (Boulton & Hindmarsh 1987; Evans 2000; Benn 2005; Evans & Twigg 2002; Evans et al. 2016b). Additionally, there are cases where couplets of fissile and massive diamictons appear to record both of the deforming layer components (e.g. LFs 9 and 10 at site Sk3) and can display typical upward strengthening macrofabrics (e.g. site Sk2; cf. Benn 1995), although A horizon preservation is normally low and it is more common to observe superimposed B horizons (cf. Evans & Twigg 2002; Evans et al. 2016b); the multiple layers of fissile diamicton likely represent such superimposed B horizons. Clast form signatures are all subglacial (Figures 2 and 11g), with high levels of blockiness, low angularity values and significant numbers of striated clasts, but there are no indications of deforming layer recharge through bedrock plucking (Figure 2c). It is assumed therefore that deforming layer materials are sourced from pre-existing glacifluvial outwash deposits, evidence for which is apparent in lower diamictons that either contain attenuated lenses of sandy gravel derived from underlying lithofacies (e.g. sites Sk1, Sk5) or have unusually high concentrations of clasts or a gravelly matrix (e.g. LF8 at site Sk3; cf Evans 2000). Nevertheless, the basal contacts of diamictons with underlying glacifluvial deposits are more often marked by clast lags or pavements, likely indicative of matrix removal by the downward migration of deforming layers (Boulton 1996; Eyles et al. 2016) and/or subglacial meltwater flushing (Boyce & Eyles 2000); periods of subaerial (aeolian) winnowing of till prior to further till emplacement could also be responsible for such clast lags (cf. Boulton & Dent 1974).

The analysis above indicates that a subglacial traction till origin is the most plausible for the diamictons across the Skaftafellsjökull foreland. Previous studies have identified glacier sub-marginal thickening wedges of such tills (Evans & Hiemstra 2005), whereby push moraines form the thicker end of fluted till sheets with numerous lodged surface clasts (boulder lags) indicative of downward migrating deforming layers that advect till to the ice margin (Boulton 1996). These deforming layers may migrate downwards into pre-existing outwash deposits and thereby introduce clasts with fluvial signatures, as well as stratified sediment rafts, to the subglacial shear zone. At quasi-stable glacier margins the tills can be stacked and overprinted by the process of incremental till thickening, as has been demonstrated by the emplacement of the mid-1990s readvance composite moraines in southern Iceland (Evans & Hiemstra 2005). Examples of overprinted till sequences on the proximal ramps of sub-marginal till wedges have been reported from the Breiðamerkurjökull and Skalafellsjökull forelands (see sections vii & iv respectively) by Evans and Twigg (2002) and Evans (2000) respectively, where they typically display similar features to those described above, including localized cannibalization of underlying outwash deposits, overprinted B horizons, weakly developed clast pavements and a range of clast macrofabric strengths that accord (parallel and occasionally transverse) with orientations of local flutings but are distinctly weaker than those obtained on populations of unequivocally lodged clasts. The weakening of clast macrofabrics in Icelandic field situations, and hence their apparently anomalous S1 eigenvalues when compared to laboratory-based shearing experiments (e.g. Hooyer & Iverson 2000; Thomason & Iverson 2006), has been explained by Evans et al. (2016b) as a product of clast collisions and perturbations set up by relatively larger (lodged) clasts in clast-rich tills (cf. Ildefonse et al. 1992; Kjær & Krüger 1998; Carr & Rose 2003; Thomason & Iverson 2006). This should therefore be manifest in a distinct relative weakening of clast macrofabrics in the coarser units in multiple till stacks, which appears to be demonstrated by the tills at sites Sk3 and Sk5.

The push moraine cross-section at site Sk6 (Figure 11f) represents till emplacement at the ice margin and appears to contain weakly defined multiple till units with a possible up-glacier, northeast dipping thrust represented by the sub-vertical lineament. The clast macrofabric orientations of the proximal section are consistent with sub-marginal till deposition related to southwesterly flowing ice, whereas the macrofabrics of the distal slope are more typical of deposits emplaced by sediment gravity flow and/or ice slope colluvium similar to the model of push moraine construction proposed by Sharp (1984). Such fabric signatures are likely to be inherited in subglacial deforming layer tills if they are superimposed over push moraines due to glacier overriding.

Of special interest in the Skaftafellsjökull till sequences is the pseudo-stratified zone at site Sk1 (inset photographs in Figure 11a), because it strongly resembles the outcrop characteristics of melt-out tills recently reported from Alaska by Larson et al. (2016). The normally poor preservation of melt-out till appears to have been improved in the Alaska case study because of a significant thickness and debris content of the parent (stratified) basal ice facies, thought to be the product of glaciohydraulic supercooling (cf. Alley et al., 1998, 1999; Lawson et al., 1998; Evenson et al., 1999). Supercooled ice has been reported from the southern Icelandic outlet glaciers (Roberts et al., 2002; Cook et al., 2007, 2010, 2011), including Skaftafellsjökull, but no evidence has been previously reported for the preservation of melt-out till derived from such ice, with the exception of Cook et als. (2011) identification of potential supercooling grain size signatures in ice-marginal deposits. The very localized preservation, as indicated by the discontinuous outcrop in section Sk1, is likely the result of a zone of stratified basal ice facies having been overprinted by a subglacial traction till, as recorded by the overlying fissile to massive diamicton, similar to the scenario reported from Alaska by Mickelson (1973) and Ham and Mickelson (1994). This would have slowed the melt rate and release of any meltwater by groundwater seepage. Indeed, the occurrence of a sub-vertical clastic dyke rising from the melt-out till into the overlying fissile to massive diamicton likely records localized water escape during the melt-out process. Further support for this being a prime site for melt-out till, potentially derived from supercooled ice, is the fact that it is located around an area of large melt-out hollows, which Evans et al. (2017a) have identified as a zone of controlled moraine development and melting based on mapping of spatial and temporal landsystem development and hence was an area of unusually well-developed supraglacial debris banding.

vi) Falljökull

Recently exposed subglacial deposits on the steep bedrock slopes on the eastern margin of Falljökull reveal thin (<2 m) diamictons directly overlying thicker sequences of pumice-rich conglomerates probably derived from volcanic gravity mass flows (Figure 12a). The diamictons contain numerous lodged boulders with well-developed upper facetted surfaces adorned with dense, unidirectional striae and protruding at the ground surface (Figure 12b). The logged section comprises two massive, matrix-supported diamictons capped by a thin, loosely packed, clast-supported to matrix-supported, massive diamicton. This upper diamicton appears to be the locally preserved remains of the former A horizon till which has been heavily reworked by wind deflation and mass flowage. The lower diamicton is 0.60 m thick, densely fissile and clay-rich and displays a moderately strong A-axis clast macrofabric (S1 = 0.585) orientated towards the northeast. The lower and middle diamctons are separated by an erosional boundary and the middle diamicton displays a faintly fissile and more crumbly, but still compact, structure and has a silty/sand matrix and a noticeably stronger clast A-axis macrofabric (S1 = 0.792), again orientated towards the northeast.

The Falljökull section was selected for analysis because of its strong resemblance to typical Icelandic subglacial deforming layer tills with their upper (A) and two lower, apparently superimposed, (B) horizons (Benn 1995; Evans & Twigg 2002) and hence the observations and data presented above can be considered representative of the macrofabric and textural signatures of superimposed B horizon deposits at this site. The middle and discontinuous upper diamictons display the vertical transition from a dense and faintly fissile structure to one that is more crumbly and then loose towards the top, typical of A and B horizons. The clast fabric orientations of both the lower and middle diamictons are compatible with the surface and near surface lodged clasts and striae and hence are consistent with former ice flow over the site. The fabric strength increases vertically through the lower and middle diamictons, as determined by the clast fabric shape ternary plot in Figure 12a. This shows that the middle diamicton plots in the highly clustered extreme of B horizon tills and lower diamicton plots in a similar position to the more clustered samples of A horizon tills. The relatively lower degree of clustering in the lower diamicton likely relates to the larger number of enclosed clasts and hence a greater tendency towards clast collisions and interference effects when being deposited (cf. Ildefonse et al. 1992; Kjær & Krüger 1998; Carr & Rose 2003; Thomason & Iverson 2006; Evans et al. 2016b).

vii) East Breiðamerkurjökull

Recent recession of the east lobe of Breiðamerkurjökull has exposed a subglacial surface composed of whalebacks (rock drumlins), roches moutonnées and patchy diamictons that infill or have been plastered into intervening topographic lows (Figure 13). Locally undercut cliffs reveal that the surfaces of the streamlined bedrock forms are heavily fissured, resulting in vertical cracks that cross-cut horizontal bedrock structures or partings, likely created by unloading, to form the boundaries of individual slabby incipient clasts. Where the bedrock protrudes through the sediment cover many such incipient clasts have clearly been plucked, leaving rectangular, straight-sided and shallow depressions. Where they can be viewed in cross section, the open fractures and partings that isolate the incipient clasts have been filled with massive, matrix-supported diamicton (Figure 13). Similar diamicton-filled fractures in bedrock have been reported from modern glacier forelands in Svalbard and ancient glacier beds in Scotland by Evans et al. (1998), where it has been proposed that subglacial deforming layer tills and glacitectonites have been intruded into the bedrock and thereby assisted in the liberation of freshly plucked bedrock blocks (cf. Broster et al. 1979; Harris 1991). Typical clast form signatures of bedrock plucking as a form of replenishment of patchy subglacial till layers, has been identified in angularity values by Evans et al. (2016b). They identify an abnormally wide range of clast angularity values in the subglacial tills of mountain outlet glaciers with stepped bedrock profiles, a reflection of the localised input of freshly plucked, and hence relatively highly angular, blocks to the deforming layer (Figure 2c). The influence of localised plucking in areas of poor till continuity can therefore be tested simply through clast form analysis. The occurrence of diamictic fracture fills which effectively isolate incipient clasts strongly indicates that this plucking is significantly enhanced by the subglacial deforming layer, a proposition that also can be tested by clast form analysis in that typical subglacial populations of abraded and edge rounded clasts will be diluted by plucked clasts of high angularity.

Clast forms from the fracture fills at east Breiðamerkurjökull display anomalously high C_{40} values for subglacial materials when compared to both Type I variants of the co-variance plots (compare Figures 2 & 13c), and resemble scree control samples from SE Iceland (Figure 4b). This indicates a strong lithological control not unexpected in freshly plucked material, but contrasting RA values between the two sample sites likely reflects the range of freshly plucked clasts contained within the injected tills. Clast form modification within the deforming till after initial plucking is well represented in the change in RA values in the vertical sequence depicted in Figures 13a and 13c; relatively high RA values (36%) in both the fracture fill and the directly overlying lower diamicton (till) horizon drop to 0% in the upper diamicton (till) horizon. This is consistent with a concomitant increase in average roundness from 1.84 through 1.94 to 2.32.

In addition to the increasing clast wear patterns between the lower and upper diamicton horizons, there are changes also in sediment matrix texture and clast macrofabric. Matrix texture changes vertically from compact and fissile to loose and granular. Clast macrofabrics display a subtle vertical strengthening from weak to strong girdle signatures and record a weak westerly dip in the lower horizon that is consistent with adjacent bedrock surface striae (Figure 13a). Although the pattern in matrix texture is typical of A and B horizons in Icelandic subglacial deforming tills, both clast macrofabrics are typical of weak A horizons (Figure 3a).

Discussion

The sedimentology of subglacial deforming layer tills in their type area of active temperate glacierization (Boulton et al. 1974; Boulton & Hindmarsh 1987; Benn 1995; Boulton & Dobbie 1998; Boulton et al. 2001; Evans & Twigg 2002) is now characterized conceptually based upon the observations from the various sampling sites detailed above (Figure 14; Table 1) and employing data previously reported from southeast Iceland. A conceptual model is proposed (Figure 15) in which the roles of debris transport pathways, substrate inheritance, subglacial deformation and glacier sub-marginal processes in the production of till characteristics are illustrated in terms of sedimentological data. This is portrayed using the three main end members in terms of stratigraphic architecture, which include: a) thin and patchy tills over bedrock erosional landforms; b) push moraine complexes and single push moraines; and c) overridden/drumlinized moraines or outwash fans. Although these end members are compiled using data predominantly from this study, they also incorporate important data from some other studies for some sediment-landform associations, including single push moraine data from Sharp (1984) and lodged boulder prow data from Evans (2018). Representative clast form and fabric data for each till type on the SE Iceland glacier forelands are related to the three architectural end members in Figure 15 and arranged schematically to illustrate data trends, which are now discussed.

The clast form covariance graph (Figure 2a) tailored for use in Iceland by Lukas et al. (2013; Figure 2b, sub-Type I) highlights a more restricted range of C_{40} values than those originally identified by Benn and Ballantyne (1994) but nonetheless clearly discriminates between two end member populations critical to the development of a typical subglacial clast form sample (Figure 4). Scree clasts represent “fresh” material unaffected by glacial wear processes, at one end of the spectrum, and glacifluvial clasts represent the most widespread deposit on the SE Iceland forelands, sandur plains and fans, in which clasts accumulate after leaving the subglacial traction zone and hence are modified by fluvial processes. Despite a restricted range of C_{40} values, the sub-Type I covariance graph highlights a discrete envelope defined by low RA, a range of RWR values and average roundness scores that are clearly intermediate between scree and glacifluvial samples. This is classified as a subglacial clast form population for the Fláajökull foreland, because not only was it sampled from glacially overridden frontal moraine arcs comprising stacked till sheets overlying glacifluvial outwash, but also the data distribution on the covariance plot conforms to previously reported subglacial samples (Benn & Ballantyne 1994; Lukas et al 2013), albeit with some indications of elevated RWR values and hence some inheritance of glacifluvial material. The underlying glacifluvial deposits are significant also in that their thickness restricts bedrock subglacial bedrock erosion and this is reflected in the lack of evidence for clast plucking in terms of elevated RA values (Evans et al. 2016b; Figure 2c). Not unrelated to the inheritance of glacifluvial clasts is the indistinct influence of passive debris transfer, as indicated by the lack of a strong down-glacier trend in clast form modification, conditioned primarily by relatively low RA and C_{40} values in lateral moraine samples in comparison to alpine glacierized catchments (cf. Matthews & Petch 1982; Benn 1989; Evans 1999; Spedding & Evans 2002).

Despite the absence of the strong down-glacier trends in clast modification that have been predicted in previous studies, compounded here by the restricted range in C_{40}, the data trends summarized above indicate that subglacial tills in SE Iceland can be differentiated from other deposits based upon standard clast form measurements (Figure 14a). Representative clast form data for the range of subglacial till types (Table 1), depicted schematically in Figure 15, reveal a subglacial wear trend from relatively immature to mature clast populations (Figure 14a). Such trends can be identified vertically between A and B horizons, especially over bedrock, and horizontally over bedrock between crag-and-tail flutings to lodged clasts and flutings, and are manifest as a decrease in RA and an increase in RWR and average roundness. Aggregated samples for undefined or overprinted tills unsurprisingly display the data ranges for a mature till sample in that they cover the ranges for A and B horizons over drift and glacitectonite (i.e. covering any glacifluvial inheritance) as well as lodged clasts and flutings and hence can be clearly differentiated from the scree and glacifluvial control samples. In thin and patchy tills over bedrock, inheritance is manifest in subtle evidence for freshly plucked debris, specifically in relatively elevated RA values in crag-and-tail fluting tills and B horizons (cf. Evans et al. (2016b). This angularity signal is also evident in fracture infills but such samples also appear to be influenced by relatively high C_{40} values similar to those of scree control samples; lower tills or B horizons over bedrock also contain clast samples with abnormally high C_{40} values. High C_{40} or relative slabbiness is likely influenced by the naturally flat plucked blocks on the Breiðamerkurjökull and Skalafellsjökull forelands, evidenced by the shallow nature of the fresh source depressions from which joint-controlled fragments have been removed by glacial erosion (Figures 10 & 13; cf. Hooyer et al. 2012). Hence elevated C_{40} here, in tandem with elevated RA (Evans et al. 2016b), is an indication of immaturity in clast modification but it reflects fresh introduction at the glacier bed rather than from extraglacial sources as in alpine glacial systems (cf. Benn & Ballantyne 1994). All of the clast form trends representative of wear patterns in subglacial traction till define a range of partially overlapping envelopes in a covariance plot that depicts progressive clast modification towards mature forms (Figure 14a). Importantly, these overlapping envelopes are clearly differentiated from those of the scree and glacifluvial control samples.

The clast macrofabric strengths reported here, especially those of A/B planes, are variable in terms of what has been traditionally expected of subglacial deforming layer tills (Figure 14b-d) but nevertheless do consistently record former glacier flow direction (Figure 15). Laboratory shearing experiments indicate that subglacial tills, due to their production in the ice-bed interface or traction zone, should be highly strained and that this should be reflected in compaction, consolidation and shear-induced fissility as well as strong clast macrofabrics (e.g. Thomason & Iverson 2006; Iverson et al. 2008; Hiemstra & Rijsdijk 2003). Field-based observation on subglacial processes, specifically at Breiðamerkurjökull, indicates also that such deforming layer tills more specifically comprise upper and lower (A and B) horizons, related to different styles of shearing (Boulton & Hindmarsh 1987); it is the B horizon in particular which displays the characteristics of shearing reproduced in laboratory experiments, because it is subject to brittle deformation, in contrast to the ductile response of the dilatant A horizon with its greater void ratio. Clast macrofabric signatures of the two-tiered deforming layer that formerly operated beneath Breiðamerkurjökull were reported by Benn (1995), who demonstrated relatively stronger B horizon ($S1 = \leq 0.72$) than unfluted A horizon (≤ 0.56) fabric strengths, in line with those at the lower end of the range of laboratory experiments on field sampled tills. Strengths at the upper end of the range of such experiments (i.e. $S1 = 0.98$) are rarely recorded in field till exposures, and even then predominantly in samples of clearly lodged clasts or in thin tills over roches moutonnées (Catto 1990, 1998; Evans & Hiemstra 2005; Evans et al. 2016b); notable exceptions are some samples from the multiple tills of Larsen and Piotrowski (2003) and the melt-out tills of Lawson (1979a, b, 1981). Some stronger A horizon fabrics ($S1 = \leq 0.71$) arise in situations where the till has been fluted (Benn 1995), potentially reflecting the greater number of lodged clasts in such landforms.

The clast macrofabric strengths collectively cover the envelopes describing the complete range of previously reported subglacial till fabrics from SE Iceland (Figure 14b) but do demonstrate some important trends when put into context of their collection sites. Significantly in this respect, the macrofabrics verify the strengthening in clast orientation from lower to upper tills, especially where they lie at the top of multiple till sequences or directly on bedrock (Figure 15). In contrast, the underlying (undefined/overprinted) tills in such sequences display a range of macrofabric strengths, plotting almost entirely within the upper till envelope on Figure 14b. Their similarities to the fabric strengths of upper and some lower tills in this study indicate that these undefined tills could represent former A or B horizons, but overprinting or complex modifications of strain signatures (cf. MacClintock & Dreimanis 1964; Ramsden & Westgate 1971; Catto 1998) as well as clast interference effects in coarser diamictons (cf. (cf. Ildefonse et al. 1992; Kjær & Krüger 1998; Carr & Rose 2003; Thomason & Iverson 2006; Evans et al. 2016b) are also likely explanations of their positioning on Figure 14b. Consideration should be made also of the widespread evidence for clast ploughing (Boulton 1976; Tulaczyk 1999) on the glacier forelands, the variable impact of which on clast macrofabric is depicted on Figure 15c using the data of Evans (2018). As this process is integral to till deformation and fluting production, its macrofabric signature is inevitably going to be coded into most subglacial tills in the region.

With the exception of lodged clasts, lower tills on bedrock display some of the strongest macrofabrics but also range from weak girdles to strong clusters. The stronger end of this spectrum likely reflects the dominance of lodgement in areas of thin deforming layers (cf. Figure 14c) but at the weaker end we have to acknowledge the additional influences of bedrock protuberances, clast clusters (interference) and freshly imported plucked clasts at the till-bedrock interface. Similarly, variability in fabric strengths in crag-and-tail flutings is related to the positioning of the sample with respect to the coupled (deforming) till layer at the top of the cavity infill (Boulton 1975, 1982). The influence of larger bedrock protuberances, such as roches moutonnées and whalebacks, on clast fabric orientations are also manifest in the data collected in this study and presented diagrammatically in Figure 15. It appears that in addition to the classic herringbone fabrics of crag-and-tail flutings (e.g. Rose, 1989, 1992; Benn, 1994b; Evans et al., 2010; Eyles et al., 2015), reverse herringbone patterns can be set up on the stoss sides of bedrock protuberances (cf. Catto 1990). Also evident are down-ice dipping, rather than the somewhat more traditionally predicted up-ice dipping, clast macrofabrics created on down-ice sloping segments of undulatory glacier beds (cf. Catto 1990; Sommerville 1997).

Clearly demarcated A and B horizons are not strongly developed at the outer edges of sub-marginally thickening till wedges (push moraines), where seasonally driven cycles of squeezing/flowage, freeze-on/melt-out and bulldozing give rise to a range of often superimposed deformation signatures related to the advection of subglacial till to the glacier snout (cf. Price 1970; Sharp 1984; Evans & Hiemstra 2005; Chandler et al. 2016a, b). The till macrofabrics are predominantly moderately strong (Figure 14b) and mostly conform to former ice flow directions as defined by local flutings and striae. However, sub-marginal till stacks, even if individual tills are thin or repeatedly overprinted, are likely to display a range of clast macrofabric strengths due to their changing rheological characteristics. Such changes are driven by changing environmental temperatures and concomitant porewater pressures beneath seasonally oscillating glacier snouts as well as localised processes involved in push moraine construction (Sharp 1984; Figure 15b). In addition to the highly variable clast orientations imparted by clast ploughing, unexpectedly weak strain signatures in till can also arise through smaller size fractions becoming relatively more mobile in the liquefaction and dewatering of matrixes (Phillips et al. 2018); in the sub-marginal till wedges this appears to be conditioned by lower basal shear stresses in the outer wedge during the ablation season when push/squeeze moraines are constructed (Price, 1970). At the thin end of such sub-marginal till wedges, the combined subglacial processes of lodgement, deformation and ice keel and clast ploughing repeatedly rework and advect till to produce overprinted strain signatures and clast pavements, a process similar to the excavational deformation invoked in the 'erodent layer hypothesis' (ELH) by Eyles et al. (2016; cf. Hart 1997). Hence, the ice-proximal ramps could contain typical A and B horizons but also superimposed horizons, potentially with strong cumulative strain signatures but equally conceivably displaying a range of clast macrofabric strengths (Figure 15b). Hence some unexpectedly low shear strain magnitudes are possible for the tills in the region, despite the associated lodged clasts displaying evidence of high strains.

Typical thicknesses for multiple tills advected to glacier margins in Iceland are modest, being less than 1.20 m per deformation event, whether that is driven seasonally (e.g. Evans & Hiemstra 2005; Evans et al 2016b) or by surging (Johnson et al. 2010; Benediktsson et al. 2016; McCracken et al. 2016). This is consistent with the subglacial deformation observations reported by Boulton and Hindmarsh (1987) and Boulton and Dobbie (1998) wherein A and B horizons were typically around 0.45m and 0.30m thick respectively. Individual till units measured in this study range from 0.10 m for B horizons to 1.40 m for undefined tills in multiple stacks, with a combined maximum thickness for A and B horizons being 1.35 m, again compatible with process observations by Boulton et al. (2001) that identified a 1 m thick shear zone beneath west Breiðamerkurjökull. Hence modern glacial systems in Iceland, especially in the type region for subglacial deforming layer tills in the southeast, lay down modest till thicknesses and may only accrete the substantial thicknesses of tens of metres, as reported from ancient glacial deposits, in increments, either on a seasonal basis at a quasi-stationary ice margin or by repeat surges of similar extent. An interesting aspect of the multiple tills at Skaftafellsjökull is the apparent survival of a discontinuous lens of melt-out till. This likely represents the localized development of stratified basal ice, potentially due to supercooling (Roberts et al., 2002; Cook et al., 2007, 2010, 2011), and its overriding by a subglacial deforming layer, which then entombed the ice-debris mix and allowed its passive melt-out. Given that this small exposure is clast-poor, it is impossible at this stage to produce typical clast form and fabric data for a typical SE Iceland melt-out till.

Conclusions

The sedimentology of subglacial deforming layers in their type area of active temperate glacierization in SE Iceland has been characterized by combining facies descriptions with clast macrofabric and form data to assess the roles of debris transport pathways, substrate inheritance, subglacial deformation and glacier sub-marginal processes in the production of sub-marginal till deposits. The main till types are characterized according to their depositional contexts, which include three main end members in terms of stratigraphic architecture: a) thin and patchy tills over bedrock erosional landforms; b) push moraine complexes and single push moraines; and c) overridden/drumlinized moraines or outwash fans.

Typical thicknesses for the individual tills in these settings range from 0.10 - 1.40 m, with combined A and B horizons being up to 1.35 m thick. Each till relates to a deformation event driven by seasonally tuned sets of processes including glacier sub-marginal shearing, freeze-on, squeezing and bulldozing. Such modest till thicknesses are consistent with subglacial deformation observations reported from Breiðamerkurjökull, where the deforming A and B horizons are typically 0.75m thick. Such glaciers, if they are typical of those responsible for the deposition of ancient tills measuring tens of metres thick, can accrete substantial till thicknesses only incrementally, either on a seasonal basis at a quasi-stationary ice margin or by repeat surges of similar extent.

The apparent survival of a discontinuous lens of melt-out till at Skaftafellsjökull is significant in that no convincing evidence has previously been reported for melt-out till preservation in the region, despite the fact that supercooling and its signature debris-rich basal ice, necessary for melt-out till production, is operating locally.

Clast form trends representative of wear patterns in subglacial traction till, defined by C_{40}, RA, RWR and average roundness values, are depicted as a range of partially overlapping envelopes in covariance plots. This clearly demonstrates a progressive clast modification towards mature forms in subglacial traction zones. Importantly, these overlapping envelopes are clearly differentiated from those of scree and glacifluvial control samples and more precisely refine the subglacial till clast form signature by identifying the roles of various subglacial processes operating at the glacier bed in SE Iceland. This is best displayed in the traditional C_{40}/RA covariance graph despite the narrow range of C_{40} values dictated by the basalt bedrock of the region.

Clast macrofabric strengths collectively cover the envelopes describing the complete range of previously reported subglacial till fabrics from SE Iceland. Hence fabric strengths, especially for A/B planes, are variable and rarely reach the S1 eigenvalues reported from laboratory shearing experiments, with the exception of lower tills on bedrock wherein clast lodgement is widespread due to thin nature of the deforming layer. However, orientations do consistently record former glacier flow directions, albeit with localized variability related to bedrock protuberances, cavity infill, clast interference and freshly imported plucked clasts at the till-bedrock interface. Some of the variability can be ascribed to the development of both classic herringbone and apparent reverse herringbone fabrics on the lee and stoss sides of protuberances respectively. Down-ice dipping clast macrofabrics are also created on down-ice sloping segments of undulatory glacier beds.

Macrofabrics verify the previously reported strengthening in clast orientation from lower (B horizon) to upper (A horizon) tills, especially where they lie at the top of multiple till sequences or directly on bedrock. The similarities between macrofabric strengths from undefined/overprinted tills and the upper and some lower tills indicate that the undefined tills could represent former A or B horizons, but a range of potential processes might explain their lack of strong clustering, including overprinting or complex modifications of strain signatures, clast interference effects in the coarser diamictons and clast ploughing/fluting construction.

At the outer edges of sub-marginally thickening till wedges or push moraines, seasonally-driven cycles of squeezing/flowage, freeze-on/melt-out and bulldozing give rise to a range of clast macrofabric strengths as well as superimposed deformation signatures. At the two extremes of till emplacement in terms of solid state deformation are: a) the more mobile, flowing and often liquefied matrixes in push/squeeze moraines; and b) the combined subglacial processes of lodgement, brittle to ductile deformation and ploughing at the thin end of sub-marginal till wedges.

Acknowledgements

Research in Iceland has been funded over a number of years by the Royal Geographical Society/IBG. Scientific research permits allowing work at the various field sites have been provided on numerous occasions by Regina Hreinsdottir on behalf of the Vatnajökull National Park and by RANNIS (The Icelandic Centre for Research). Thanks to two anonymous reviewers for their helpful comments on an earlier version of this paper. Assistance with data collection in Iceland was provided by Durham University students L. Brzeskwinski, C. Chantler, S. Charles, H. Diamond, M. Dinnage, B. Freer, C. Goodchild, B. Hearn and M. Kay, who hopefully now all know how to make poppadoms and proper coffee!

References

Alley, R.B., Cuffey, K.M., Evenson, E.B., Strasser, J.C., Lawson, D.E., Larson, G.J., 1997. How glaciers entrain and transport basal sediment: physical constraints. Quaternary Science Reviews 16, 1017–1038.

Alley, R.B., Lawson, D.E., Evenson, E.B., Strasser, J.C., Larson, G.J., 1998. Glaciohydraulic supercooling: a freeze-on mechanism to create stratified, debris-rich basal ice: II. Theory. *Journal of Glaciology* 44, 563-569.

Alley, R. B., Strasser, J. C., Lawson, D. E., Evenson, E. B., Larson, G. J., 1999. Glaciological and geological implications of basal-ice accretion in overdeepenings. In: Mickelson, D.M., Attig, J.W. (Eds.), *Glacial Processes Past and Present, Geological Society of America Special Paper* 337, 1-9.

Benediktsson, Í.Ö., Jónsson, S.A., Schomacker, A., Johnson, M.D., Ingólfsson, Ó., Zoet, L.K., Iverson, N.R., Stötter, J.. 2016. Progressive formation of modern drumlins at Múlajökull, Iceland: stratigraphical and morphological evidence. Boreas, 45, 567-583.

Benn, D.I.. 1989. Debris transport by Loch Lomond Readvance glaciers in northern Scotland – basin form and the within-valley asymmetry of lateral moraines. *Journal of Quaternary Science* 4, 243-254.

Benn, D.I., 1994a. Fabric shape and the interpretation of sedimentary fabric data. Journal of Sedimentary Research A 64, 910–915.

Benn, D.I., 1994b. Fluted moraine formation and till genesis below a temperate glacier: Slettmarkbreen, Jotunheimen, Norway. *Sedimentology* 41, 279-292.
Benn, D.I., 1995. Fabric signature of subglacial till deformation, Breiðamerkurjokull, Iceland. *Sedimentology* 42, 735–747.
Benn, D.I., 2004a. Clast morphology. In: Evans, D.J.A., Benn, D.I. (Eds.), A Practical Guide to the Study of Glacial Sediments. Arnold, London, pp. 77-92.
Benn, D.I., 2004b. Macrofabric. In: Evans, D.J.A. and Benn, D.I. (Eds): A Practical Guide to the Study of Glacial Sediments. Arnold, London, pp. 93–114.
Benn, D.I., 2007. Clast form analysis. In *Encyclopedia of Quaternary Science*, Elias SA (ed). Elsevier: Amsterdam; 904–909.
Benn, D.I., Ballantyne, C.K., 1993. The description and representation of clast shape. Earth Surface Processes and Landforms 18, 665–72.
Benn, D.I., Ballantyne, C.K., 1994. Reconstructing the transport history of glaciogenic sediments: a new approach based on the co-variance of clast form indices. Sedimentary Geology 91, 215-227.
Benn, D.I., Evans, D.J.A., 1996. The interpretation and classification of subglacially-deformed materials. Quaternary Science Reviews 15, 23–52.
Benn, D.I., Evans, D.J.A., Phillips, E.R., Hiemstra, J.F., Walden, J., Hoey, T.B., 2004. The research project – a case study of Quaternary glacial sediments. In: Evans, D.J.A., Benn, D.I. (Eds.), A Practical Guide to the Study of Glacial Sediments. Arnold, London, pp. 209–234.
Bennett, G. L., Evans, D. J. A., 2012. Glacier retreat and landform production on an overdeepened glacier foreland: The debris-charged glacial landsystem at Kvíárjökull, Iceland. Earth Surface Processes and Landforms, 37, 1584–1602.
Bennett, G. L., Evans, D. J. A., Carbonneau, P., Twigg, D. R., 2010. Evolution of a debris-charged glacier landsystem, Kvíárjökull, Iceland. *Journal of Maps* 6, 40–67.
Bennett, M. R., Huddart, D., McCormick, T., 2000. The glaciolacustrine landform-sediment assemblage at Heinabergsjokull, Iceland. Geografiska Annaler, 82A, 1–16.
Boulton, G.S., 1975. Processes and patterns of subglacial sedimentation: a theoretical approach. In: Wright, A.E.,Moseley, F. (Eds.), Ice Ages: Ancient and Modern. Seel House Press, Liverpool, pp. 7–42.
Boulton, G.S., 1976. The origin of glacially fluted surfaces – observations and theory. *Journal of Glaciology* 17, 287-309.
Boulton, G.S., 1978. Boulder shapes and grain size distributions of debris as indicators of transport paths through a glacier and till genesis. Sedimentology 25, 773–799.
Boulton, G.S., 1979. Processes of glacier erosion on different substrata. Journal of Glaciology 23, 15–38.
Boulton, G.S., 1982. Subglacial processes and the development of glacial bedforms. In: Davidson-Arnott, R., Nickling, W., Fahey, B.D. (Eds.), Research in Glacial, Glacio-fluvial and Glaciolacustrine Systems. Geo Books, Norwich, pp. 1–31.
Boulton, G.S., 1986. Push moraines and glacier contact fans in marine and terrestrial environments. *Sedimentology* 33, 677-698.
Boulton, G.S., 1987. A theory of drumlin formation by subglacial sediment deformation. In: Menzies, J., Rose, J. (Eds.), *Drumlin Symposium*. Balkema, Rotterdam, 25-80.
Boulton, G.S., 1996. Theory of glacial erosion, transport and deposition as a consequence of subglacial sediment deformation. Journal of Glaciology 42, 43–62.
Boulton, G.S., Dent, D.L., 1974. The nature and rates of post-depositional changes in recently deposited till from south-east Iceland. Geografiska Annaler 56A, 121–134.

Boulton, G.S., Dobbie, K.E., 1998. Slow flow of granular aggregates: the deformation of sediments beneath glaciers. *Philosophical Transactions of the Royal Society of London A* **356**(1747): 2713–2745.

Boulton, G.S., Hindmarsh, R.C.A., 1987. Sediment deformation beneath glaciers: rheology and sedimentological consequences. *Journal of Geophysical Research: Earth Surface* 92, 9059–9082.

Boulton, G.S., Dent, D.L., Morris, E.M., 1974. Subglacial shearing and crushing, and the role of water pressures in tills from southeast Iceland. Geografiska Annaler 56A, 135–145.

Boulton, G.S., Dobbie, K.E., Zatsepin, S., 2001. Sediment deformation beneath glaciers and its coupling to the subglacial hydraulic system. Quaternary International 86, 3–28.

Boyce, J.I., Eyles, N., 2000. Architectural element analysis applied to glacial deposits: internal geometry of a late Pleistocene till sheet, Ontario, Canada. Bulletin of the Geological Society of America 112, 98–118.

Bradwell, T., Sigurðsson, O., Everest, J., 2013. Recent, very rapid retreat of a temperate glacier in SE Iceland. Boreas 42, 959–973.

Broster, B.E., Dreimanis, A., White, J.C., 1979. A sequence of glacial deformation, erosion and deposition at the ice–rock interface during the last glaciation: Cranbrook, British Columbia, Canada. Journal of Glaciology 23, 283–295.

Carr, S.J., Rose, J., 2003. Till fabric patterns and significance: particle response to subglacial stress. Quaternary Science Reviews 22, 1415–1426.

Catto, N.R., 1990. Clast fabric of diamictons associated with some roches moutonnées. Boreas 19, 289-296.

Catto, N.R., 1998. Comparative study of striations and basal till clast fabrics, Malpeque-Bedeque region, Price Edward Island, Canada. Boreas 27, 259-274.

Chandler, B.M.P., Evans, D.J.A., Roberts, D.H., 2016a. Characteristics of recessional moraines at a temperate glacier in SE Iceland: Insights into patterns, rates and drivers of glacier retreat. *Quaternary Science Reviews* 135, 171-205.

Chandler B.M.P., Evans D.J.A., Roberts D.H., Ewertowski M., Clayton A.I., 2016b. Glacial geomorphology of the Skálafellsjökull foreland, Iceland: A case study of 'annual' moraines. *Journal of Maps* 12, 905-916.

Clark, P.U., 1991. Striated clast pavements, products of deforming subglacial sediment? Geology 19, 530–533.

Clark, P.U., 1992. Comment and reply on "Striated clast pavements: products of deforming subglacial sediment?" Geology 20, 285-286.

Clark, P.U., Hansel, A.K., 1989. Clast ploughing, lodgement and glacier sliding over a soft glacier bed. Boreas 18, 201–207.

Clarke, G.K.C., 2005. Subglacial processes. Annual Review of Earth and Planetary Sciences **33**, 247–276.

Cook, S.J., Knight, P.G., Waller, R.I., Robinson, Z.P., Adam, W.G., 2007. The geography of basal ice and its relationship to glaciohydraulic supercooling: Svínafellsjökull, southeast Iceland. *Quaternary Science Reviews* 26, 2309-2315.

Cook, S.J., Graham, D.J., Swift, D.A., Midgeley, N.G., Adam, W.G., 2011. Sedimentary signatures of basal ice formation and their preservation in ice-marginal sediments. Geomorphology 125, 122–131.

Cook S.J., Robinson, Z.P., Fairchild, I.J., Knight, P.G., Waller, R.I., Boomer, I., 2010. Role of glaciohydraulic supercooling in the formation of stratified facies basal ice: Svínafellsjökull and Skaftafellsjökull, southeast Iceland. Boreas 39, 24–38.

Dowdeswell, J.A., Sharp, M., 1986. Characterization of pebble fabrics in modern terrestrial glacigenic sediments. Sedimentology 33, 699–710.

Dowdeswell, J.A., Hambrey, M.J., Wu, R., 1985. A comparison of clast fabric and shape in Late Precambrian and modern glacigenic sediments. Journal of Sedimentary Petrology 55, 691-704.

Evans, D.J.A., 1999. Glacial debris transport and moraine deposition: a case study of the Jardalen cirque complex, Sogn-og-Fjordane, western Norway. *Zeitshcrift fur Geomorphologie* 43, 203–234.

Evans, D.J.A., 2000. A gravel outwash/deformation till continuum, Skalafellsjokull, Iceland. *Geografiska Annaler* 82A, 499–512.

Evans, D. J. A., 2005. The glacier-marginal landsystems of Iceland. In: Caseldine, C.J., Russell, A.J., Harjardottir, J., Knudsen, O. (Eds.), Iceland: Modern processes and past environments (pp. 93–126). Amsterdam: Elsevier.

Evans, D.J.A., 2010. Controlled moraine development and debris transport pathways in polythermal plateau icefields: examples from Tungnafellsjökull, Iceland. *Earth Surface Processes and Landforms* 35, 1430–1444.

Evans, D.J.A., 2018. *Till: A Glacial Process Sedimentology*. Wiley-Blackwell: Chichester.

Evans, D.J.A., Benn, D.I., 2004. Facies description and the logging of sedimentary exposures. In: Evans, D.J.A., Benn, D.I. (Eds.), A Practical Guide to the Study of Glacial Sediments. Arnold, London.

Evans D.J.A., Hiemstra J.F., 2005. Till deposition by glacier submarginal, incremental thickening. *Earth Surface Processes and Landforms* 30, 1633-1662.

Evans, D. J. A., Orton, C., 2015. Heinabergsjökull and Skálafellsjökull, Iceland: Active temperate piedmont lobe and outwash head glacial landsystem. *Journal of Maps* 11, 415-431.

Evans, D.J.A., Twigg, D.R., 2002. The active temperate glacial landsystem: a model based on Breiðamerkurjökull and Fjallsjökull, Iceland. *Quaternary Science Reviews* 21, 2143–2177.

Evans, D.J.A., Ewertowski, M., Orton, C., 2016a. Fláajökull (north lobe), Iceland: active temperate piedmont lobe glacial landsystem. *Journal of Maps* 12, 777-789.

Evans D.J.A., Ewertowski M., Orton C., 2017a. Skaftafellsjokull, Iceland: glacial geomorphology recording glacier recession since the Little Ice Age. *Journal of Maps* 13, 358-368.

Evans D.J.A., Ewertowski M., Orton C., 2017b. The glaciated valley landsystem of Morsárjökull, southeast Iceland. *Journal of Maps* 13, 909-920.

Evans, D.J.A., Hiemstra, J.F., Ó Cofaigh, C., 2007. An assessment of clast macrofabrics in glaciogenic sediments based on A/B plane data. Geografiska Annaler A89, 103-120.

Evans, D.J.A., Nelson, C.D., Webb, C., 2010. An assessment of fluting and till esker formation on the foreland of Sandfellsjökull, Iceland. Geomorphology 114, 453–465.

Evans, D.J.A., Phillips, E.R., Hiemstra, J.F., Auton, C.A., 2006. Subglacial till: Formation, sedimentary characteristics and classification. *Earth-Science Reviews* 78, 115–176.

Evans, D.J.A., Rea, B.R., Benn, D.I., 1998. Subglacial deformation and bedrock plucking in areas of hard bedrock. Glacial Geology and Geomorphology (rp04/1998—http://ggg.qub.ac.uk/ggg/papers/full/1998/rp041998/rp04.html).

Evans D.J.A., Roberts D.H. & Evans S.C., 2016b. Multiple subglacial till deposition: a modern exemplar for Quaternary palaeoglaciology. *Quaternary Science Reviews* 145, 1-21.

Evans, D. J. A., Shand, M., Petrie, G., 2009. Maps of the snout and proglacial landforms of Fjallsjökull, Iceland (1945, 1965, 1998). *Scottish Geographical Journal* 125, 304–320.

Evenson, E.B., Lawson, D.E., Strasser, J.C., Larson, G.J., Alley, R.B., Ensminger, S.L., Stevenson, W.E., 1999. Field evidence for the recognition of glaciohydraulic supercooling. In: Mickelson, D.M., Attig, J.W. (Eds.), *Glacial Processes Past and Present. Geological Society of America Special Paper* 337, 23-35.

Everest, J., Bradwell, T., Jones, L., Hughes, L., 2017. The geomorphology of Svínafellsjökull and Virkisjökull-Falljökull glacier forelands, southeast Iceland. Journal of Maps 13, 936-945.

Eyles, N., 1979. Facies of supraglacial sedimentation on Icelandic and Alpine temperate glaciers. Canadian *Journal of Earth Sciences* 16, 1341– 1361.

Eyles, N., 1983. Modern Icelandic glaciers as depositional models for 'hummocky moraine' in the Scottish Highlands. In: Evenson, E.B., Schluchter, C., Rabassa, J. (Eds.), *Tills and Related Deposits: Genesis, Petrology, Stratigraphy*. Balkema, Rotterdam, pp. 47– 60.

Eyles, N., Boyce, J., Putkinen, N., 2015. Neoglacial (<3000 years) till and flutes at Saskatchewan Glacier, Canadian Rocky Mountains, formed by subglacial deformation of a soft bed. Sedimentology 62, 182–203.

Eyles, N., Eyles, C.H., Menzies, J., Boyce, J., 2011. End moraine construction by incremental till deposition below the Laurentide Ice Sheet: Southern Ontario, Canada. Boreas 40, 92-104.

Eyles, N., Eyles, C.H., Miall, A.D., 1983a. Lithofacies types and vertical profile models; an alternative approach to the description and environmental interpretation of glacial diamict and diamictite sequences. Sedimentology 30, 393–410.

Eyles, N., Putkinen, N., Sookhan, S., Arbelaez-Moreno, L., 2016. Erosional origin of drumlins and megaridges. Sedimentary Geology 338, 2-23.

Ham, N.R., Mickelson, D.M., 1994. Basal till fabric and deposition at Burroughs Glacier, Glacier Bay, Alaska. Bulletin of the Geological Society of America 106, 1552–1559.

Harris, C., 1991. Glacially deformed bedrock at Wylfa Head, Anglesey, North Wales. In: Forster, A., Culshaw, M.G., Cripps, J.C., Little, J.A., Moon, C.F. (Eds.), Quaternary Engineering Geology. Geological Society Engineering Geology Special Publication 7, London, pp. 135–142.

Hart, J.K., 1997. The relationship between drumlins and other forms of subglacial glaciotectonic deformation. Quaternary Science Reviews 16, 93-107.

Hart, J.K., Clayton, A.I., Martinez, K., Robson, B.A., 2018. Erosional and depositional subglacial streamlining processes at Skálafellsjökull, Iceland: an analogue for a new bedform continuum model, GFF, DOI: 10.1080/11035897.2018.1477830

Hicock, S.R., Goff, J.R., Lian, O.B., Little, E.C., 1996. On the interpretation of subglacial till fabric. Journal of Sedimentary Research 66, 928–934.

Hiemstra, J.F., Rijsdijk, K.F., 2003. Observing artificially induced strain: implications for subglacial deformation. Journal of Quaternary Science 18, 373–383.

Hooyer, T.S., Iverson, N.R., 2000. Diffusive mixing between shearing granular layers: constraints on bed deformation from till contacts. Journal of Glaciology 46, 641–651.

Hooyer, T.S., D. Cohen, N.R. Iverson, 2012. Control of glacial quarrying by bedrock joints. Geomorphology, 153, 91-101.

Ildefonse, B., Mancktelow, N.S., 1993. Deformation around rigid particles: the influence of slip at the particle/matrix interface. Tectonophysics 221, 345–359.

Ildefonse, B., Launeau, P., Bouchez, J.L., Fernandez, A., 1992. Effects of mechanical interactions on the development of preferred orientations: a two-dimensional experimental approach. Journal of Structural Geology 14, 73–83.

Iverson, N.R., Hooyer, T.S., Thomason, J.F., Graesch, M., Shumway, J.R. 2008. The experimental basis for interpreting particle and magnetic fabrics of sheared till. Earth Surface Processes and Landforms 33, 627-645.

Iverson, N.R., Baker, R.W., Hooyer, T.S., 1997. A ring-shear device for the study of till deformation tests on tills with contrasting clay contents. Quaternary Science Reviews 16, 1057–1066.

Iverson, N.R., Hooyer, T.S., Baker, R.W., 1998. Ring-shear studies of till deformation: Coulomb-plastic behaviour and distributed strain in glacier beds. Journal of Glaciology 44, 634–642.

Iverson, N. R., Hooyer, T. S., Hooke, R. L., 1996. A laboratory study of sediment deformation: stress heterogeneity and grain-size evolution. Annals of Glaciology 22, 167–175.

Johnson, M.D., Schomacker, A., Benediktsson, Í.Ö., Geiger, A.J., Ferguson, A., Ingólfsson, Ó., 2010. Active drumlin field revealed at the margin of Múlajökull, Iceland: a surge-type glacier. Geology 38, 943–946.

Jónsson, S.A., Benediktsson I.O., Ingolfsson, I., Schomacker, A., Bergsdottir, H.L., Jacobson, W.R., Linderson, H., 2016. Submarginal drumlin formation and late Holocene history of Fláajökull, southeast Iceland. Annals of Glaciology 57, 128-141.

Jónsson, S. A., Schomacker, A., Benediktsson, Í. Ö., Ingólfsson, Ó., Johnson. M. D., 2014. The drumlin field and the geomorphology of the Múlajökull surge type glacier, central Iceland. Geomorphology, 207, 213–220.

Kjær, K.H., Krüger, J., 1998. Does clast size influence fabric strength? Journal of Sedimentary Research 68, 746–749.

Krüger, J., 1979. Structures and textures in till indicating subglacial deposition. *Boreas* 8, 323-340.

Krüger, J., 1984. Clasts with stoss-lee form in lodgement tills: a discussion. Journal of Glaciology 30, 241–243.

Krüger, J., 1993. Moraine ridge formation along a stationary ice front in Iceland. Boreas 22, 101–109.

Krüger, J., 1994. Glacial processes, sediments, landforms and stratigraphy in the terminus region of Mýrdalsjökull, Iceland. *Folia Geographica Danica* **21**: 1–233.

Krüger, J., 1995. Origin, chronology and climatological significance of annual moraine ridges at Mýrdalsjökull, Iceland. *The Holocene* **5**: 420–427.

Krüger, J., 1996. Moraine ridges formed from subglacial frozen-on sediment slabs and their differentiation from push moraines. *Boreas* **25**: 57–63.

Larsen, N.K., Piotrowski, J.A., 2003. Fabric pattern in a basal till succession and its significance for reconstructing subglacial processes. Journal of Sedimentary Research 73, 725–734.

Larson, G.J., Lawson, D.E., Evenson, E.B., Alley, R.B., Knudsen, Ó., Lachniet, M.S., Goetz, S.L., 2006. Glaciohydraulic supercooling in former ice sheets? *Geomorphology* 75, 20-32.

Larson, G.J., Lawson, D.E., Evenson, E.B., Knudsen, O., Alley, R.B., Phanikumar, M.S., 2010. Origin of stratified basal ice in outlet glaciers of Vatnajökull and Öraefajökull, Iceland. *Boreas* 39, 457-470.

Larson, G.J., Menzies, J., Lawson, D.E., Evenson, E.B., Hopkins, N.R., 2016. Macro- and micro-sedimentology of a modern melt-out till – Matanuska Glacier, Alaska, USA. Boreas 45, 235–251.

Lawson, D.E., 1979a. Sedimentological analysis of the western terminus region of the Matanuska Glacier, Alaska. CRREL Report 79-9, Hanover, NH. .

Lawson, D.E., 1979b. A comparison of the pebble orientations in ice and deposits of the Matanuska Glacier, Alaska. Journal of Geology 87, 629–645.

Lawson, D.E., 1981. Distinguishing characteristics of diamictons at the margin of the Matanuska Glacier, Alaska. Annals of Glaciology 2, 78–84.

Lawson, D.E., Strasser, J.C., Evenson, E.B., Alley, R.B., Larson, G.J., Arcone, S.A., 1998. Glaciohydraulic supercooling a freeze-on mechanism to create stratified, debris-rich basal ice: I. Field evidence. *Journal of Glaciology* 44, 547-562.

Le Heron, D.P., Etienne, J.L., 2005. A complex subglacial clastic dyke swarm, Solheimajökull, southern Iceland. Sedimentary Geology 181, 25–37.

Li, D., Yi, C., Ma, B., Wang, P., Ma, C., Cheng, G., 2006. Fabric analysis of till clasts in the upper Urumqi River, Tian Shan, China. Quaternary International 154–155, 19–25.

Lliboutry, L., 1994. Monolithologic erosion of hard beds by temperate glaciers. *Journal of Glaciology* 40, 433–450.

Lukas, S., Benn, D.I., Boston, C.M., Brook, M., Coray, S., Evans, D.J.A., Graf, A., Kellerer-Pirklbauer, A., Kirkbride, M.P., Krabbendam, M., Lovell, H., Machiedo, M., Mills, S.C., Nye, K., Reinardy, B.T.I., Ross, F.H., Signer, M., 2013. Clast shape analysis and clast transport paths in glacial environments: a critical review of methods and the role of lithology. Earth-Science Reviews 121, 96-116.

MacClintock, P., Dreimanis, A., 1964. Reorientation of till fabric by overriding glacier in the St. Lawrence Valley. American Journal of Science 262, 133–142.

MacGregor K.R., Anderson R.S., Waddington E.D., 2009. Numerical modeling of glacial erosion and headwall processes in alpine valleys. *Geomorphology* 103, 189–204.

Maizels, J.K., 1989. Sedimentology, palaeoflow dynamics and flood history of jökulhlaup deposits: palaeohydrology of Holocene sediment sequences in southern Iceland sandur deposits. Journal of Sedimentary Petrology 59, 204-223.

Maizels, J.K., 1993. Lithofacies variations within sandur deposits: the role of runoff regime, flow dynamics and sediment supply characteristics. *Sedimentary Geology* 85, 299–325.

Maizels, J.K., 1995. Sediments and landforms of modern proglacial terrestrial environments. In: Menzies J. (ed.), Modern Glacial Environments. Butterworth-Heinemann, Oxford, 365-416.

March, A., 1932. Mathematische Theorie der Regelung nach der Korngestalt bei affiner Deformation. Zeitschrift fur Kristallographie 81, 285–297.

Marren, P.M., 2005. Magnitude and frequency in proglacial rivers: a geomorphological and sedimentological perspective. *Earth Science Reviews* 70, 203-251.

Matthews, J.A., Petch, J.R., 1982. Within-valley asymmetry and related problems of Neoglacial lateral moraine development at certain Jotunheimen glaciers, southern Norway. *Boreas* 11, 225–247.

McCracken, R.G., Iverson, N.R. Benediktsson, Í.Ö. Schomacker, A., Zoet, L.K., Johnson, M.D., Hooyer, T.S., Ingólfsson, Ó., 2016. Origin of the active drumlin field at Múlajökull, Iceland: New insights from till shear and consolidation patterns. Quaternary Science Reviews, 148, 243-260.

Mickelson, D.M., 1973. Nature and rate of basal till deposition in a stagnating ice mass, Burroughs Glacier, Alaska. Arctic and Alpine Research 5, 17–27.

Phillips, E.R., Evans, D.J.A., van der Meer, J.J.M., Lee, J.R., 2018. Potential triggers for till liquefaction during glacier flow by "soft-bed sliding". Quaternary Science Reviews 181, 123-143..

Powers, M.C., 1953. A new roundness scale for sedimentary particles. *Journal of Sedimentary Petrology* 23, 117–19.

Price, R.J., 1969. Moraines, sandar, kames and eskers near Breiðamerkurjökull, Iceland. *Transactions of the Institute of British Geographers* 46, 17–43.

Price, R.J., 1970. Moraines at Fjallsjökull, Iceland. *Arctic and Alpine Research* 2, 27-42.

Ramsden, J., Westgate, J.A., 1971. Evidence for reorientation of a till fabric in the Edmonton area, Alberta. In: Till-a symposium. R.P. Goldthwait (Ed.). Ohio State University Press, Columbus, OH, pp. 335–344.

Rijsdijk, K.F., Owen, G., Warren, W.P., McCarroll, D., van der Meer, J.J.M., 1999. Clastic dykes in over-consolidated tills: evidence for subglacial hydrofracturing at Killiney Bay, eastern Ireland. Sedimentary Geology 129, 111–126.

Roberts, M.J., Tweed, F.S., Russell, A.J., Knudsen, Ó., Lawson, D.E., Larson, G.J., Evenson, E.B., Björnsson, H., 2002. Glaciohydraulic supercooling in Iceland. *Geology* 30, 439-442.

Ronnert, L., Mickelson, D.M., 1992. High porosity of basal till at Burroughs Glacier, southeastern Alaska. Geology 20, 849–852.

Rose, J., 1989. Glacier stress patterns and sediment transfer associated with the formation of superimposed flutes. Sedimentary Geology 62, 151–176.

Rose, J., 1992. Boulder clusters in glacial flutes. Geomorphology 6, 51–58.

Russell, A.J., Marren, P.M., 1999. Proglacial fluvial sedimentary sequences in Greenland and Iceland: a case study from active proglacial environments subject to jokulhlaups. In, Jones A.P., Tucker M.E., Hart J.K. (Eds.), *The Description and Analysis of Quaternary Stratigraphic Field Sections*. Quaternary Research Association Technical Guide 7, 171-208.

Russell, A.J., Knight, P.G., van Dijk, T.A.G.P., 2001. Glacier surging as a control on the development of proglacial, fluvial landforms and deposits, Skeiðarársandur, Iceland. *Global and Planetary Change* 28, 163-174.

Russell, A.J., Roberts, M.J., Fay, H., Marren, P.M., Cassidy, N.J., Tweed, F.S., Harris, T., 2006. Icelandic jökulhlaup impacts: implications for ice-sheet hydrology, sediment transfer and geomorphology. *Geomorphology* 75, 33-64.

Sharp, M.J., 1982. Modification of clasts in lodgement tills by glacial erosion. Journal of Glaciology 28, 475–481.

Sharp, M.J., 1984. Annual moraine ridges at Skalafellsjökull, southeast Iceland. *Journal of Glaciology* 30, 82-93.

Sommerville, A., 1997. The Late Quaternary History of Terra Nova National Park and Vicinity, Northeast Newfoundland. Unpublished M.Sc. thesis, Department of Geography, Memorial University of Newfoundland.

Spedding, N., Evans, D.J.A., 2002. Sediments and landforms at Kviarjokull, south-east Iceland: a reappraisal of the glaciated valley landsystem. Sedimentary Geology 149, 21–42.

Thomason, J.F., Iverson, N.R., 2006. Microfabric and microshear evolution in deformed till. Quaternary Science Reviews 25, 1027–1038.

Þórarinsson, S., 1939. Vatnajökull. The scientific results of the Swedish-Icelandic investigations 1936-37-38. Chapter IX. The ice dammed lakes of Iceland with particular reference to their values as indicators of glacier oscillations. *Geografiska Annaler* 21, 216–242.

Tulaczyk, S., 1999. Ice sliding over weak, fine-grained tills: dependence of ice-till interactions on till granulometry. In: Mickelson, D.M., Attig, J.W. (Eds.), Glacial Processes: Past and Present. Geological Society of America, Special Paper, vol. 337, pp. 159–177.

van der Meer, J.J.M., Kjær, K.H., Krüger, J., 1999. Subglacial water escape structures and till structure, Slettjokull, Iceland. Journal of Quaternary Science 14, 191–205.

van der Meer, J.J.M., Kjær, K.H., Krüger, J., Rabassa, J., Kilfeather, A.A., 2009. Under pressure: clastic dykes in glacial settings. Quaternary Science Reviews 28, 708–720.

Figure captions

Figure 1: Location map, showing the seven glacier forelands where sedimentological analyses were undertaken. The specific sampling sites are arrowed.

Figure 2: Existing clast form co-variance plots used for comparisons with data in this study: a) "Type 1" co-variance plot of Lukas et al. (2013) for low anisotropy basalt clast lithologies; b) sub-Type 1 co-variance plot for Fláajökull (Lukas et al. 2013) for settings with tills that have inherited glacifluvial roundness signatures; c) sub-Type 1 co-variance plot (Evans et al. 2016b) for settings with tills that have ingested freshly plucked fragments from bedrock outcrops.

Figure 3: Templates for analytical plots of clast fabric strength: a) clast fabric shape ternary plot (Benn, 1994) containing envelopes of fabric shapes for lodged clasts, subglacial traction tills (Icelandic upper A and lower B horizons) and glacitectonites, as well as the influence trends for consolidation (black arrow) and shear strain (grey arrow) proposed by Iverson et al. (2008); b) modality-isotropy plot (after Hicock et al., 1996; Evans et al., 2007) containing a sample envelope for lodged clasts (dotted line) and a shaded area representing that part of the graph in which stronger modality and isotropy in previously reported subglacial traction tills or glacitectonites reflects an increasing lodgement component (un, unimodal; su, spread unimodal; bi, bi-modal; sb, spread bi-modal; mm, multi-modal).

Figure 4: Clast form data for the scree and glacifluvial control samples: a) ternary clast form diagrams and histograms of roundness with values for C_{40}, RA, RWR and average roundness (AvR). Abbreviations: VA= very angular; A= angular; SA= sub angular; SR= sub rounded; R= rounded; WR= well rounded; b) co variance plots for the scree and glacifluvial control samples (note that these samples were employed by Lukas et al. (2013) to define a sub-Type I co-variance plot, represented here as Figure 2b).

Figure 5: Google Earth image of the Fláajökull foreland annotated with the clast form sampling transects.

Figure 6: Clast form data for the Fláajökull moraines: a) down-glacier trends in clast form criteria based upon the sampling transect along the eastern lateral moraine (L1-34). Two trend lines have been calculated for linear (red) and second order polynomial (black) regression; b) covariance plots for the eastern lateral moraine clast form data (L1-34); c) covariance plots for the LIA maximum frontal moraine clast form data (F1-6); d) down-latero-frontal moraine trends in clast form criteria based upon the combined sampling transects, with distance being measured along the eastern lateral moraine and across the LIA maximum frontal moraine (L1-34 & F1-6). Two trend lines have been calculated for linear (red) and polynomial (black) regression; e) covariance plots for the mid-1990s readvance moraine clast form data (P1-13) with bracketed values for R2 and Pearson's r representing calculations on the dataset excluding site P1.

Figure 7: The Fláajökull study site: a) ground photograph showing the main lithofacies; b) vertical profile log and clast fabric and form data.

Figure 8: The Fjallsjökull study site: a) photographs of main exposure, showing the details of a vertical clastic dyke containing laminated silts and clays and a branching base, the stack of capping diamictons, and details (i & ii) of the nature of their internal fissile to crumbly structure; b) scaled section sketch and vertical profile logs, together with and clast fabric and form data. Sediments bracketed and labelled GT are classified as glacitectonite.

Figure 9: The Heinabergsjökull study site, showing ground photograph and vertical profile log together with clast fabrtic and form data.

Figure 10: The Skalafellsjökull study sites: a) lower foreland site, showing vertical profile log and clast fabric and form data; b) glacially abraded bedrock/patchy till site, showing ground photographs and clast fabric and form data, together with fabric for adjacent lodged boulders; c) glacially abraded bedrock/crag-and-tail fluting site, showing ground photograph and clast fabric and form data, together with fabric for adjacent lodged boulders; d) clast macrofabric shape ternary plot containing the data (in b & c) from the two glacially abraded bedrock sites; e) covariance plots for the data (in b & c) from the two glacially abraded bedrock sites.

Figure 11: The Skaftafellsjökull study sites: a) section SK1, showing vertical profile log and photographs of the diamictons together with clast macrofabric and form data; b) section SK2, showing photomontage, vertical profile log and detailed photograph of the changing structure of the capping diamicton, together with clast macrofabric and form data; c) section SK3, showing vertical profile log and detailed photographs of the structures in the upper and lower diamictons, together with clast macrofabric data; d) section SK4, showing vertical profile log and detailed photographs of the structures in the diamictons, together with clast macrofabric data; e) section SK5, showing ground photograph of the landform and stratigraphic exposure, vertical profile log and detailed photographs of the structures in the upper diamicton, together with clast macrofabric data; f) section SK6, showing ground photograph of the landform and stratigraphic exposure and detailed photographs of the structures in the upper diamictons, together with clast macrofabric and form data; g) covariance plots of the clast form data from all the Skaftafellsjökull study sites; h) clast macrofabric shape ternary plot containing all data from the Skaftafellsjökull study sites.

Figure 12: The Falljökull study site: a) vertical profile log, photographs showing details of the lower and middle diamictons and clast macrofabric data; b) ground photograph of lodged and striated boulders.

Figure 13: The east Breiðamerkurjökull abraded bedrock and patchy till site: a) photograph of till section over bedrock with vertical and horizontal fracture infills, together with clast macrofabric and form data; b) photograph of patchy till veneer over bedrock with vertical fracture infills, together with clast form data; c) covariance plots for the data (in a & b) from the two glacially abraded bedrock and patchy till sites.

Figure 14: Aggregate plots of all the data reported in this study: a) covariance plots for all clast form data; b) ternary plot for all clast macrofabric shape data; c) modality/isotropy plot for all A axes clast macrofabrics; d) modality/isotropy plot for all A/B plane clast macrofabrics, using the envelopes for A/B plane data from Evans et al. (2007).

Figure 15: Idealized sketches of the three main stratigraphic architectural end members and the typical range of associated clast macrofabric and form data, including: a) thin and patchy tills over bedrock erosional landforms; b) push moraine complexes and single push moraines; and c) overridden/drumlinized moraines or outwash fans.

Table 1: Sedimentological data (where available) relevant to inferred till genesis with data from previous studies in SE Iceland unless otherwise stated.

	This study								Previous studies*							
Sediment	**C_{40}%**	**RA %**	**RWR %**	**Av. R**	**Striae %**	**S1 A**	**S1 A/B**	**Thick-ness (m)+**	**C_{40}%**	**RA %**	**RWR %**	**Av. R**	**Striae %**	**S1 A**	**S1 A/B**	**Thick-ness (m)+**
Upper tills on drift (A horizons)	16-27	13-20	0-10	1.97-2.24	20-46	0.54-0.63	0.42	0.35-0.50	32	0	8	2.75	32	0.48-0.56	0.46-0.52	0.45-1.00
Lower tills on drift (B horizons)	12-28	14-33	0-12	1.80-2.44	14-42	0.55-0.70	0.42	0.10-0.65	14-28	0-8	13-18	2.88-2.92	0-28	0.61-0.72	0.47-0.67	0.30-0.65
Upper tills on bedrock (A horizons)	10-40	0-17	0-2	2.3-2.4	10-25	0.46-0.53		0.15-0.60								
Lower tills on bedrock (B horizons)	24-68	26-36	0-1	1.94-2.00	6-15	0.47-0.79		0.30-0.75								
Tills (undefined/ overprinted) on drift	0-34	0-17	4-26	2.13-3.10	8-40	0.44-0.62	0.41-0.51	0.35-1.40	6-38	0-10	3-35	2.64-3.26	14-70	0.45-0.79	0.46-0.67	0.40-2.00
Fluted tills	13-27	10-16	10-11	1.97 2.24	20-27	0.51-0.63	0.42	0.20-1.20						0.60-0.72		
Lodged boulder prow/incipient fluting														0.37-0.63		0.30-0.40
Crag-&-tail fluting tills	20-30	14-44	4-8	1.72-2.20	6-25	0.54-0.64		0.80								
Glacitectonite	18-30	2-12	0-26	2.40-2.76	12-20	0.48-0.52	0.40-0.54	0.20-1.50	2-30	0	20-32	2.50-3.25	0-5		0.43-0.68	0.60-1.20
Lodged clasts	16	0	1	3.00	90	0.89		N/A	8-28	8-16	10-31	2.24-2.92	14-26	0.83-0.94		N/A
Fracture infills	54-62	10-36	0	1.84-2.08	0-5			N/A								N/A
Push moraine tills	13-33	7-20	3-13	1.53-2.57	8-46	0.48-0.67	0.66	0.20-0.75							0.38-0.58	0.2-1.5
Scree (control)	44-64	90-98	0	0.80-0.94	0	N/A	N/A	N/A								
Glacifluvial (control)	36-54	0	22-36	3.26-3.34	0-1	N/A	N/A	N/A								

*Includes: Sharp (1982), Dowdeswell et al. (1985), Dowdeswell & Sharp (1986), Benn (1995), Evans (2000), Evans & Twigg (2002), Evans & Hiemstra (2005), Jónsson et al. (2016). Boulder prow data from Bruarjökull foreland (Evans 2018). Ranges indicate multiple samples and single figures indicate one sample.

+ Thickness measurements relate to individual till units.

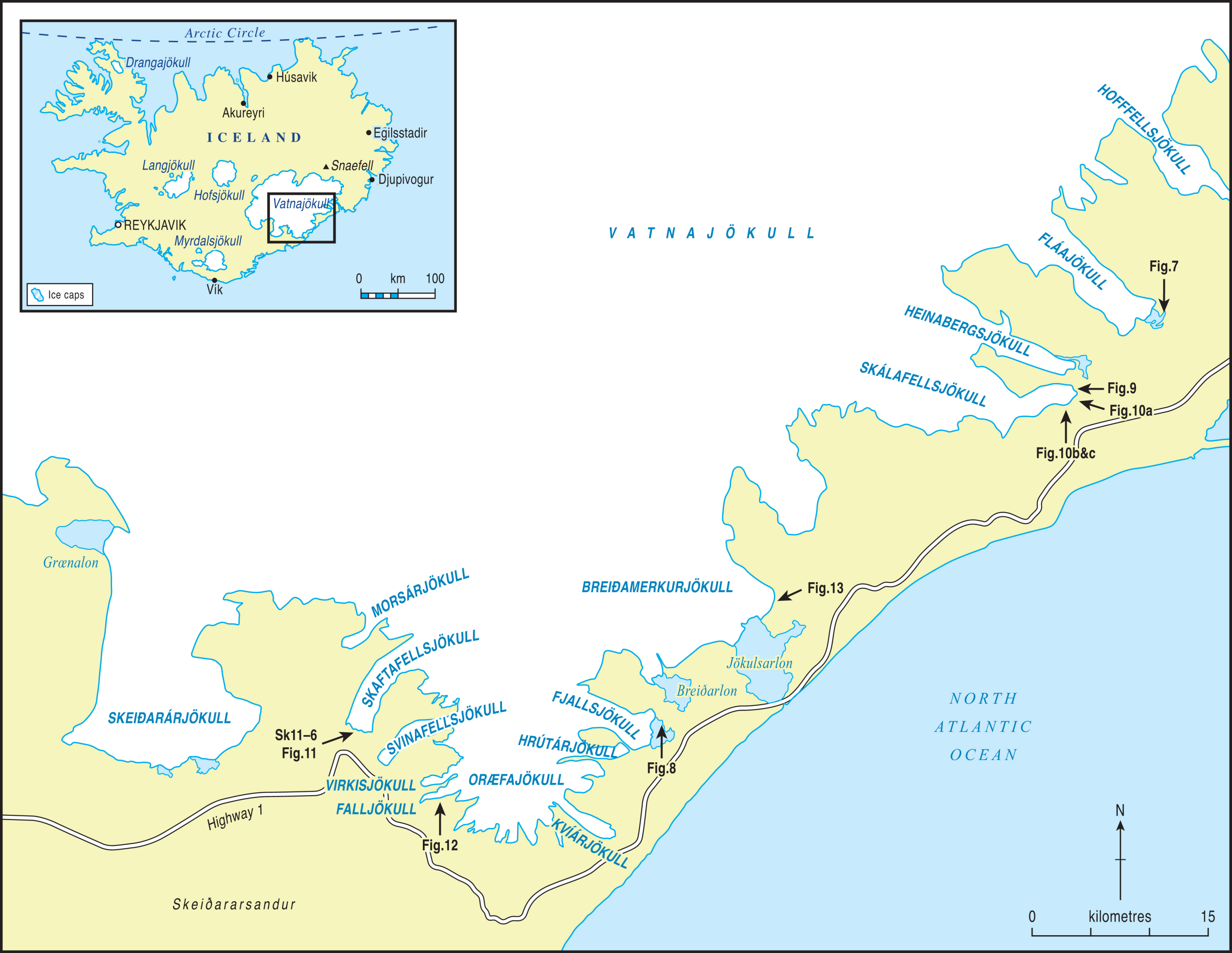

Arctic Circle
Drangajökull
Húsavik
Akureyri
ICELAND
Egilsstadir
Langjökull
Snaefell
Djupivogur
Hofsjökull
Vatnajökull
REYKJAVIK
Myrdalsjökull
Vík
Ice caps
0
km
100
VATNAJÖKULL
HOFFELLSJÖKULL
FLÁAJÖKULL
Fig.7
HEINABERGSJÖKULL
SKÁLAFELLSJÖKULL
Fig.9
Fig.10a
Fig.10b&c
Grænalon
BREIÐAMERKURJÖKULL
Fig.13
MORSÁRJÖKULL
SKAFTAFELLSJÖKULL
Jökulsarlon
Breiðarlon
SVINAFELLSJÖKULL
FJALLSJÖKULL
SKEIÐARÁRJÖKULL
Sk11–6
Fig.11
HRÚTÁRJÖKULL
Fig.8
NORTH
ATLANTIC
OCEAN
VIRKISJÖKULL
ORÆFAJÖKULL
FALLJÖKULL
Highway 1
Fig.12
KVÍÁRJÖKULL
N
Skeiðararsandur
0
kilometres
15

a) Type I (Lukas et al. 2013)

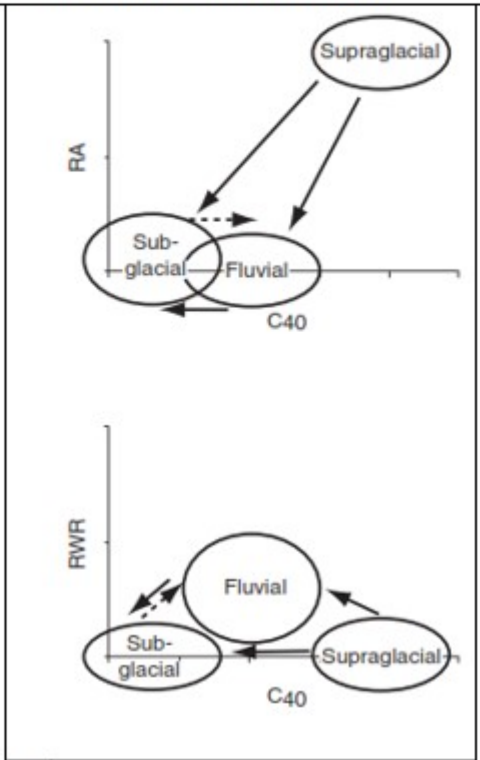

Environment	Maritime, temperate *mountain glaciers* (corrie, valley and ice cap outlet glaciers)
Clast shape	**Angularity**/roundness (**RA and**/or RWR) **and** platiness (C_{40}-index) are both nearly equally-strong discriminators
Lithology	Mainly low-anisotropy ('massive'), e.g. ortho-gneiss, eclogite
Processes	Dominant subglacial erosion and transport; limited supra-/extraglacial and fluvial input to subglacial system; fluvial reworking of subglacial sediment minimal

b) sub-Type I/Fláajökull (Lukas et al. 2013)

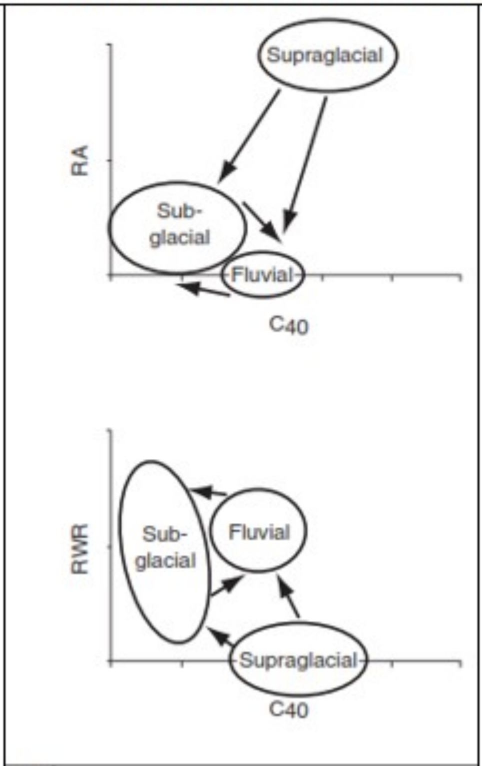

Environment	Maritime, temperate *mountain glacier* (ice cap outlet glacier)
Clast shape	Angularity/roundness (RA and RWR) are good discriminators; platiness (C_{40}-index) is less useful, because of fairly 'blocky' input
Lithology	Basalt (low-anisotropy, 'massive')
Processes	Dominant subglacial and fluvial erosion and transport; limited supraglacial input to subglacial system, but mixing of fluvially and subglacially reworked material pronounced

c) sub-Type I/with plucking (Evans et al. 2016b)

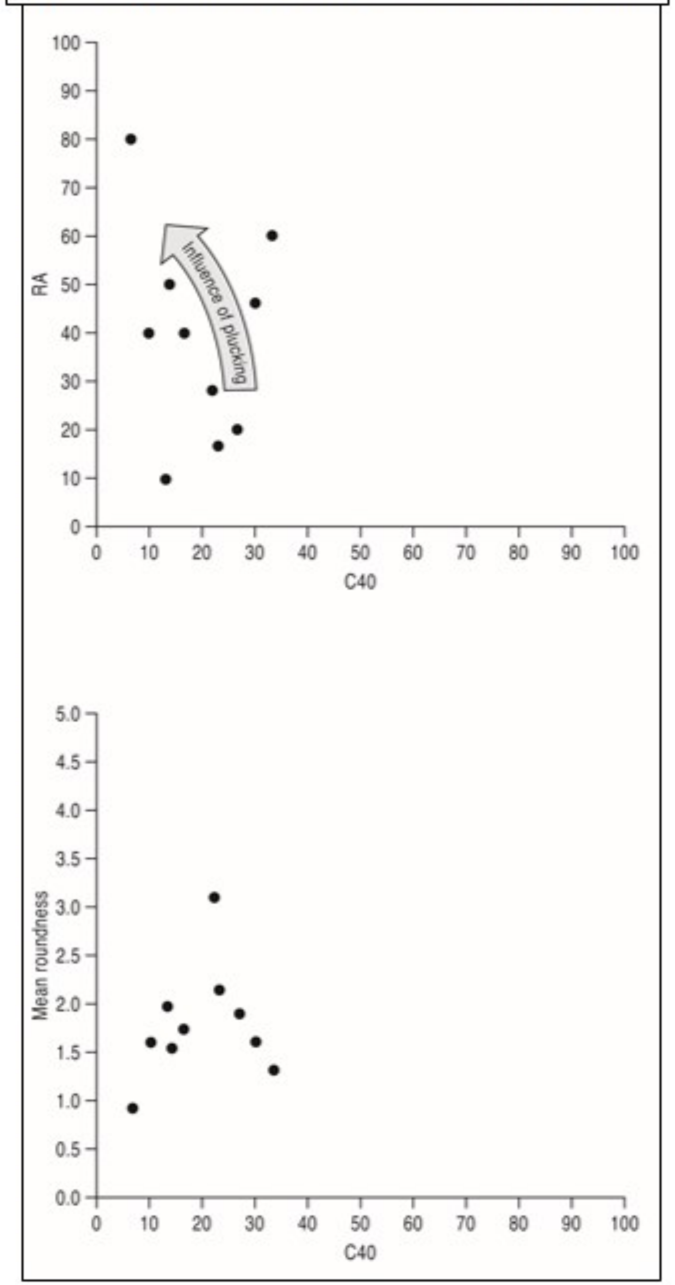

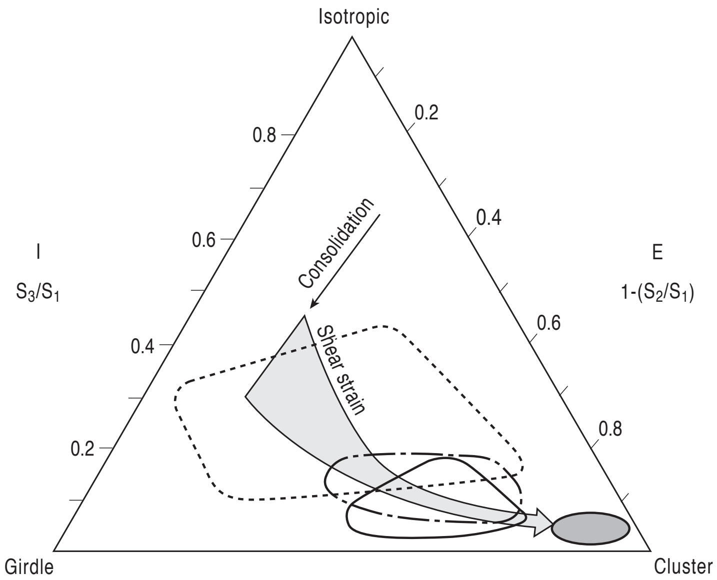

Breiðamerkurjökull upper till
(Benn & Evans, 1996)

Breiðamerkurjökull lower till
(Benn & Evans, 1996)

Glaciotectonite (Benn & Evans, 1996)

Lodged clasts (Evans and Hiemstra 2005)

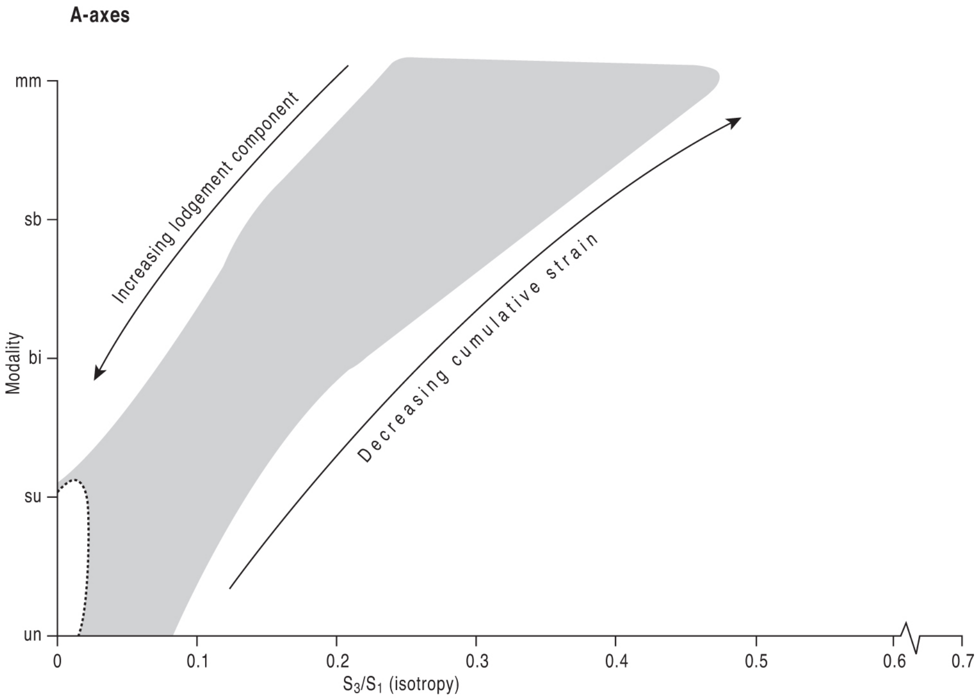
A-axes
mm
sb
bi
su
un
Modality
0
0.1
0.2
0.3
0.4
0.5
0.6
0.7
S_3/S_1 (isotropy)
Increasing lodgement component
Decreasing cumulative strain

FLÁAJÖKULL CLAST FORM CONTROL SAMPLES

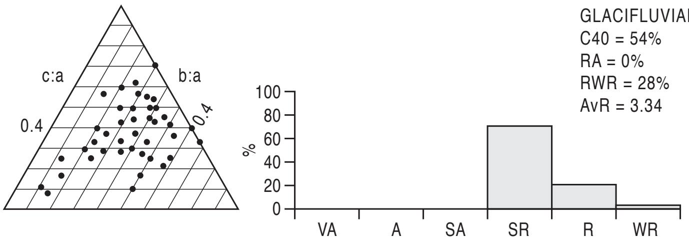

GLACIFLUVIAL 1
C40 = 54%
RA = 0%
RWR = 28%
AvR = 3.34

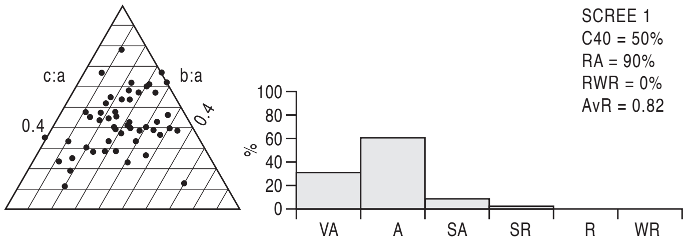

SCREE 1
C40 = 50%
RA = 90%
RWR = 0%
AvR = 0.82

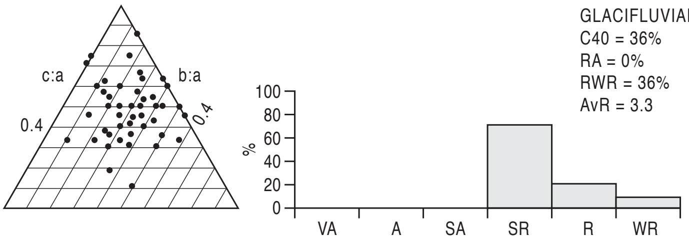

GLACIFLUVIAL 2
C40 = 36%
RA = 0%
RWR = 36%
AvR = 3.3

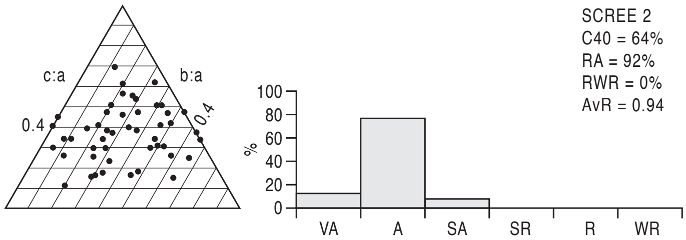

SCREE 2
C40 = 64%
RA = 92%
RWR = 0%
AvR = 0.94

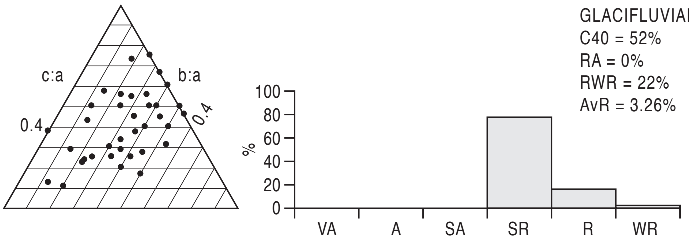

GLACIFLUVIAL 3
C40 = 52%
RA = 0%
RWR = 22%
AvR = 3.26%

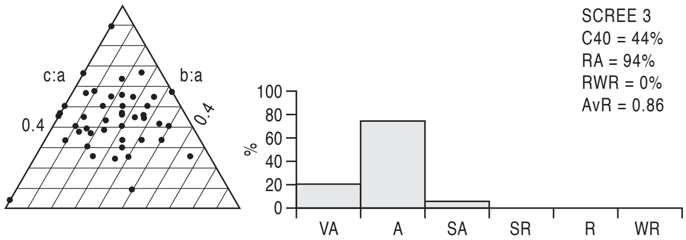

SCREE 3
C40 = 44%
RA = 94%
RWR = 0%
AvR = 0.86

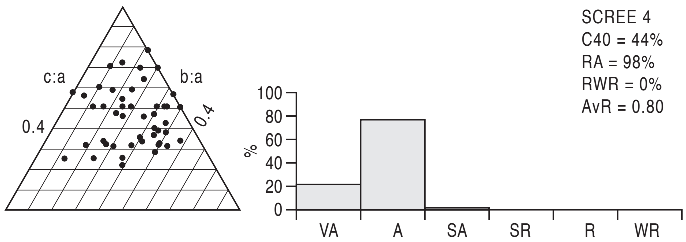

SCREE 4
C40 = 44%
RA = 98%
RWR = 0%
AvR = 0.80

Fláajökull clast form control samples (co-variance)

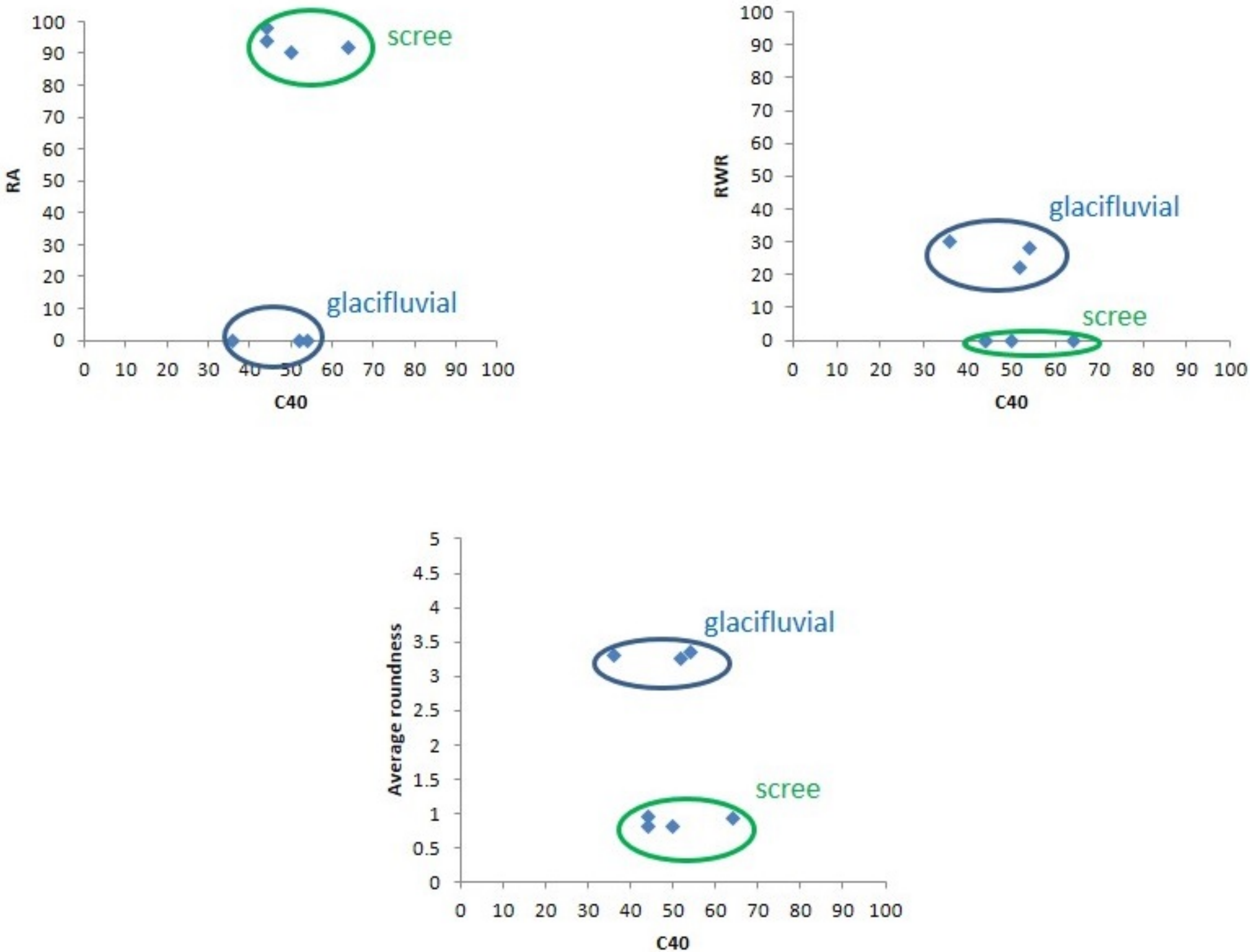


L1
L34
F1
P1
F2
section
F3
F4
P13
F5
F6


L1
L34
F1
P1
F2
section
F3
P13
F4
F5
F6

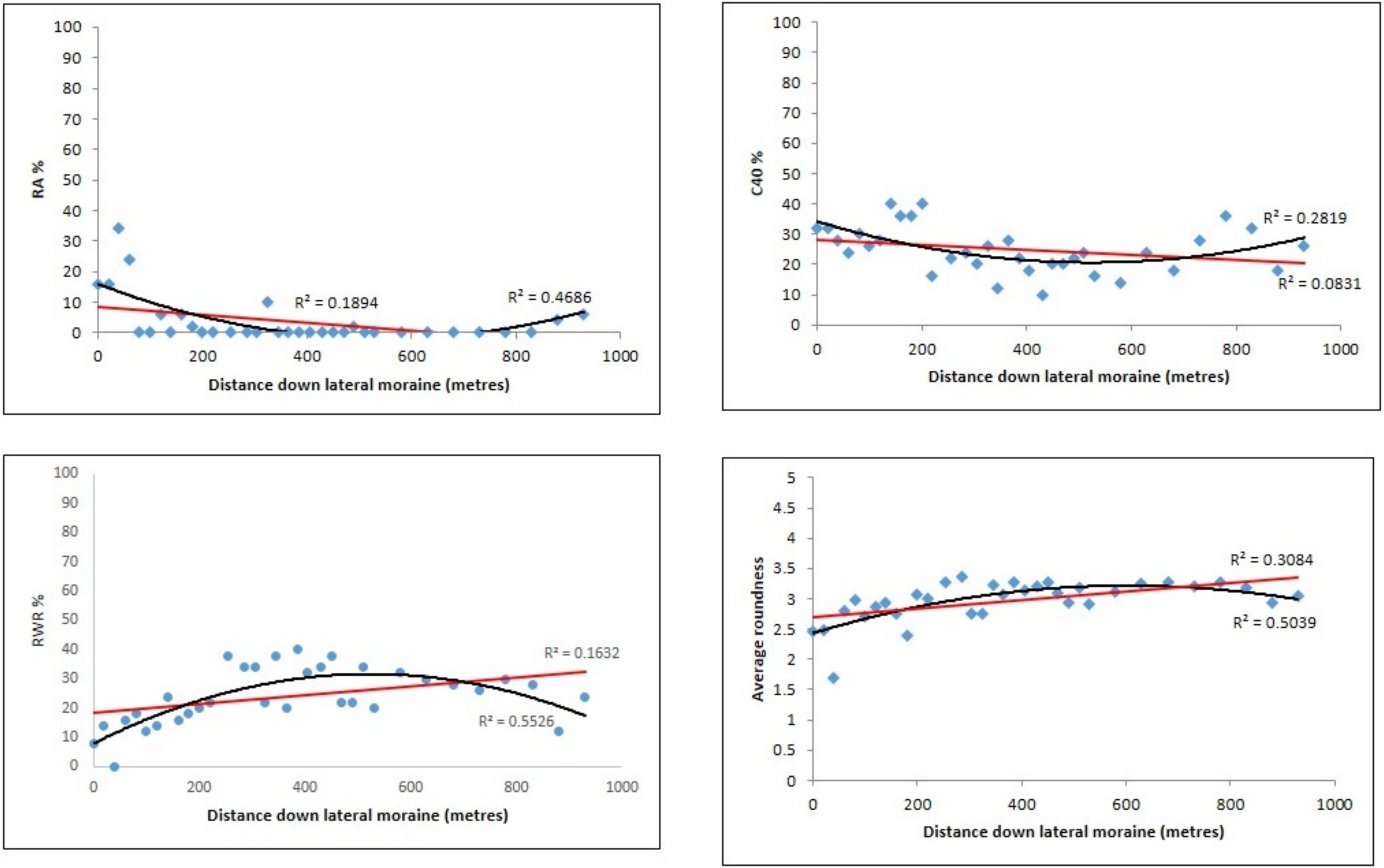

RA %
R² = 0.1894
R² = 0.4686
Distance down lateral moraine (metres)
C40 %
R² = 0.2819
R² = 0.0831
Distance down lateral moraine (metres)
RWR %
R² = 0.1632
R² = 0.5526
Distance down lateral moraine (metres)
Average roundness
R² = 0.3084
R² = 0.5039
Distance down lateral moraine (metres)

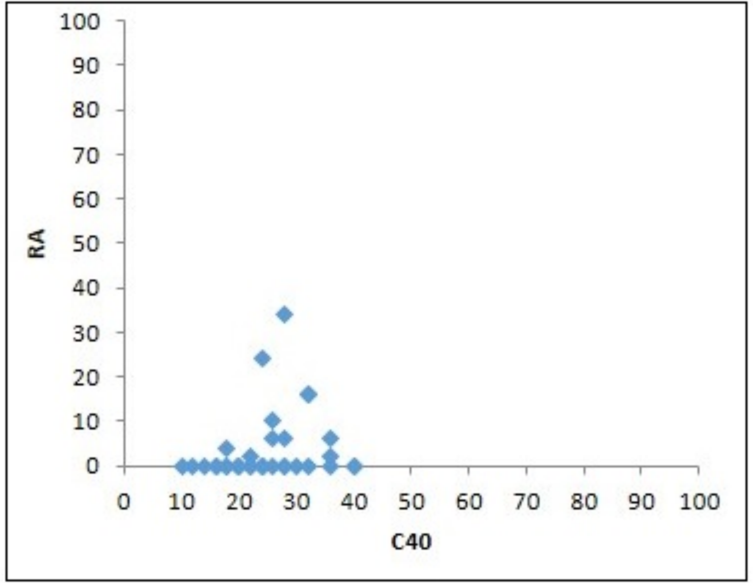
RA
C40
0
10
20
30
40
50
60
70
80
90
100

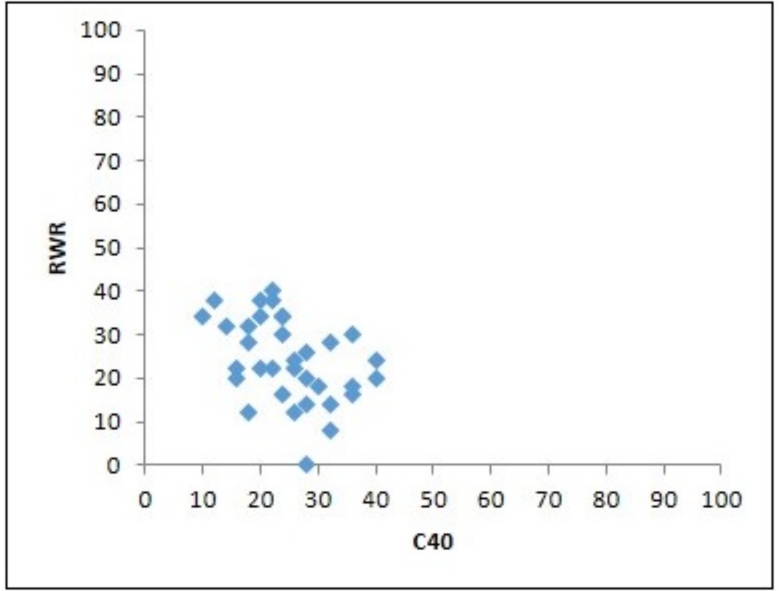
RWR
C40
0
10
20
30
40
50
60
70
80
90
100

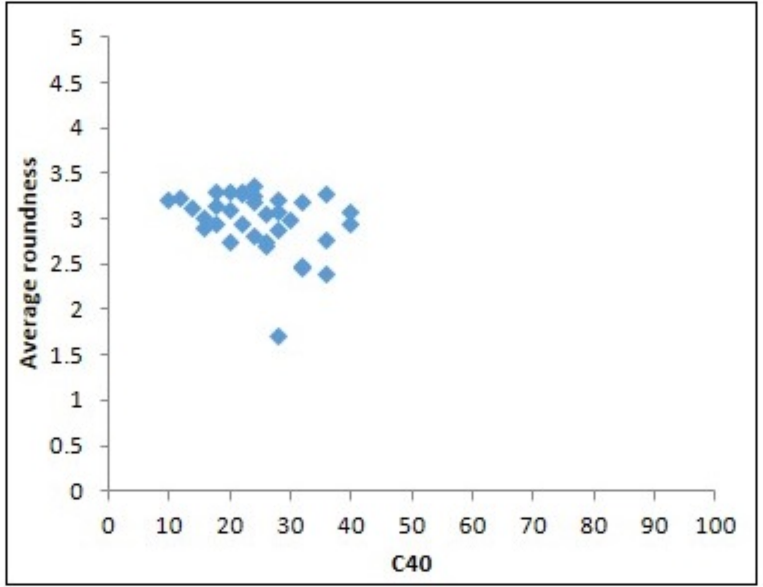
Average roundness
C40
0
0.5
1
1.5
2
2.5
3
3.5
4
4.5
5
0
10
20
30
40
50
60
70
80
90
100

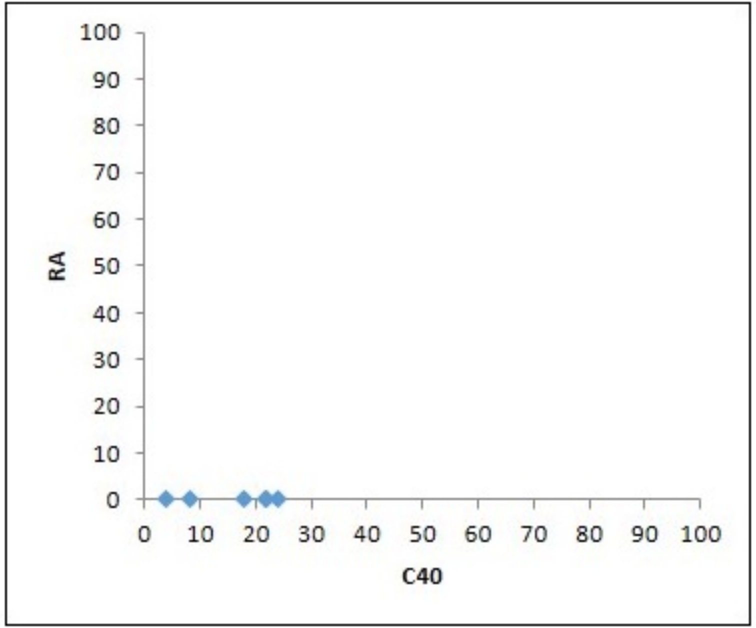
RA
C40
0
10
20
30
40
50
60
70
80
90
100

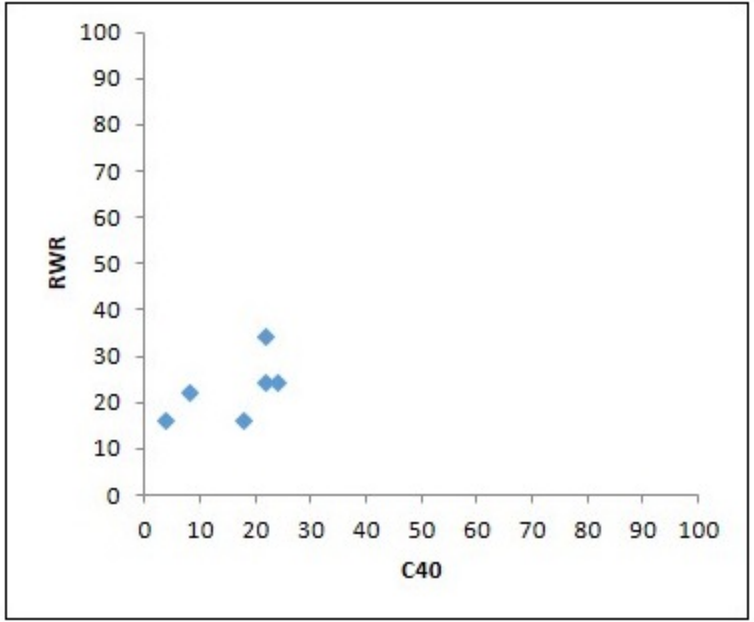
RWR
C40
0
10
20
30
40
50
60
70
80
90
100

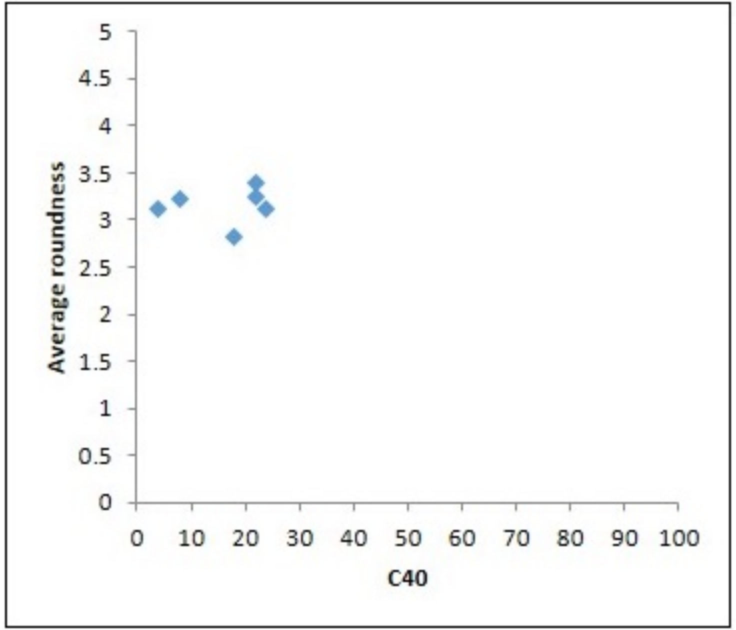
Average roundness
C40
0
0.5
1
1.5
2
2.5
3
3.5
4
4.5
5
0
10
20
30
40
50
60
70
80
90
100

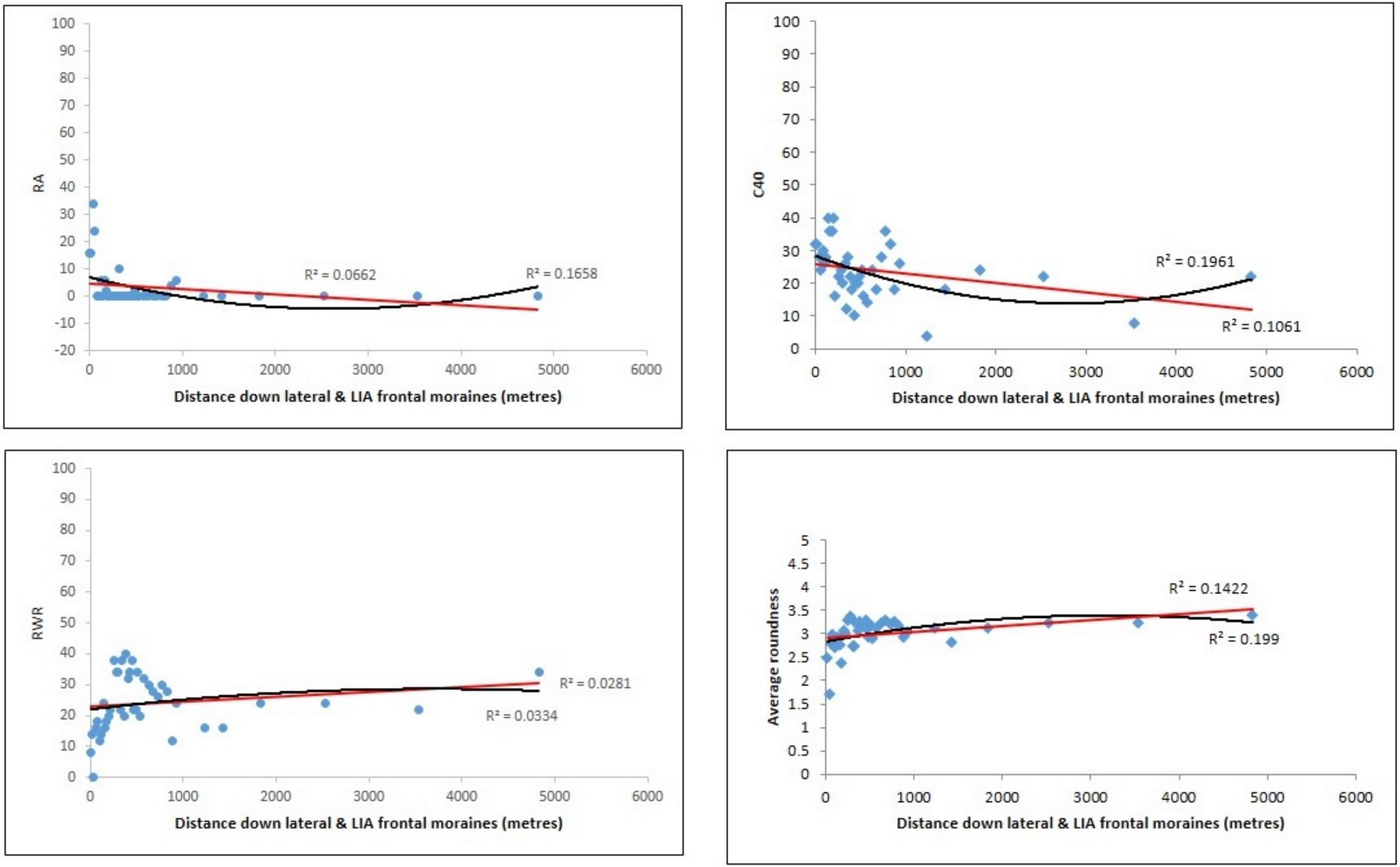
RA
R² = 0.0662
R² = 0.1658
Distance down lateral & LIA frontal moraines (metres)
C40
R² = 0.1961
R² = 0.1061
Distance down lateral & LIA frontal moraines (metres)
RWR
R² = 0.0281
R² = 0.0334
Distance down lateral & LIA frontal moraines (metres)
Average roundness
R² = 0.1422
R² = 0.199
Distance down lateral & LIA frontal moraines (metres)

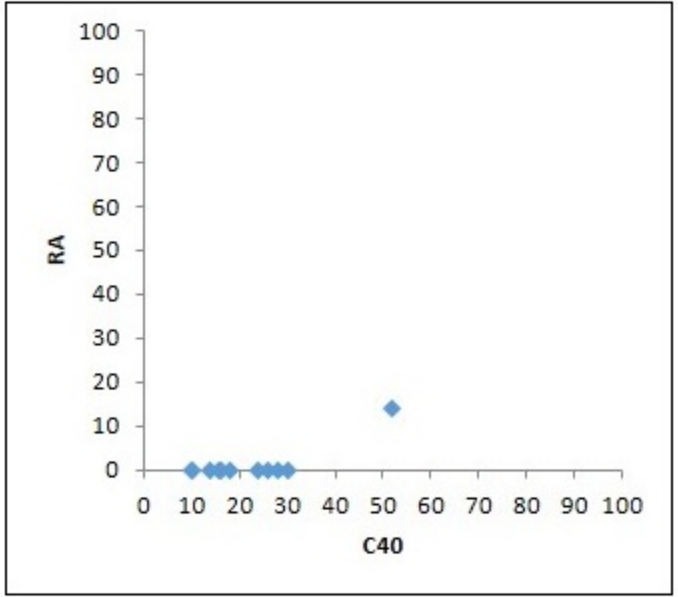
RA
C40

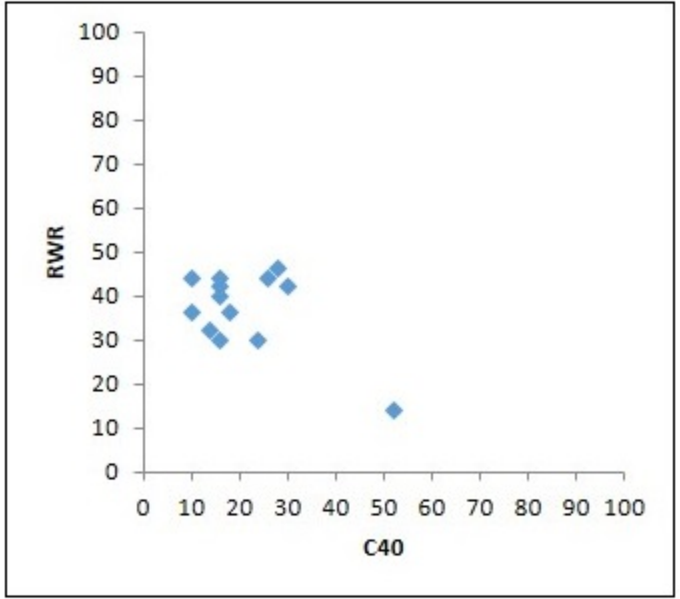
RWR
C40

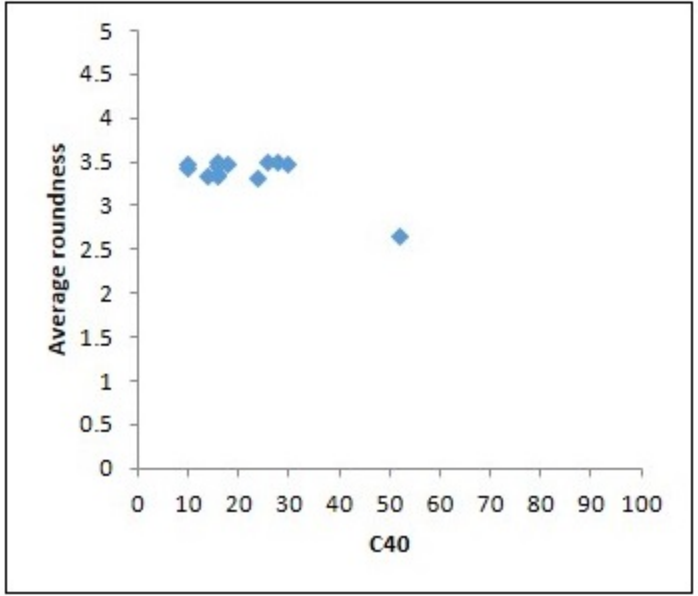
Average roundness
C40

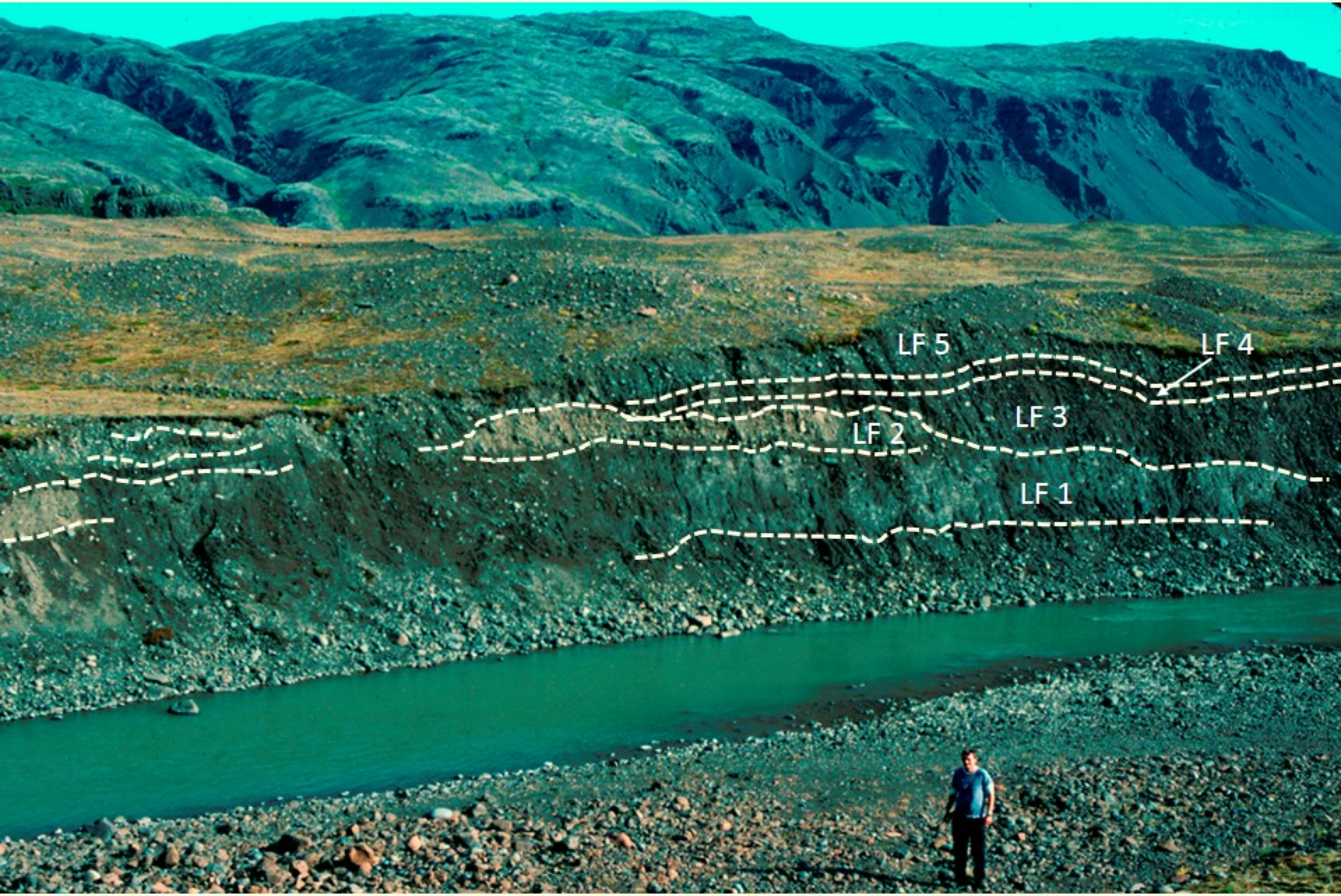
LF 5
LF 4
LF 3
LF 2
LF 1

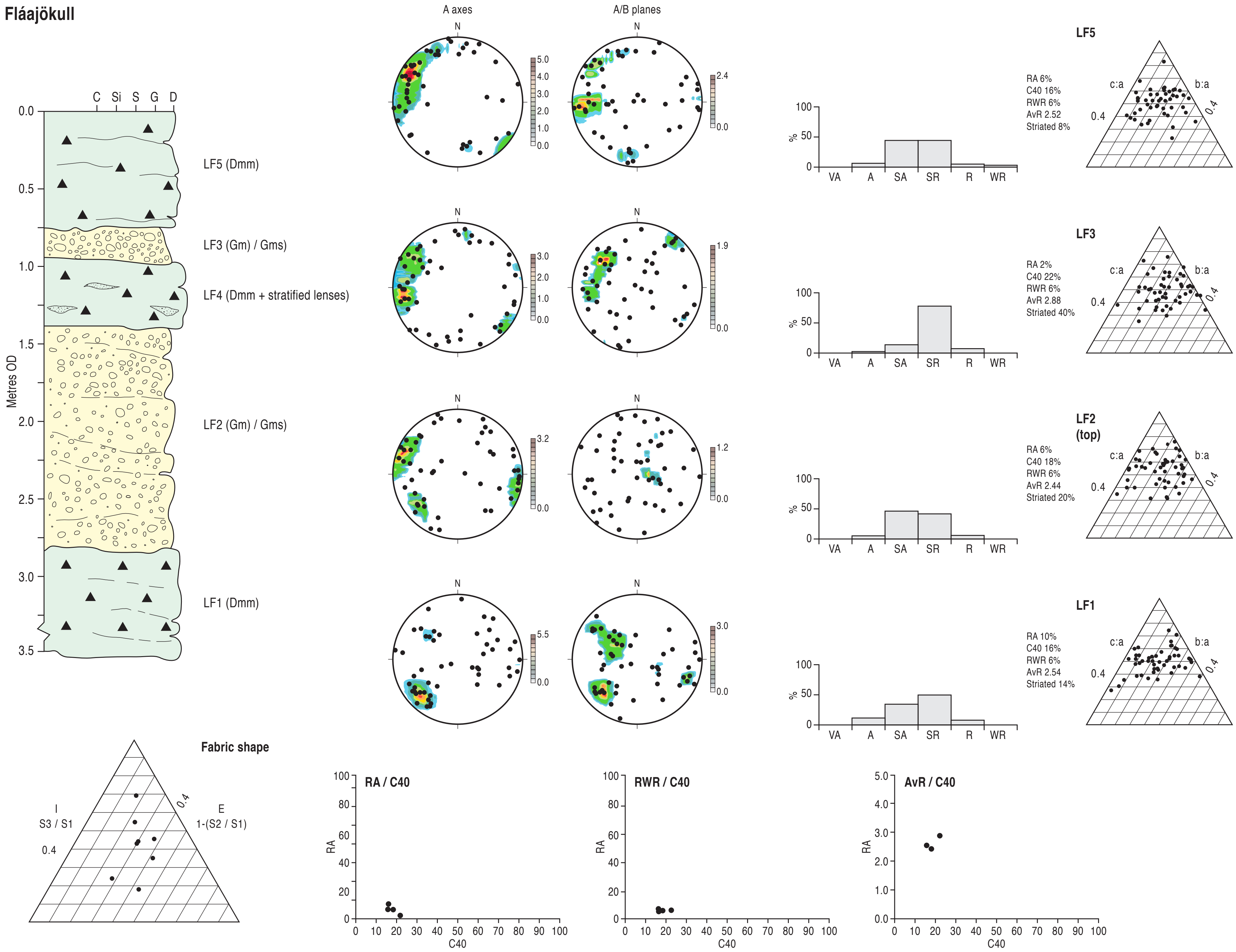

Fláajökull
A axes
A/B planes
N
C Si S G D
Metres OD
0.0
0.5
1.0
1.5
2.0
2.5
3.0
3.5
LF5 (Dmm)
LF3 (Gm) / Gms)
LF4 (Dmm + stratified lenses)
LF2 (Gm) / Gms)
LF1 (Dmm)
LF5
RA 6%
C40 16%
RWR 6%
AvR 2.52
Striated 8%
LF3
RA 2%
C40 22%
RWR 6%
AvR 2.88
Striated 40%
LF2 (top)
RA 6%
C40 18%
RWR 6%
AvR 2.44
Striated 20%
LF1
RA 10%
C40 16%
RWR 6%
AvR 2.54
Striated 14%
c:a
b:a
0.4
%
VA A SA SR R WR
Fabric shape
I
S3 / S1
E
1-(S2 / S1)
RA / C40
RWR / C40
AvR / C40
RA
C40

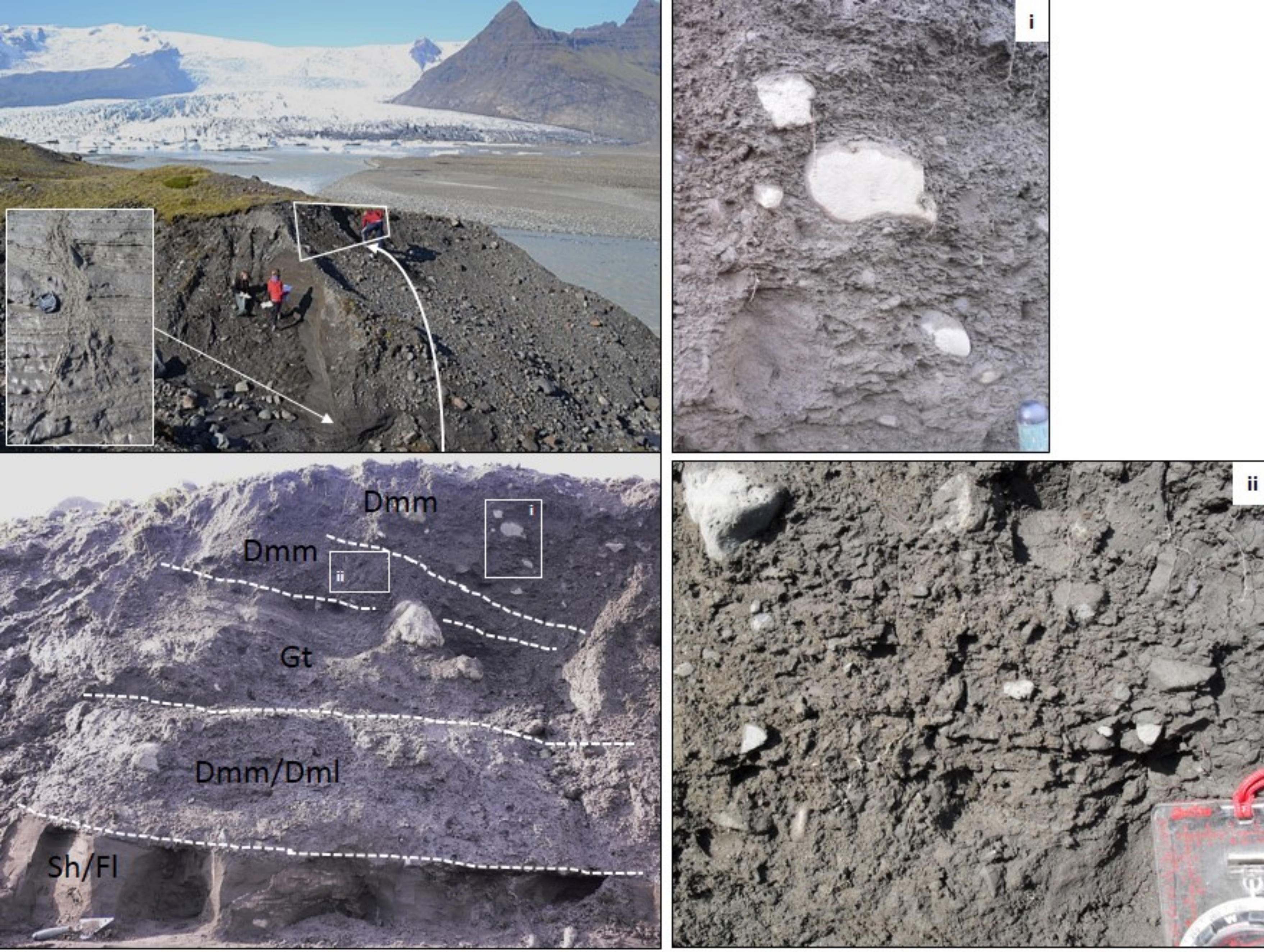
i
Dmm
Dmm
i
ii
Gt
Dmm/Dml
Sh/Fl
ii

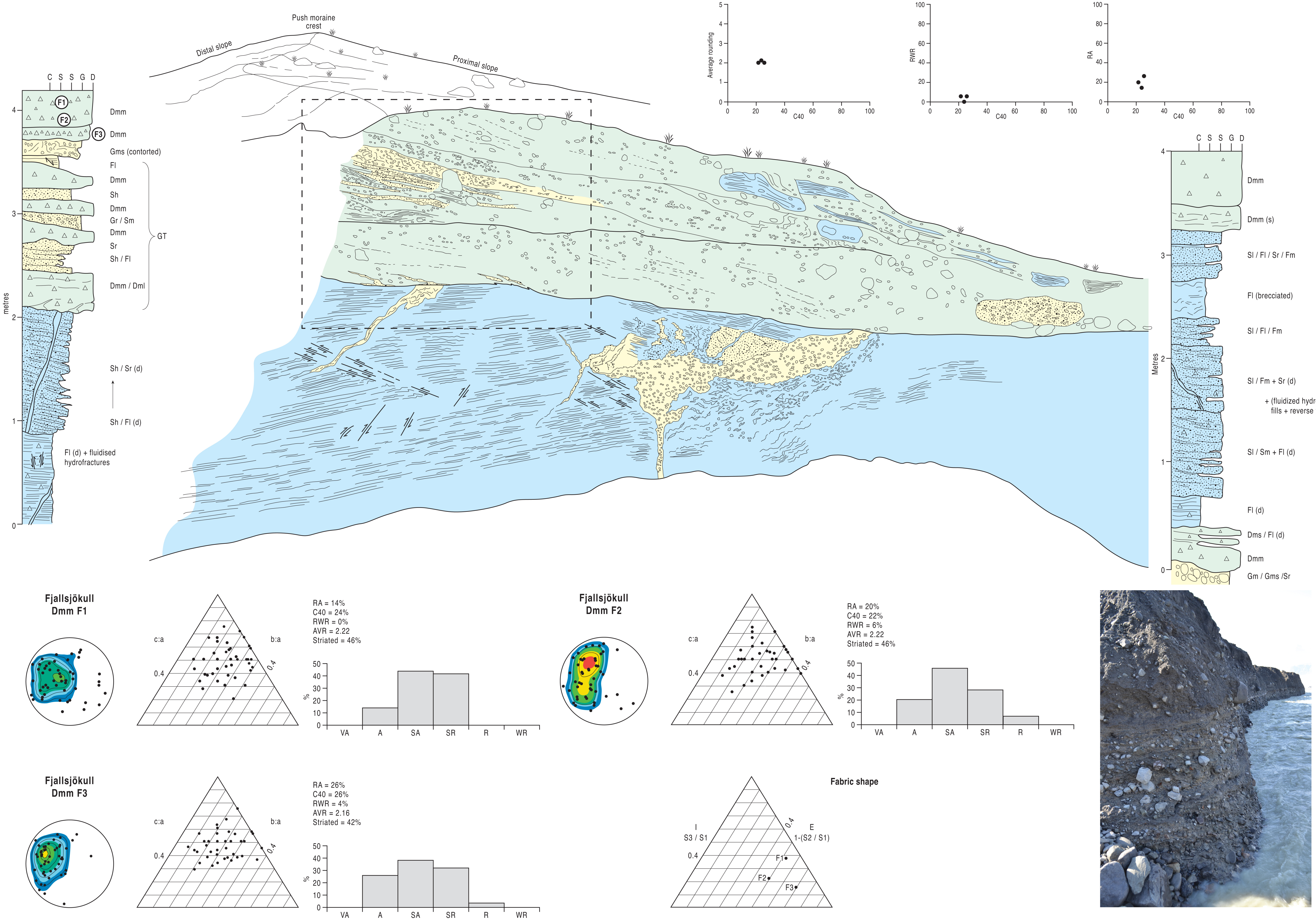

Push moraine crest
Distal slope
Proximal slope
C S S G D
metres
Dmm
F1
F2
F3
Dmm
Gms (contorted)
Fl
Dmm
Sh
Dmm
Gr / Sm
Dmm
Sr
Sh / Fl
Dmm / Dml
GT
Sh / Sr (d)
Sh / Fl (d)
Fl (d) + fluidised hydrofractures
Average rounding
RWR
RA
C40
Metres
Dmm
Dmm (s)
Sl / Fl / Sr / Fm
Fl (brecciated)
Sl / Fl / Fm
Sl / Fm + Sr (d)
+ (fluidized hydrofracture fills + reverse faults)
Sl / Sm + Fl (d)
Fl (d)
Dms / Fl (d)
Dmm
Gm / Gms /Sr
Fjallsjökull Dmm F1
c:a
b:a
0.4
RA = 14%
C40 = 24%
RWR = 0%
AVR = 2.22
Striated = 46%
%
VA A SA SR R WR
Fjallsjökull Dmm F2
RA = 20%
C40 = 22%
RWR = 6%
AVR = 2.22
Striated = 46%
Fjallsjökull Dmm F3
RA = 26%
C40 = 26%
RWR = 4%
AVR = 2.16
Striated = 42%
Fabric shape
I
S3 / S1
E
1-(S2 / S1)

Heinabergsjökull

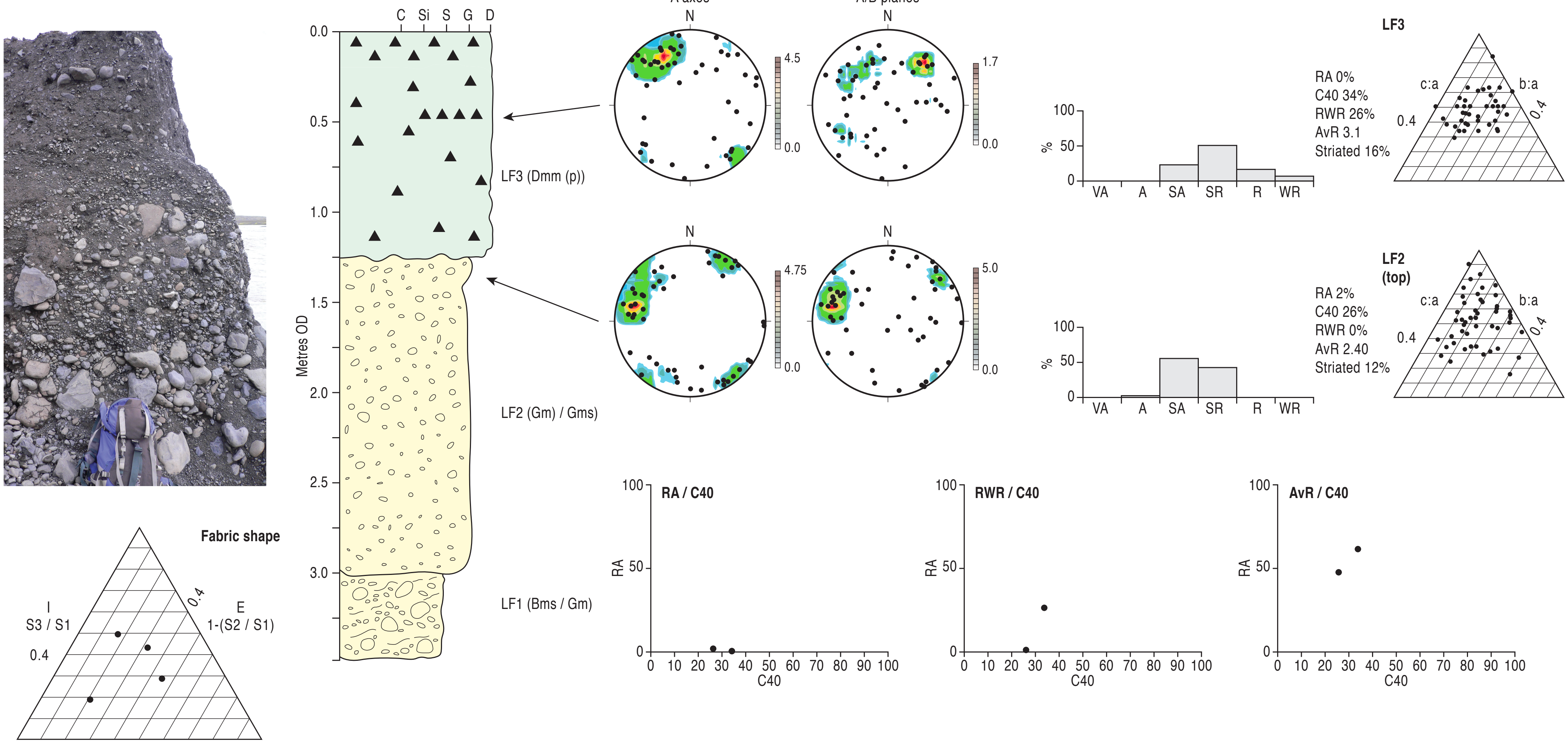

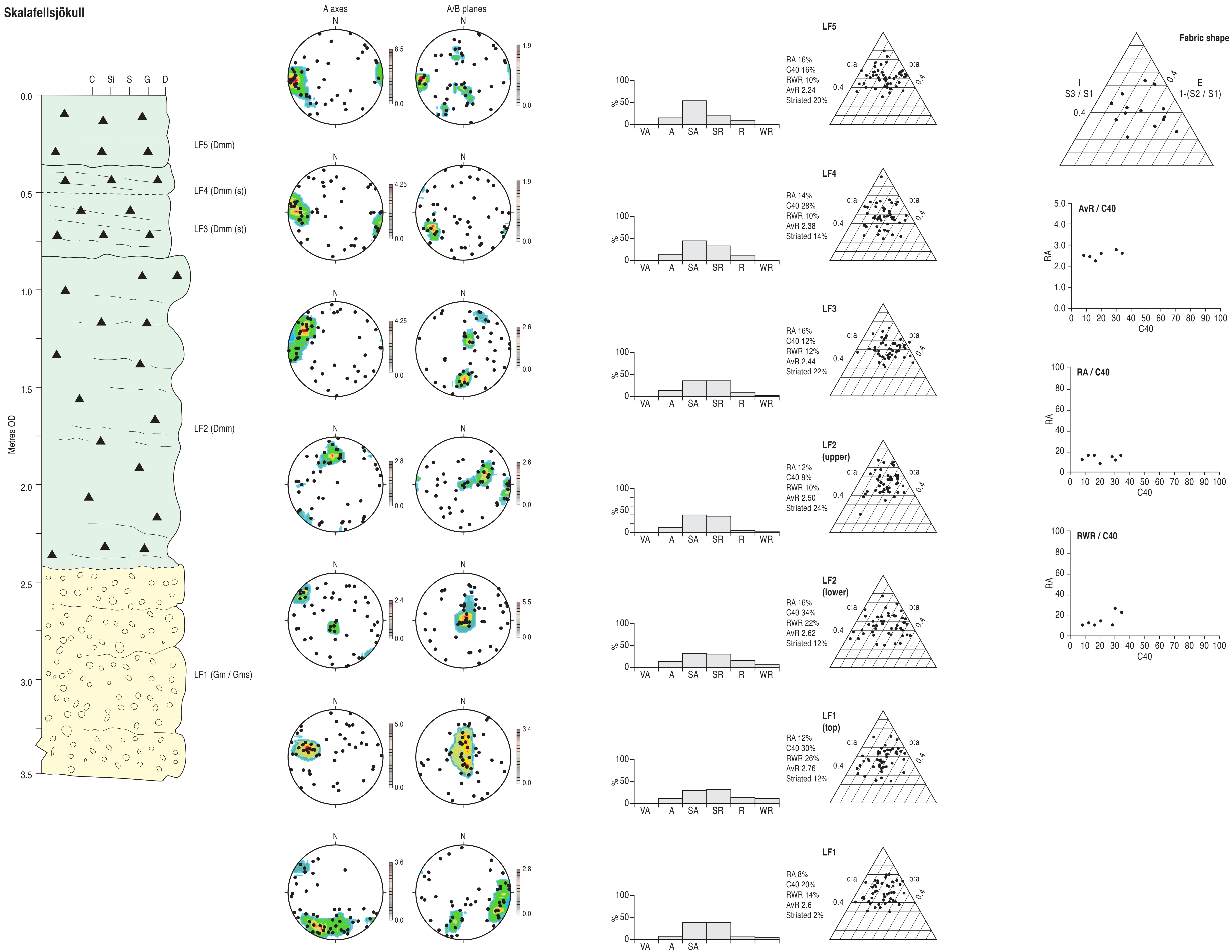
Skalafellsjökull
A axes
A/B planes
N
C Si S G D
0.0
0.5
1.0
1.5
2.0
2.5
3.0
3.5
Metres OD
LF5 (Dmm)
LF4 (Dmm (s))
LF3 (Dmm (s))
LF2 (Dmm)
LF1 (Gm / Gms)
VA A SA SR R WR
% 50
100
LF5
RA 16%
C40 16%
RWR 10%
AvR 2.24
Striated 20%
LF4
RA 14%
C40 28%
RWR 10%
AvR 2.38
Striated 14%
LF3
RA 16%
C40 12%
RWR 12%
AvR 2.44
Striated 22%
LF2 (upper)
RA 12%
C40 8%
RWR 10%
AvR 2.50
Striated 24%
LF2 (lower)
RA 16%
C40 34%
RWR 22%
AvR 2.62
Striated 12%
LF1 (top)
RA 12%
C40 30%
RWR 26%
AvR 2.76
Striated 12%
LF1
RA 8%
C40 20%
RWR 14%
AvR 2.6
Striated 2%
c:a
b:a
0.4
Fabric shape
I
S3 / S1
E
1-(S2 / S1)
AvR / C40
RA / C40
RWR / C40
RA
C40

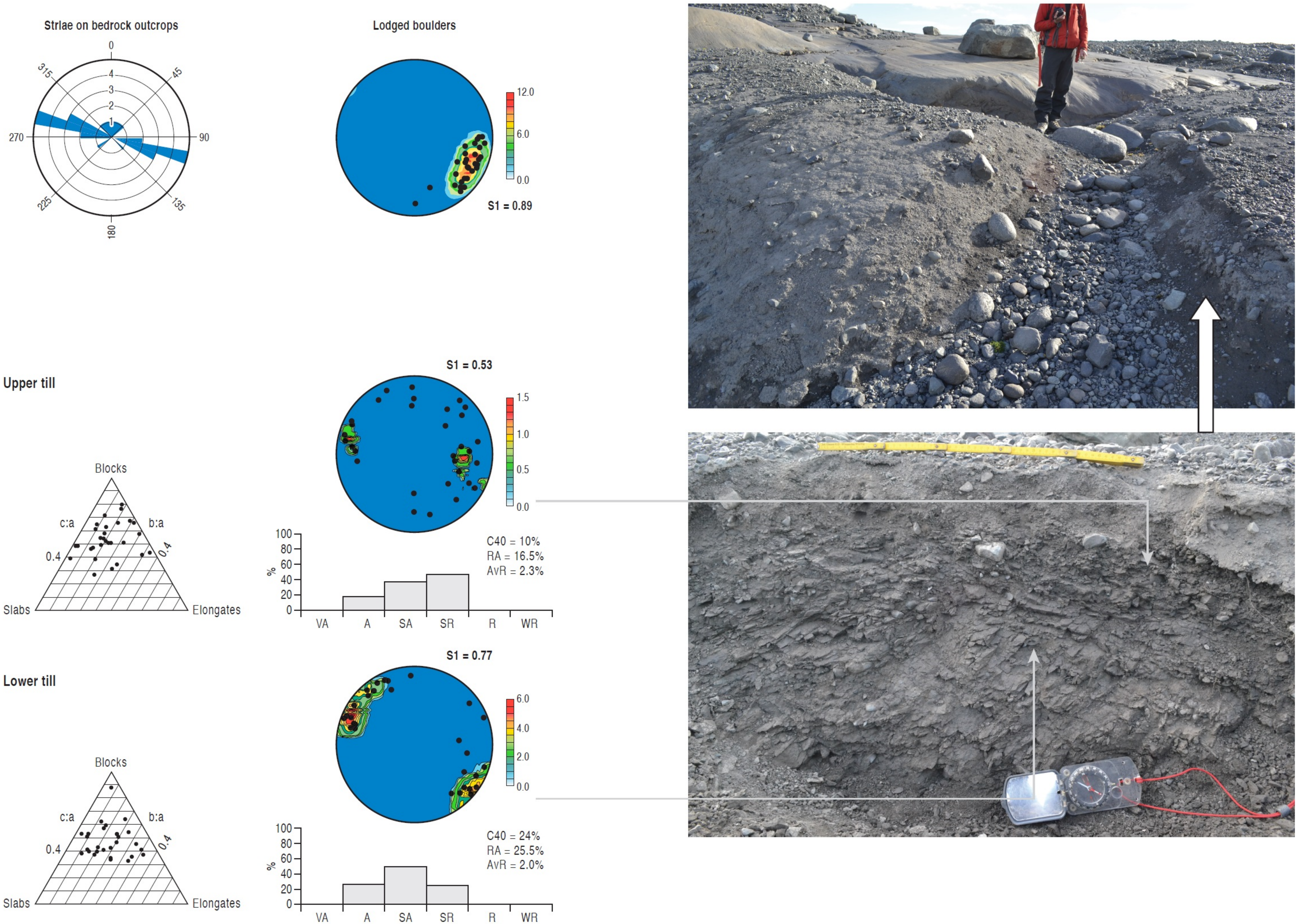

Striae on bedrock outcrops
0
45
90
135
180
225
270
315
1
2
3
4
Lodged boulders
12.0
6.0
0.0
S1 = 0.89
Upper till
S1 = 0.53
1.5
1.0
0.5
0.0
Blocks
c:a
b:a
0.4
0.4
Slabs
Elongates
C40 = 10%
RA = 16.5%
AvR = 2.3%
%
100
80
60
40
20
0
VA
A
SA
SR
R
WR
Lower till
S1 = 0.77
6.0
4.0
2.0
0.0
Blocks
c:a
b:a
0.4
0.4
Slabs
Elongates
C40 = 24%
RA = 25.5%
AvR = 2.0%
%
100
80
60
40
20
0
VA
A
SA
SR
R
WR

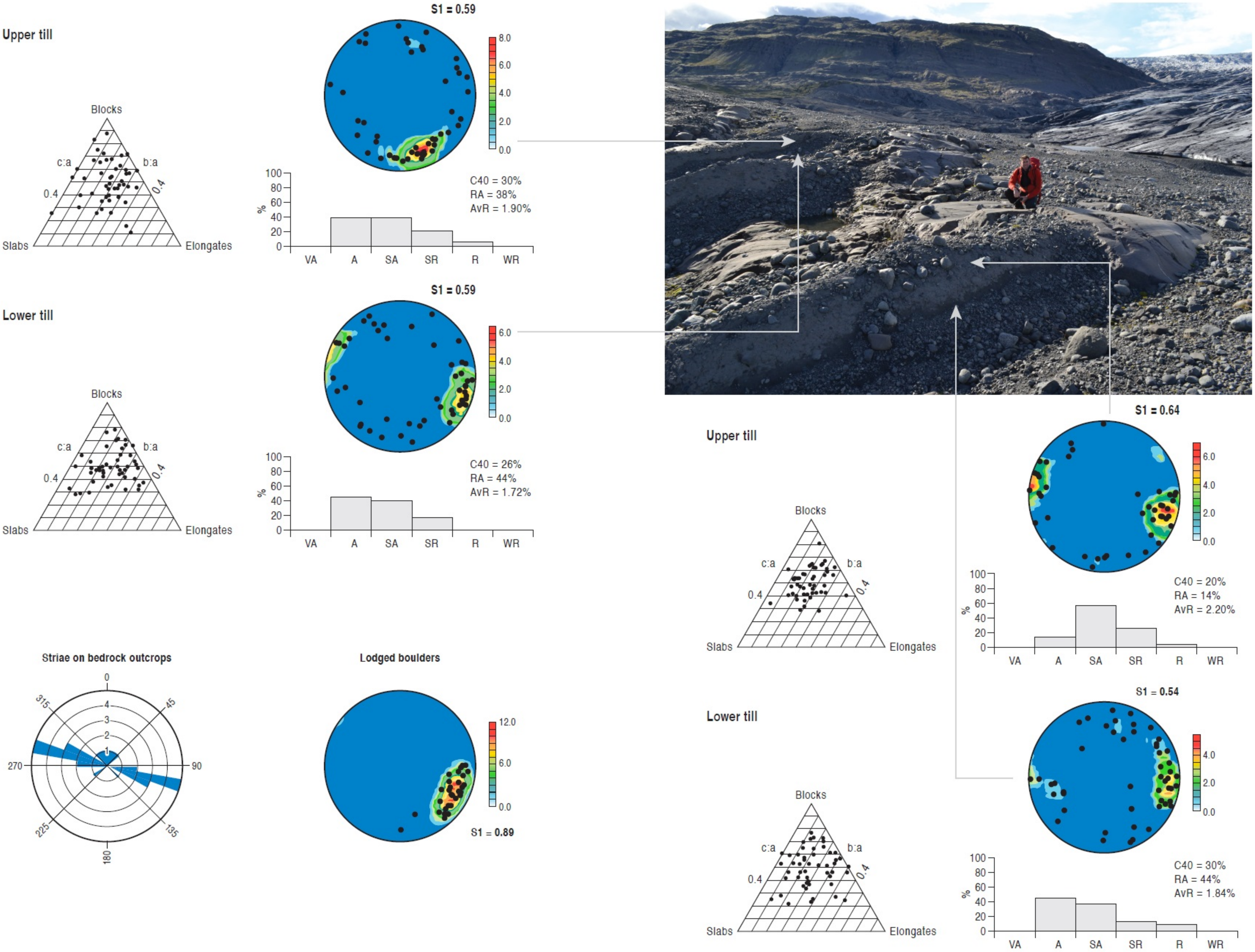
Upper till
S1 = 0.59
C40 = 30%
RA = 38%
AvR = 1.90%
Lower till
S1 = 0.59
C40 = 26%
RA = 44%
AvR = 1.72%
Blocks
c:a
b:a
0.4
Slabs
Elongates
VA A SA SR R WR
%
Striae on bedrock outcrops
Lodged boulders
S1 = 0.89
Upper till
S1 = 0.64
C40 = 20%
RA = 14%
AvR = 2.20%
Lower till
S1 = 0.54
C40 = 30%
RA = 44%
AvR = 1.84%

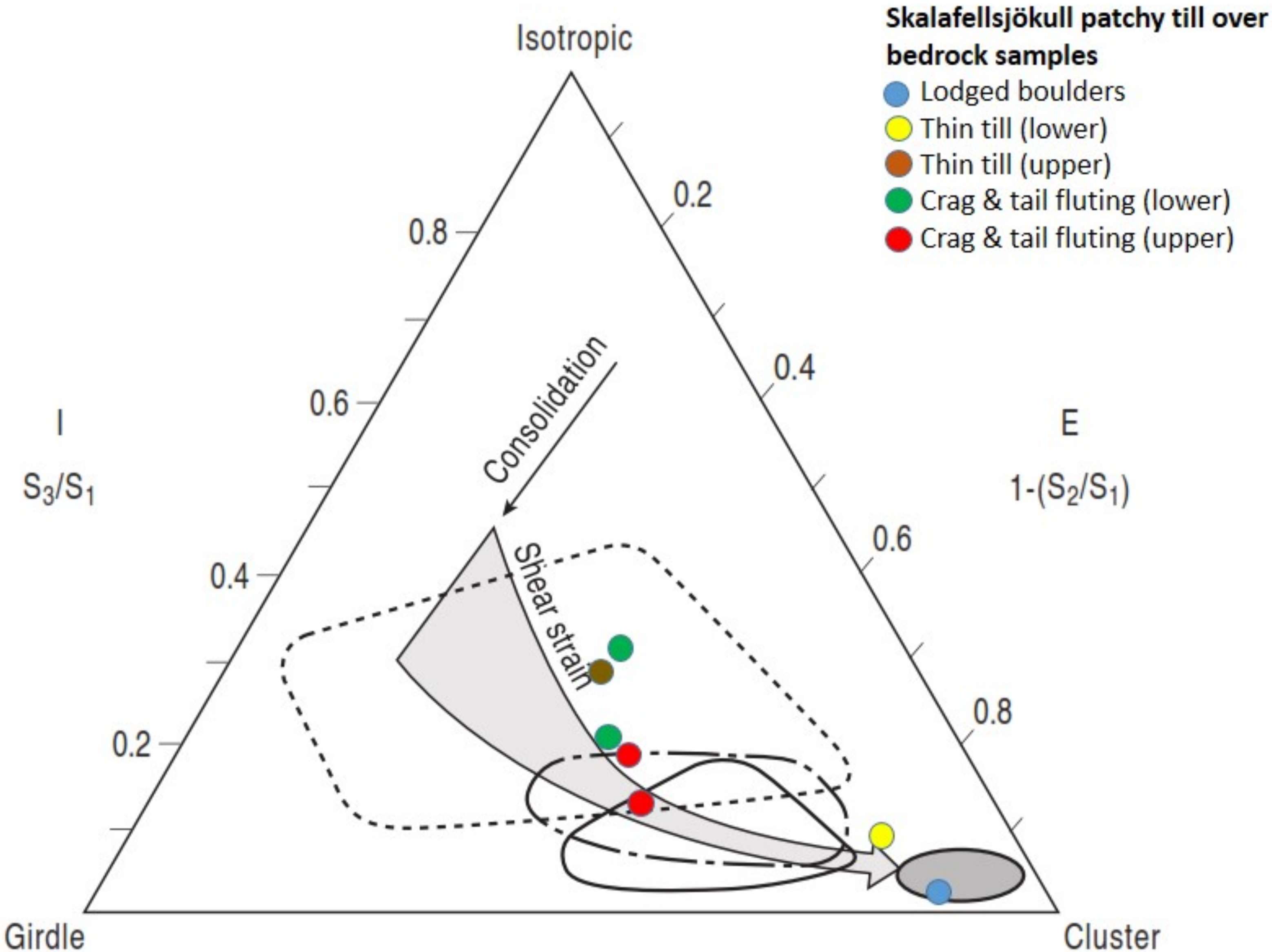

Skalafellsjökull patchy till over bedrock samples
Lodged boulders
Thin till (lower)
Thin till (upper)
Crag & tail fluting (lower)
Crag & tail fluting (upper)
Isotropic
Girdle
Cluster
I
S3/S1
E
1-(S2/S1)
0.2
0.4
0.6
0.8
Consolidation
Shear strain

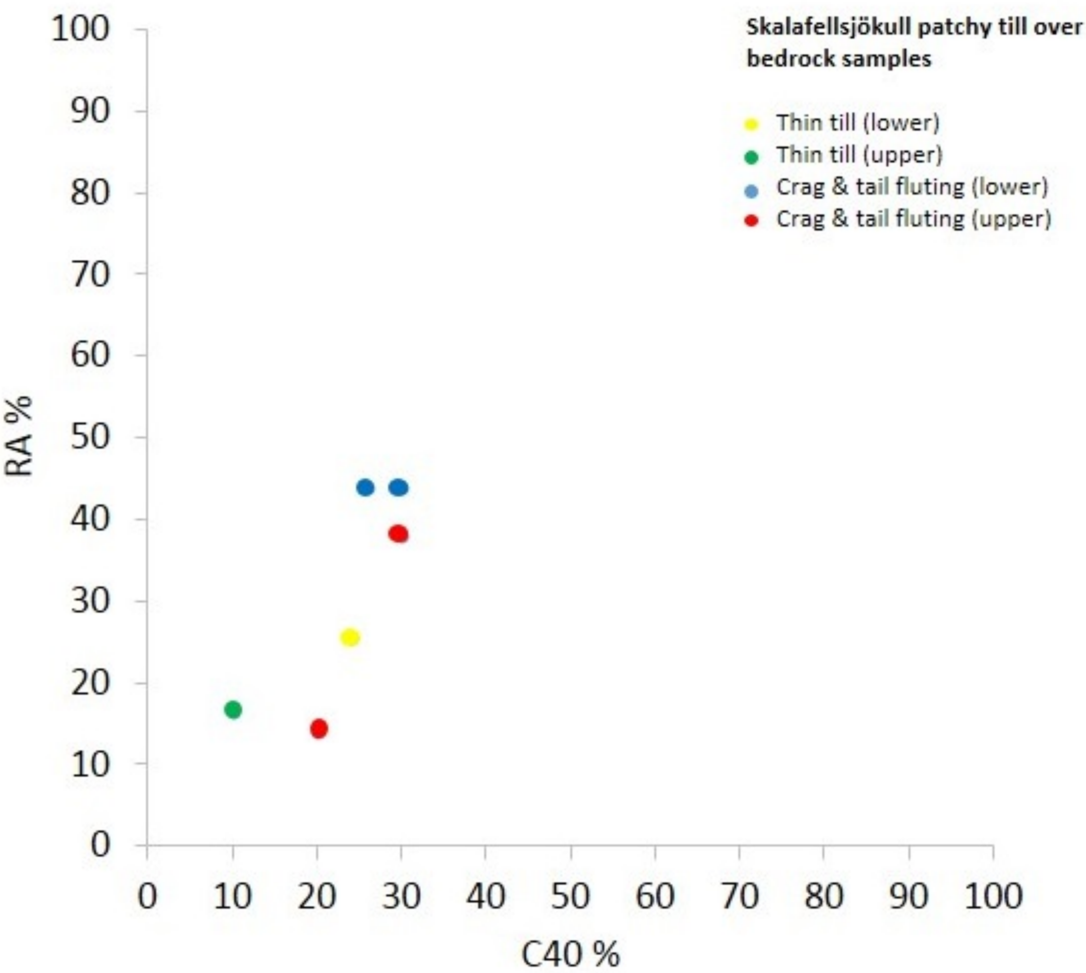

Skalafellsjökull patchy till over bedrock samples
Thin till (lower)
Thin till (upper)
Crag & tail fluting (lower)
Crag & tail fluting (upper)
RA %
C40 %
0
10
20
30
40
50
60
70
80
90
100

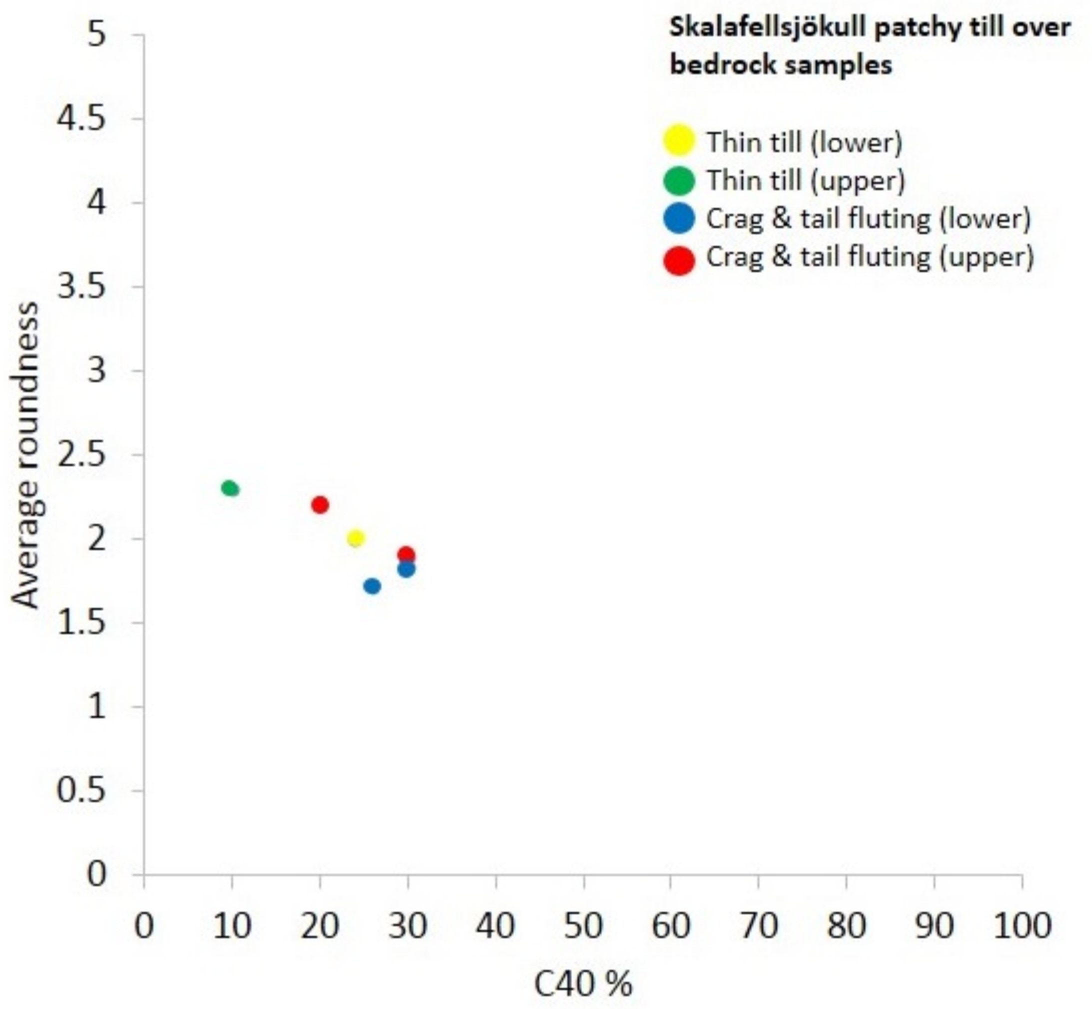
Skalafellsjökull patchy till over bedrock samples
Thin till (lower)
Thin till (upper)
Crag & tail fluting (lower)
Crag & tail fluting (upper)
Average roundness
C40 %
0
0.5
1
1.5
2
2.5
3
3.5
4
4.5
5
10
20
30
40
50
60
70
80
90
100

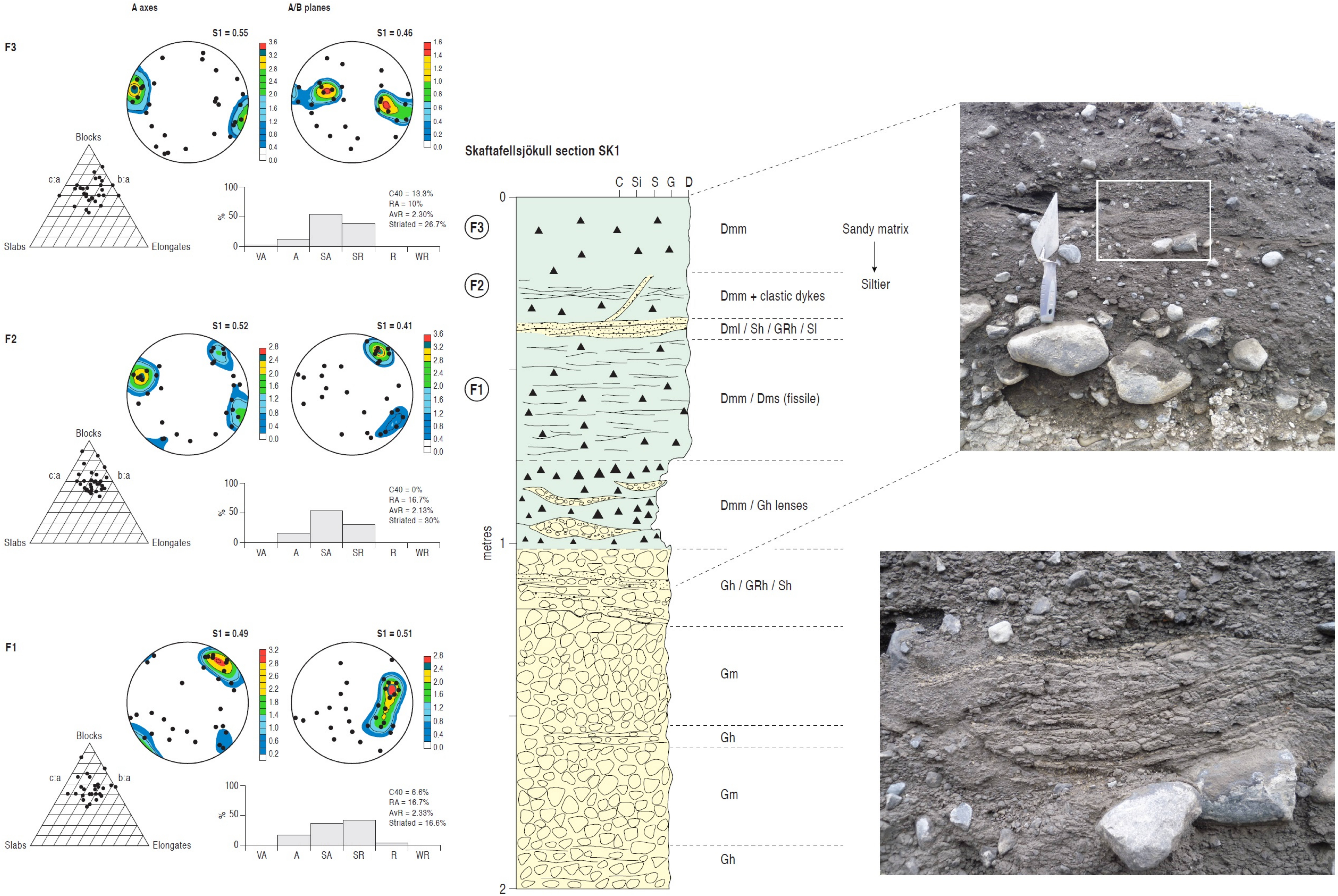
A axes
A/B planes
F3
S1 = 0.55
S1 = 0.46
Blocks
c:a
b:a
Slabs
Elongates
C40 = 13.3%
RA = 10%
AvR = 2.30%
Striated = 26.7%
F2
S1 = 0.52
S1 = 0.41
C40 = 0%
RA = 16.7%
AvR = 2.13%
Striated = 30%
F1
S1 = 0.49
S1 = 0.51
C40 = 6.6%
RA = 16.7%
AvR = 2.33%
Striated = 16.6%
VA
A
SA
SR
R
WR
%
Skaftafellsjökull section SK1
C
Si
S
G
D
metres
Dmm
Sandy matrix
Siltier
Dmm + clastic dykes
Dml / Sh / GRh / Sl
Dmm / Dms (fissile)
Dmm / Gh lenses
Gh / GRh / Sh
Gm
Gh
Gm
Gh

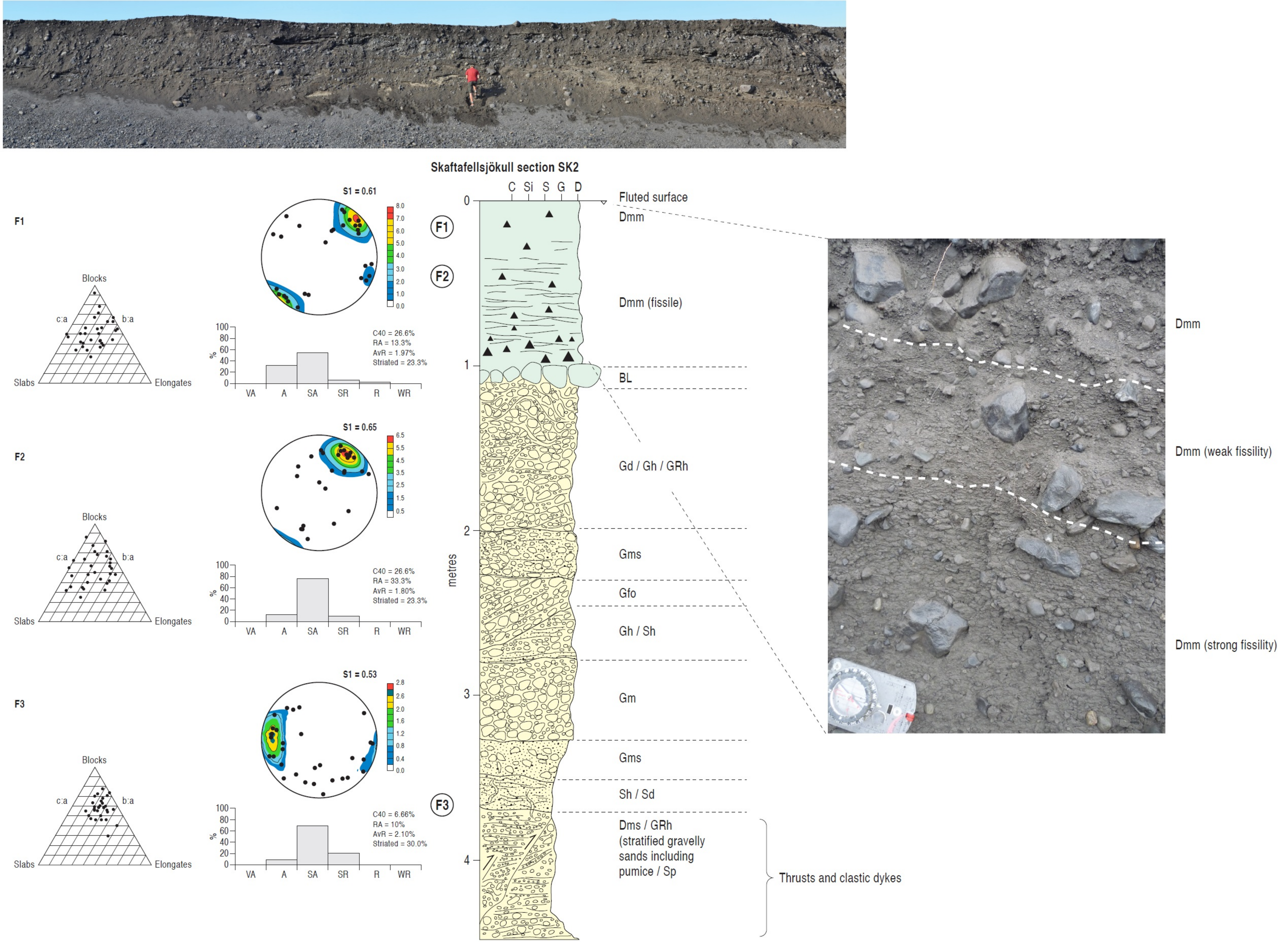

Skaftafellsjökull section SK2
C Si S G D
Fluted surface
Dmm
Dmm (fissile)
BL
Gd / Gh / GRh
Gms
Gfo
Gh / Sh
Gm
Gms
Sh / Sd
Dms / GRh
(stratified gravelly
sands including
pumice / Sp
Thrusts and clastic dykes
metres
0
1
2
3
4
F1
F2
F3
S1 = 0.61
S1 = 0.65
S1 = 0.53
Blocks
c:a
b:a
Slabs
Elongates
C40 = 26.6%
RA = 13.3%
AvR = 1.97%
Striated = 23.3%
C40 = 26.6%
RA = 33.3%
AvR = 1.80%
Striated = 23.3%
C40 = 6.66%
RA = 10%
AvR = 2.10%
Striated = 30.0%
VA A SA SR R WR
%
Dmm
Dmm (weak fissility)
Dmm (strong fissility)

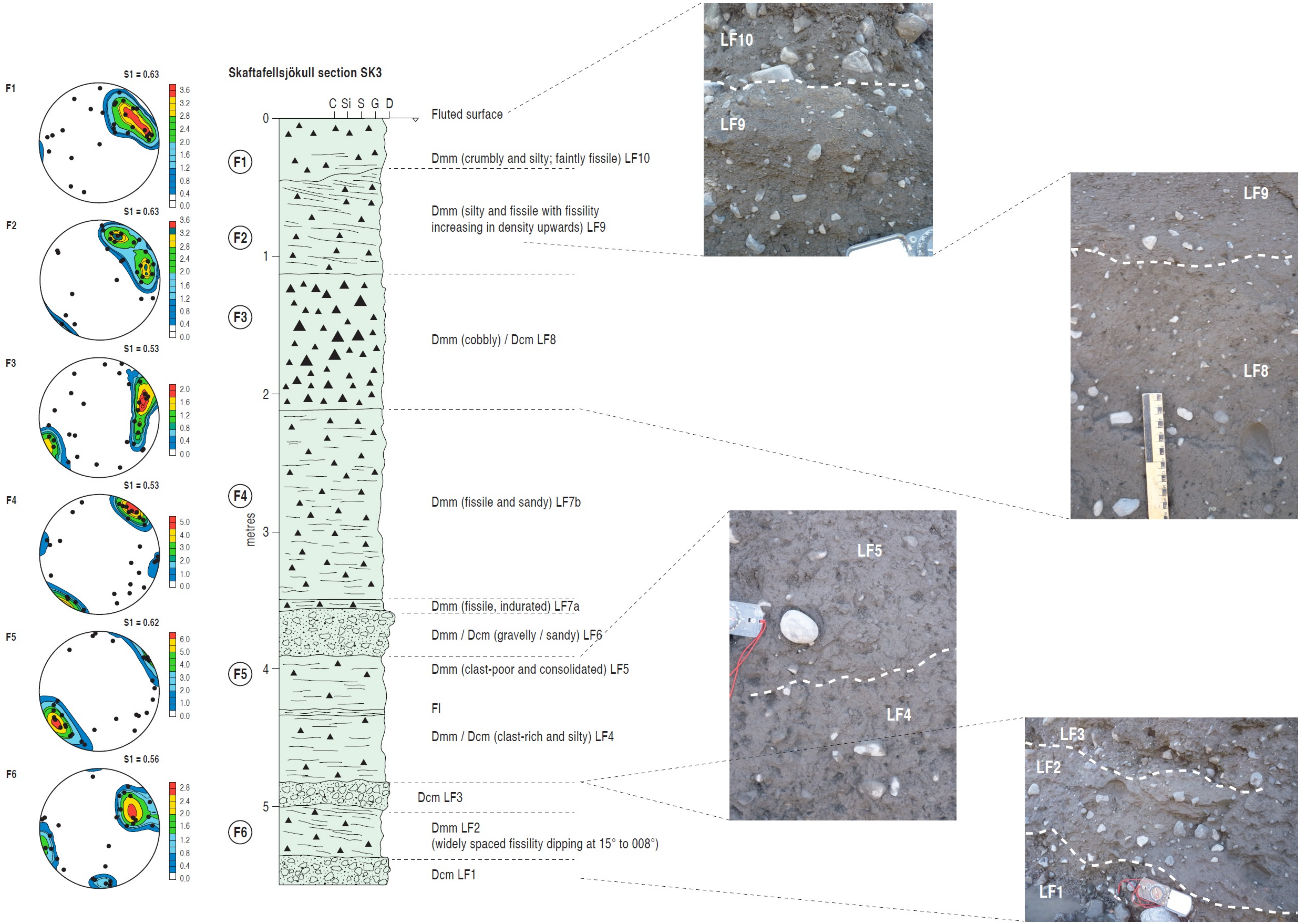

Skaftafellsjökull section SK3
C Si S G D
0
1
2
3
4
5
metres
Fluted surface
Dmm (crumbly and silty; faintly fissile) LF10
Dmm (silty and fissile with fissility increasing in density upwards) LF9
Dmm (cobbly) / Dcm LF8
Dmm (fissile and sandy) LF7b
Dmm (fissile, indurated) LF7a
Dmm / Dcm (gravelly / sandy) LF6
Dmm (clast-poor and consolidated) LF5
Fl
Dmm / Dcm (clast-rich and silty) LF4
Dcm LF3
Dmm LF2
(widely spaced fissility dipping at 15° to 008°)
Dcm LF1
F1
F2
F3
F4
F5
F6
S1 = 0.63
S1 = 0.63
S1 = 0.53
S1 = 0.53
S1 = 0.62
S1 = 0.56
LF10
LF9
LF8
LF5
LF4
LF3
LF2
LF1

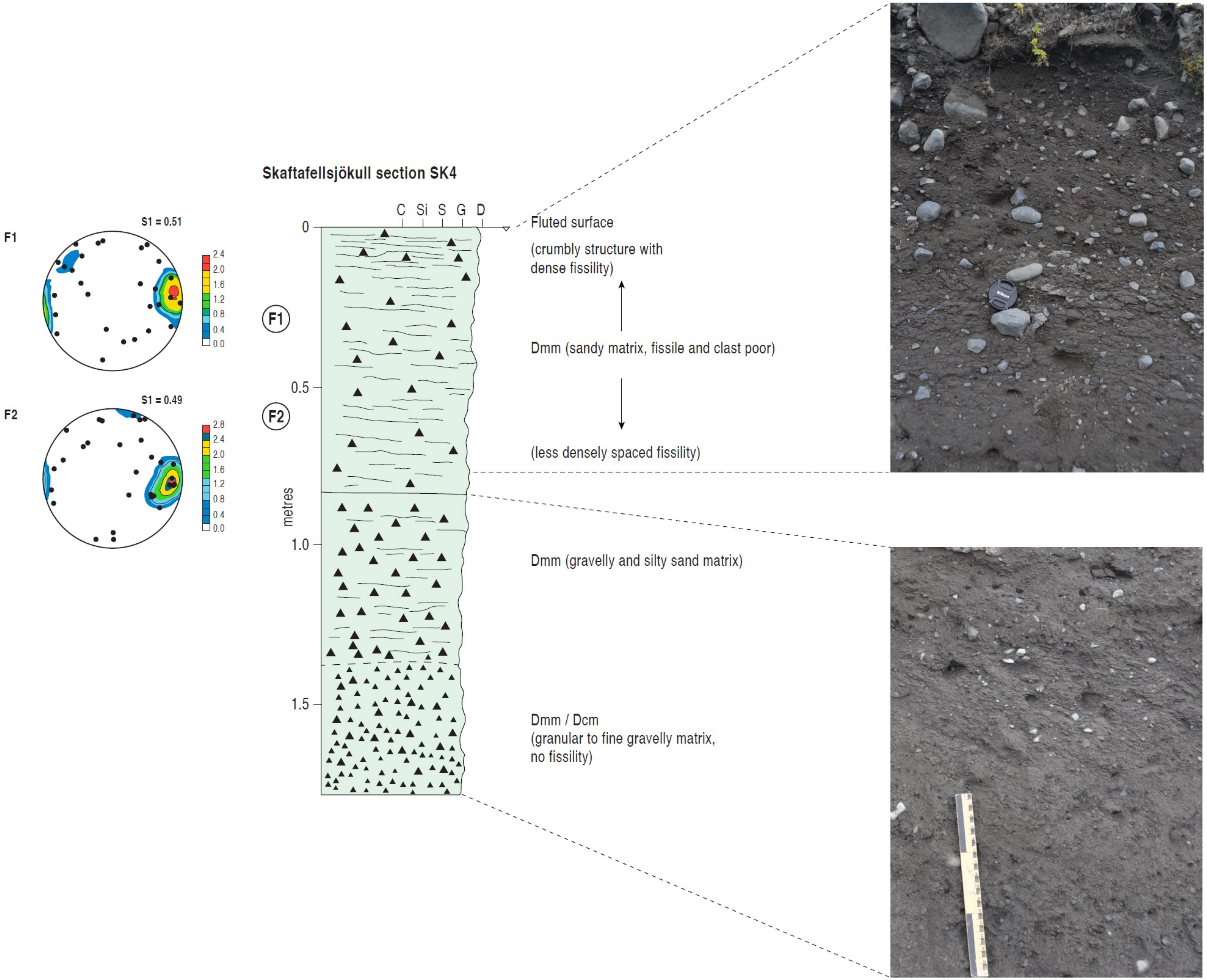
Skaftafellsjökull section SK4
F1
S1 = 0.51
F2
S1 = 0.49
C Si S G D
0
0.5
1.0
1.5
metres
F1
F2
Fluted surface
(crumbly structure with
dense fissility)
Dmm (sandy matrix, fissile and clast poor)
(less densely spaced fissility)
Dmm (gravelly and silty sand matrix)
Dmm / Dcm
(granular to fine gravelly matrix,
no fissility)

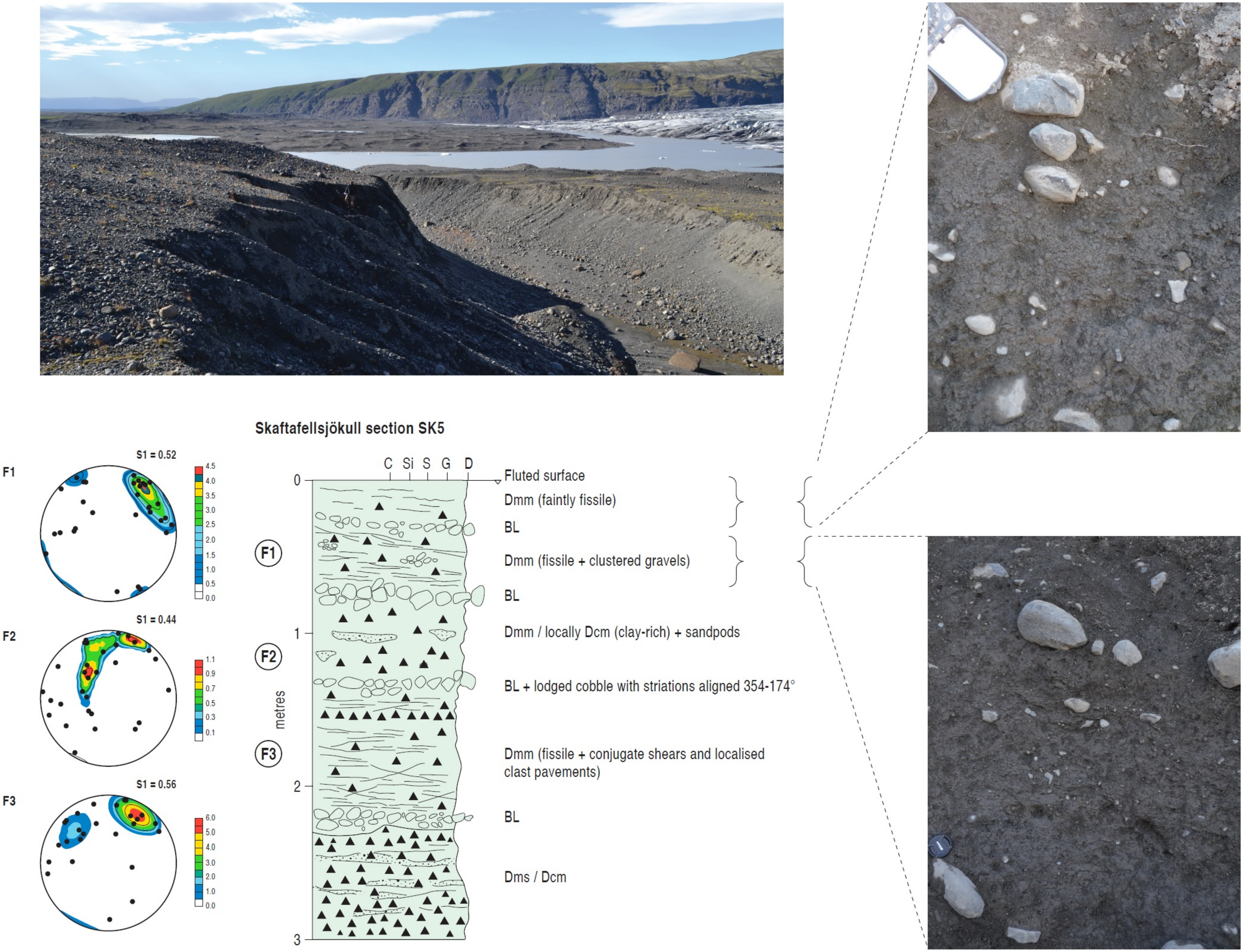
Skaftafellsjökull section SK5
F1
S1 = 0.52
F2
S1 = 0.44
F3
S1 = 0.56
C Si S G D
0
1
2
3
metres
Fluted surface
Dmm (faintly fissile)
BL
Dmm (fissile + clustered gravels)
BL
Dmm / locally Dcm (clay-rich) + sandpods
BL + lodged cobble with striations aligned 354-174°
Dmm (fissile + conjugate shears and localised clast pavements)
BL
Dms / Dcm

Skaftafellsjökull section SK6

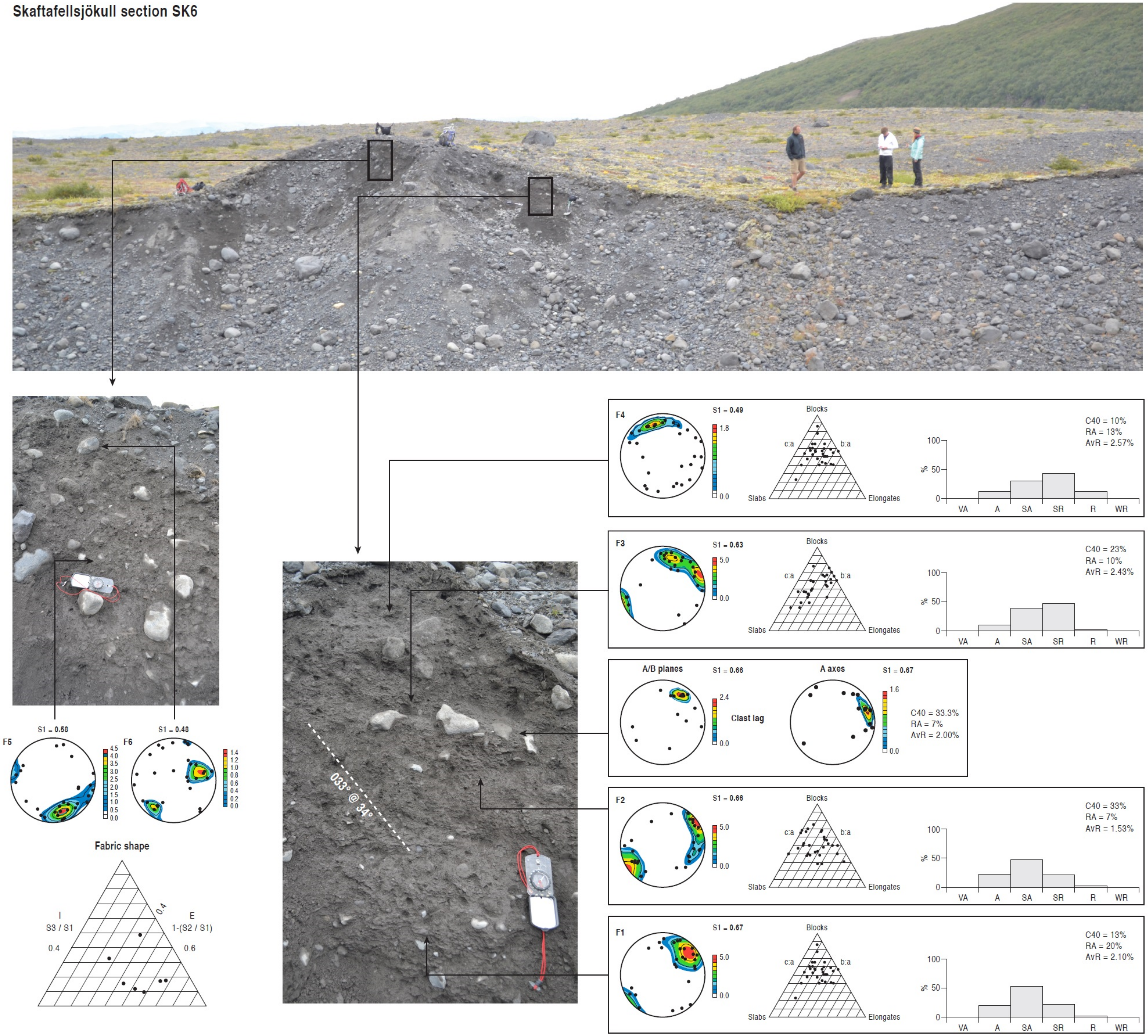

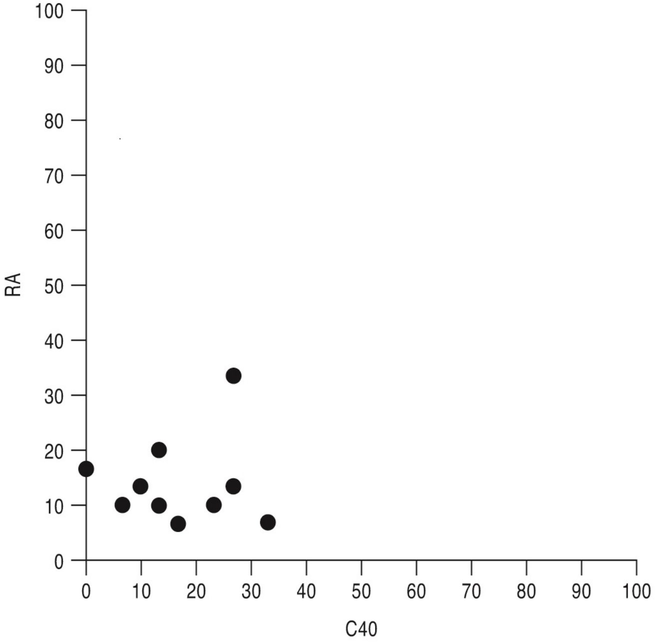

RA
C40

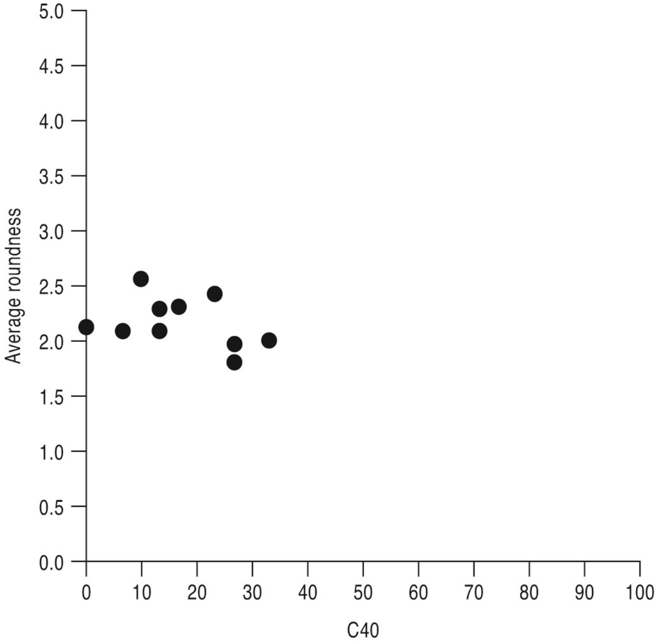

Average roundness
C40

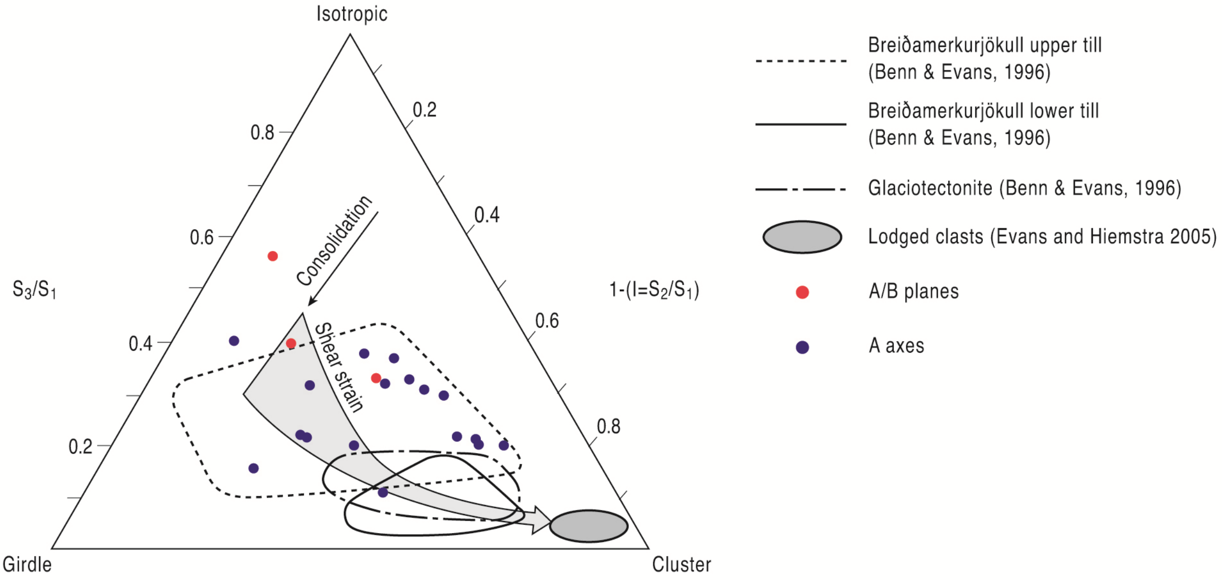
Isotropic
Girdle
Cluster
S3/S1
1-(I=S2/S1)
0.2
0.4
0.6
0.8
Consolidation
Shear strain
Breiðamerkurjökull upper till (Benn & Evans, 1996)
Breiðamerkurjökull lower till (Benn & Evans, 1996)
Glaciotectonite (Benn & Evans, 1996)
Lodged clasts (Evans and Hiemstra 2005)
A/B planes
A axes

Falljökull

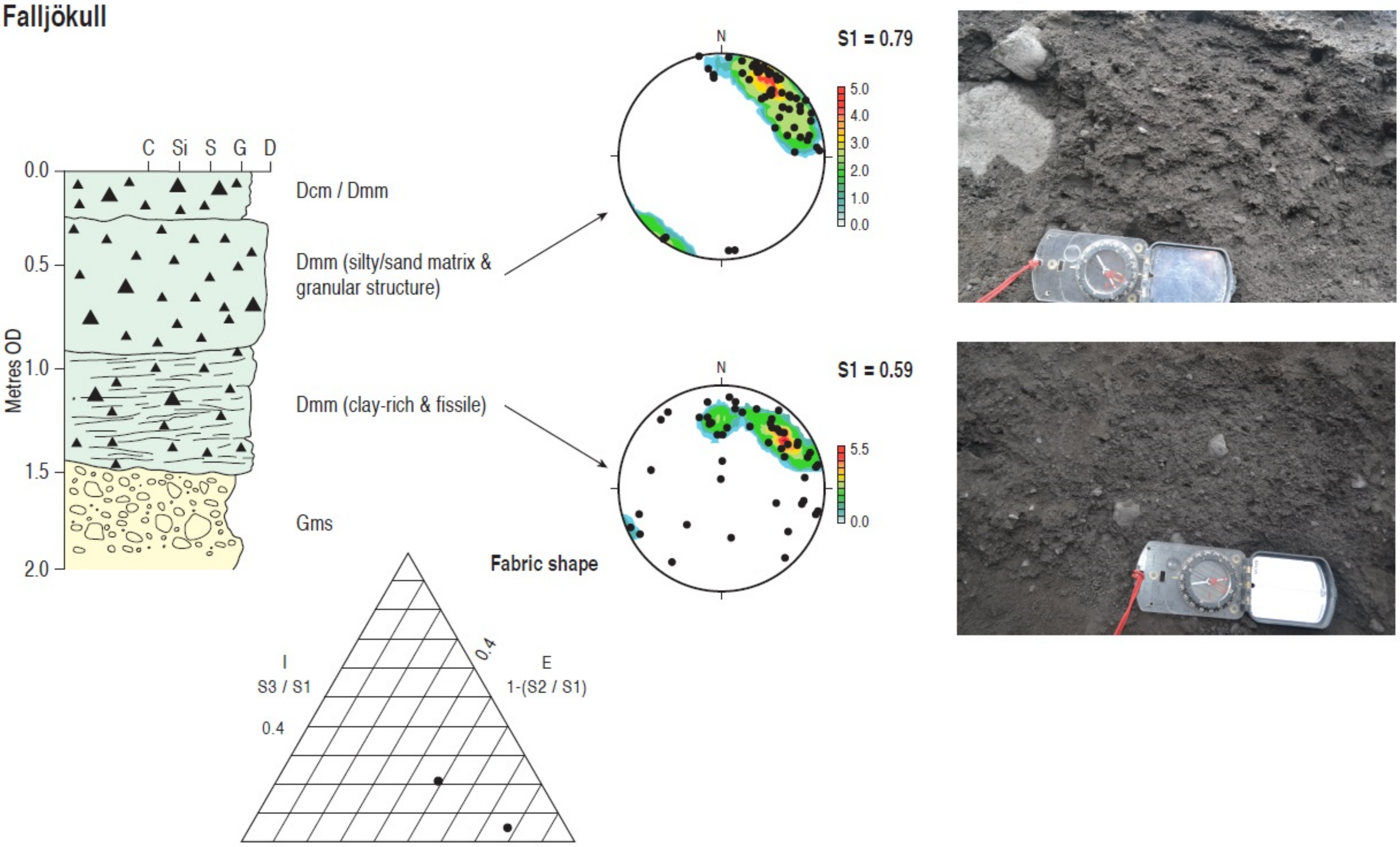

C Si S G D
0.0
0.5
1.0
1.5
2.0
Metres OD
Dcm / Dmm
Dmm (silty/sand matrix & granular structure)
Dmm (clay-rich & fissile)
Gms
N
S1 = 0.79
5.0
4.0
3.0
2.0
1.0
0.0
S1 = 0.59
5.5
0.0
Fabric shape
I
S3 / S1
0.4
E
1-(S2 / S1)
0.4

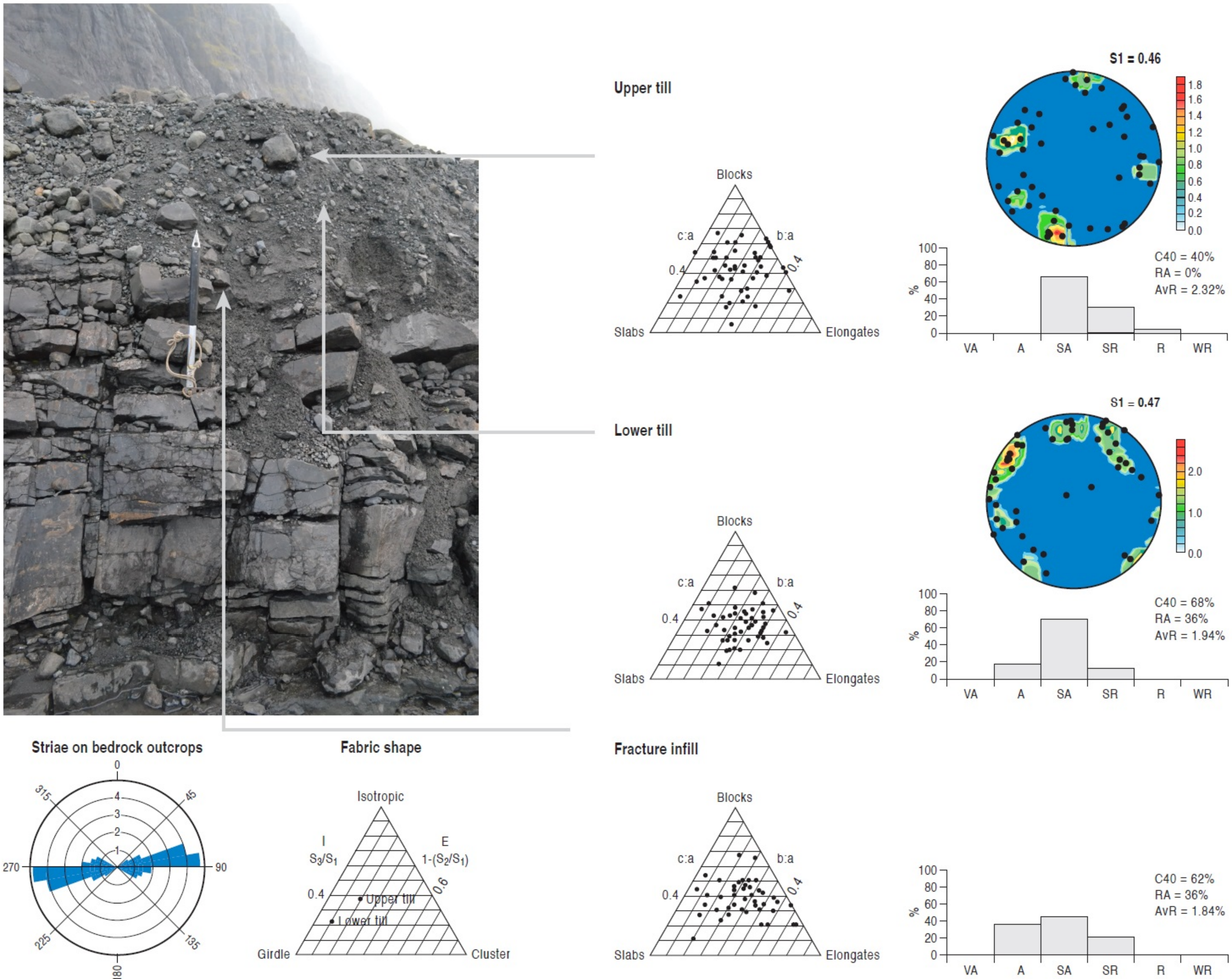
Upper till
S1 = 0.46
Blocks
c:a
b:a
0.4
Slabs
Elongates
C40 = 40%
RA = 0%
AvR = 2.32%
VA
A
SA
SR
R
WR
Lower till
S1 = 0.47
C40 = 68%
RA = 36%
AvR = 1.94%
Fracture infill
C40 = 62%
RA = 36%
AvR = 1.84%
Striae on bedrock outcrops
Fabric shape
Isotropic
I
S3/S1
E
1-(S2/S1)
0.6
Upper till
Lower till
Girdle
Cluster

Breidamerkurjökull

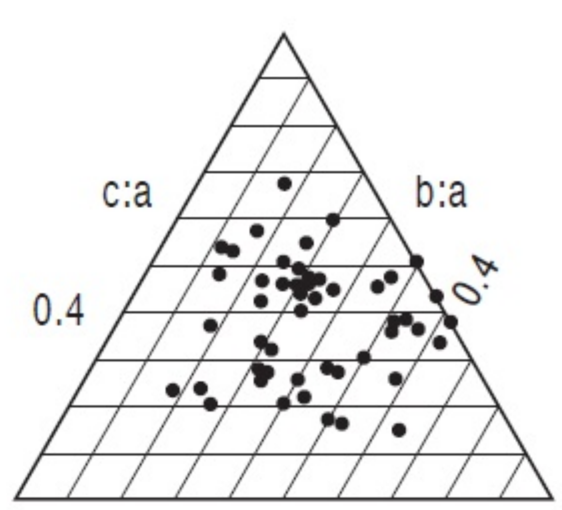

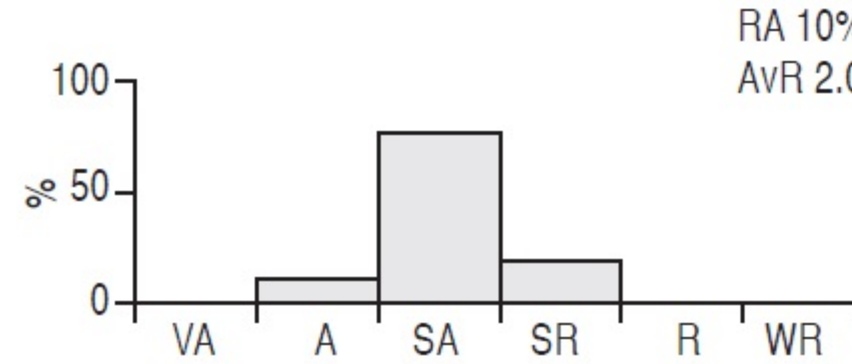

Fracture infill

C40 54%
RA 10%
AvR 2.08

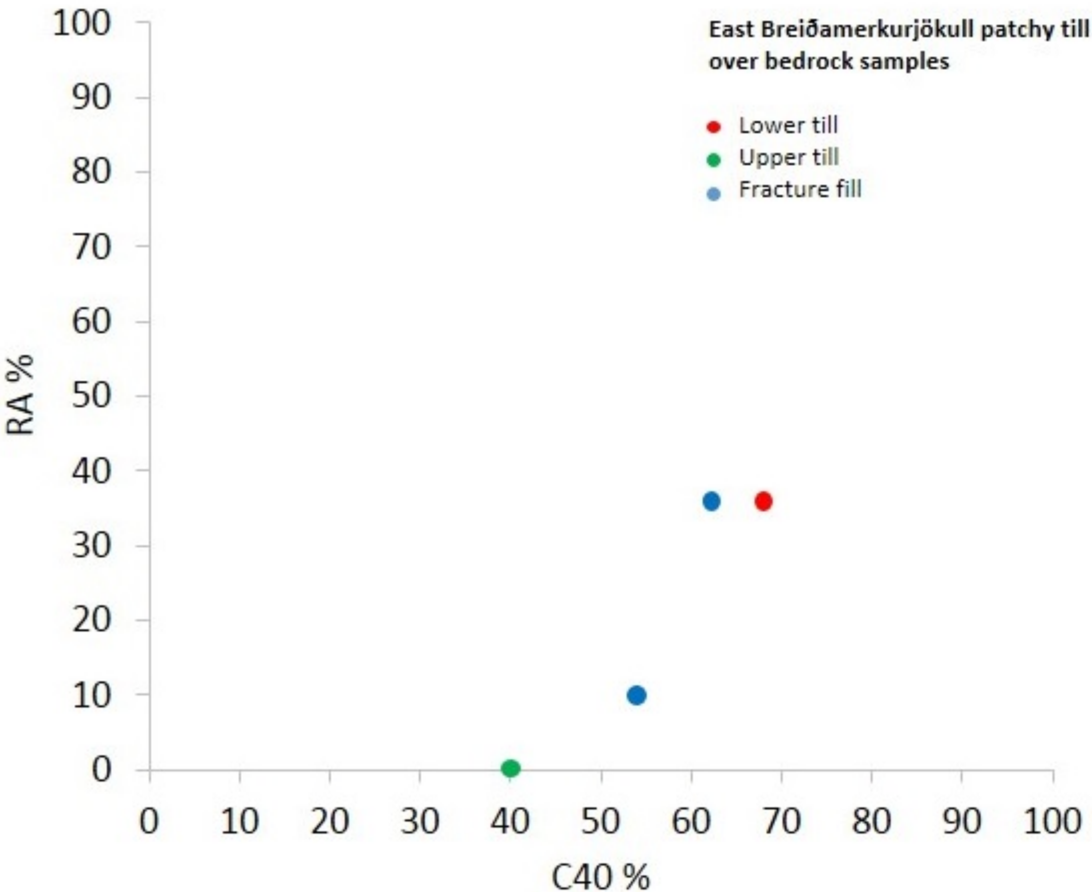
East Breiðamerkurjökull patchy till over bedrock samples
Lower till
Upper till
Fracture fill
RA %
C40 %
0
10
20
30
40
50
60
70
80
90
100

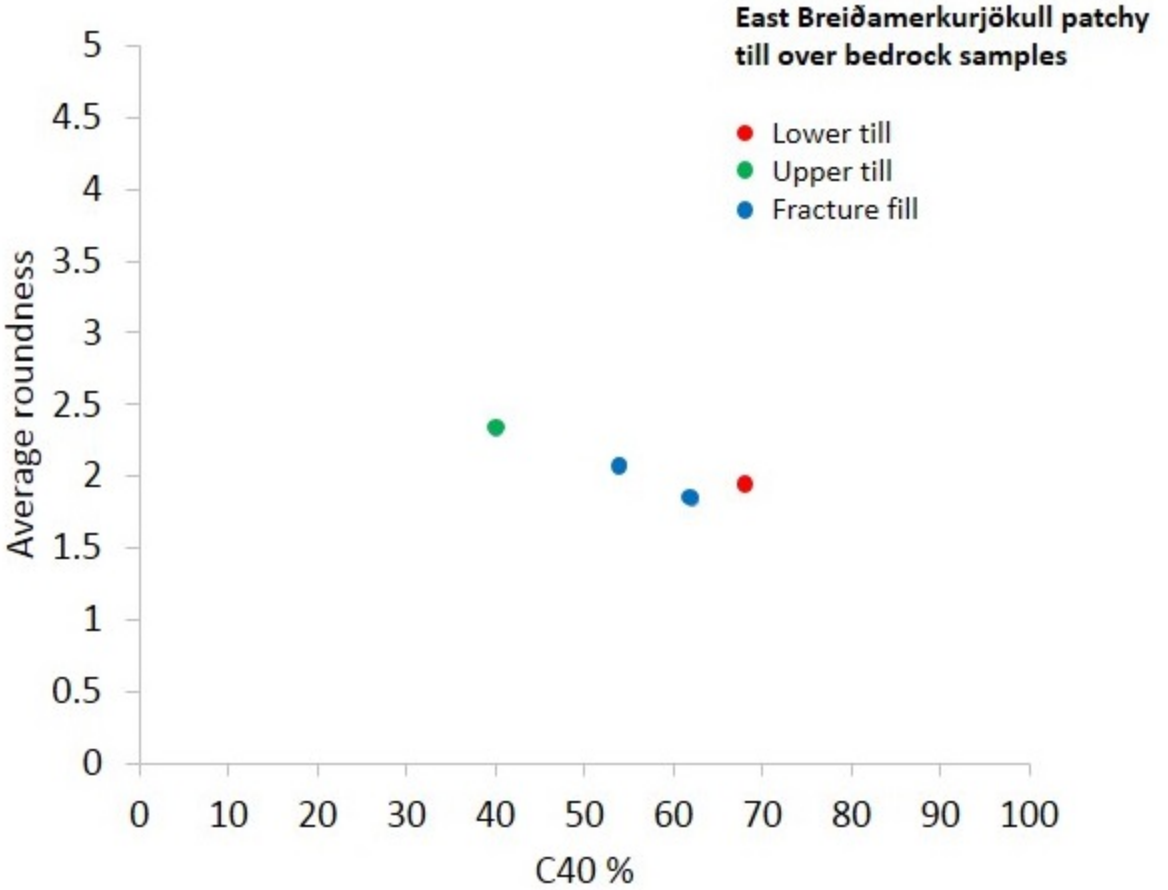
East Breiðamerkurjökull patchy till over bedrock samples
Lower till
Upper till
Fracture fill
Average roundness
5
4.5
4
3.5
3
2.5
2
1.5
1
0.5
0
0
10
20
30
40
50
60
70
80
90
100
C40 %

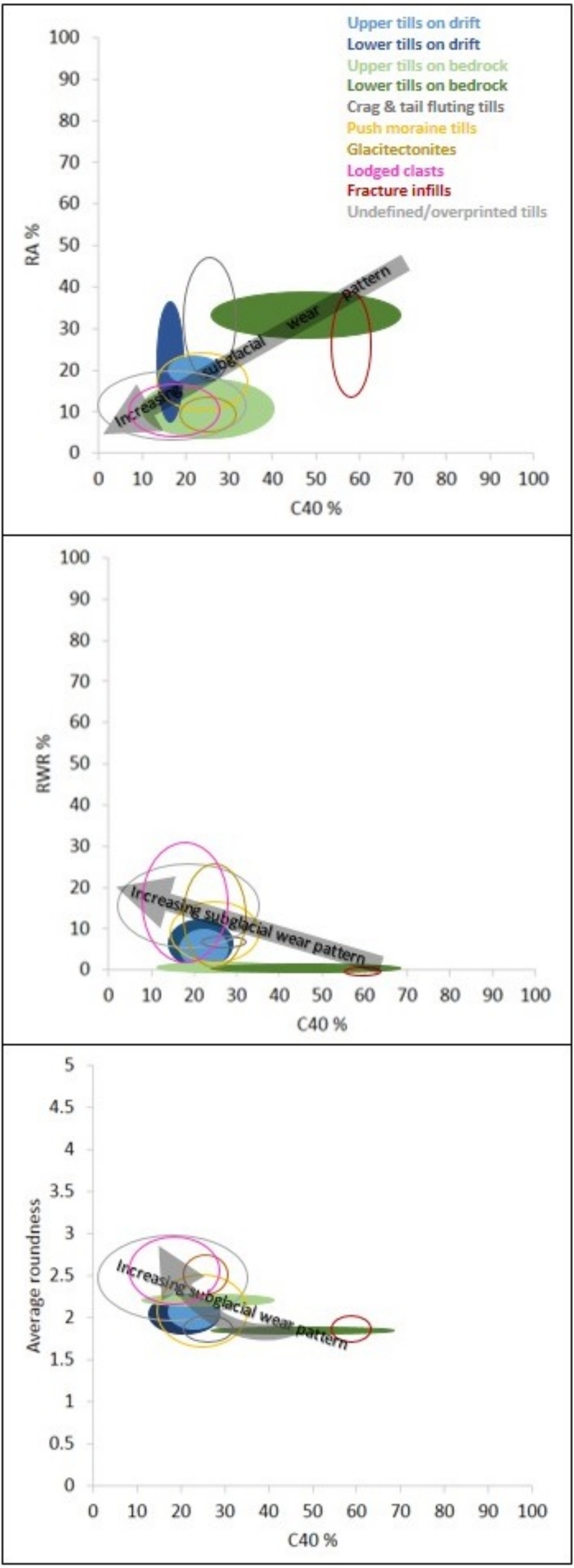
Upper tills on drift
Lower tills on drift
Upper tills on bedrock
Lower tills on bedrock
Crag & tail fluting tills
Push moraine tills
Glacitectonites
Lodged clasts
Fracture infills
Undefined/overprinted tills
RA %
C40 %
Increasing subglacial wear pattern
RWR %
C40 %
Increasing subglacial wear pattern
Average roundness
C40 %
Increasing subglacial wear pattern

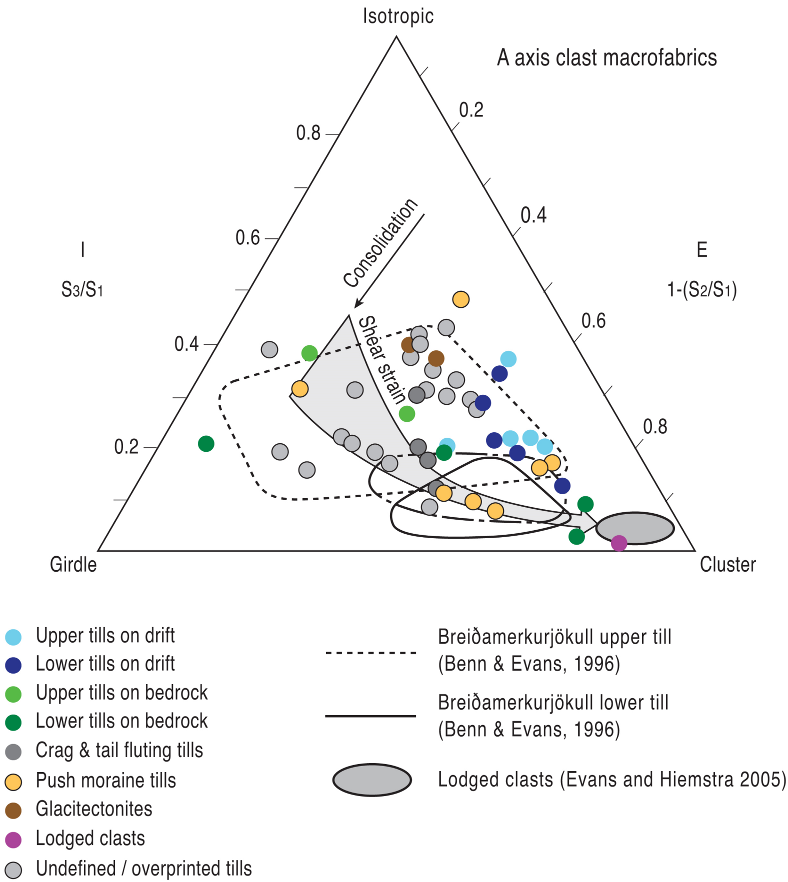
Isotropic
A axis clast macrofabrics
0.2
0.4
0.6
0.8
0.8
0.6
0.4
0.2
I
S3/S1
E
1-(S2/S1)
Consolidation
Shear strain
Girdle
Cluster
Upper tills on drift
Lower tills on drift
Upper tills on bedrock
Lower tills on bedrock
Crag & tail fluting tills
Push moraine tills
Glacitectonites
Lodged clasts
Undefined / overprinted tills
Breiðamerkurjökull upper till
(Benn & Evans, 1996)
Breiðamerkurjökull lower till
(Benn & Evans, 1996)
Lodged clasts (Evans and Hiemstra 2005)

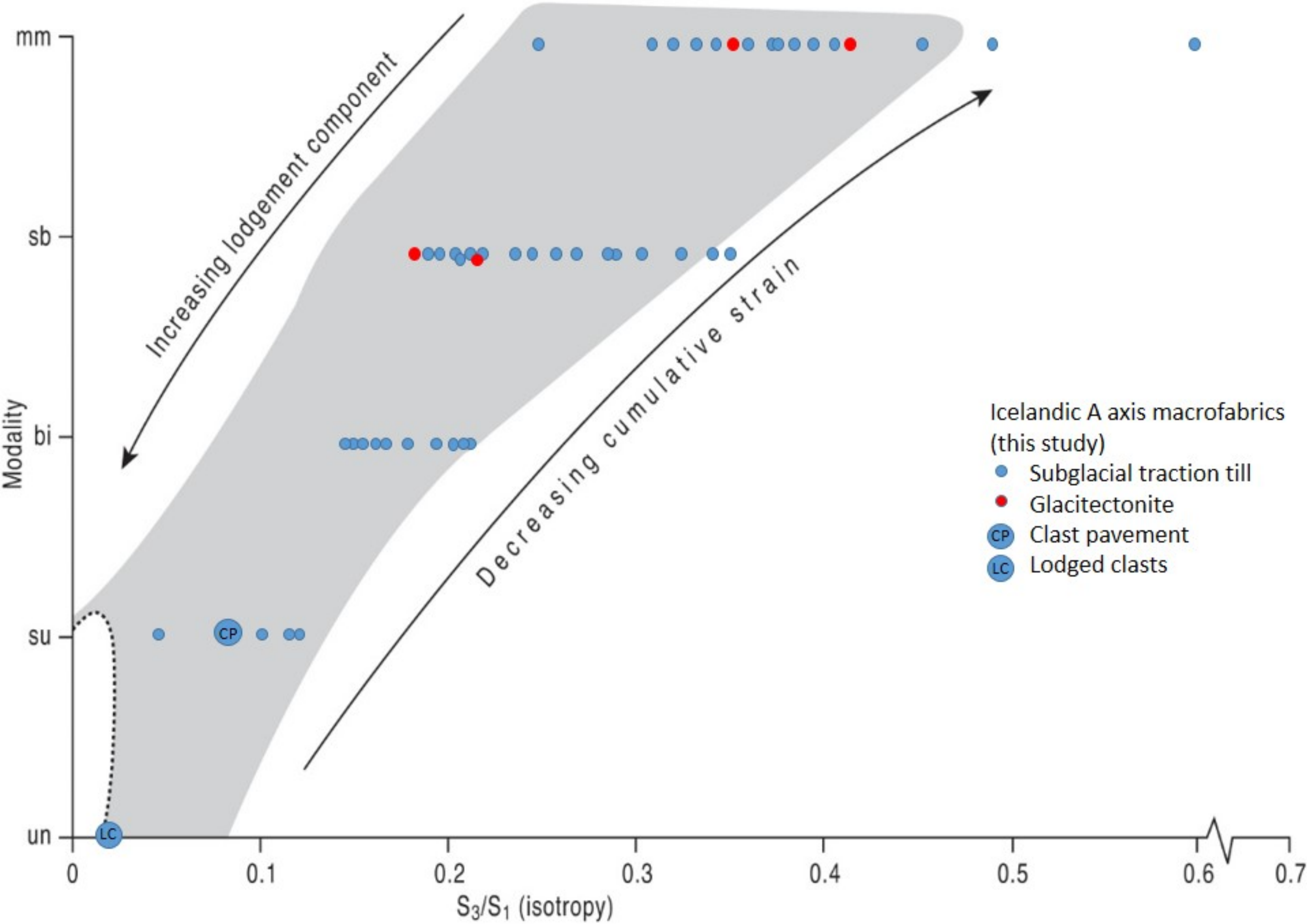

mm
sb
bi
su
un
Modality
0
0.1
0.2
0.3
0.4
0.5
0.6
0.7
S3/S1 (isotropy)
Increasing lodgement component
Decreasing cumulative strain
CP
LC
Icelandic A axis macrofabrics (this study)
Subglacial traction till
Glacitectonite
Clast pavement
Lodged clasts

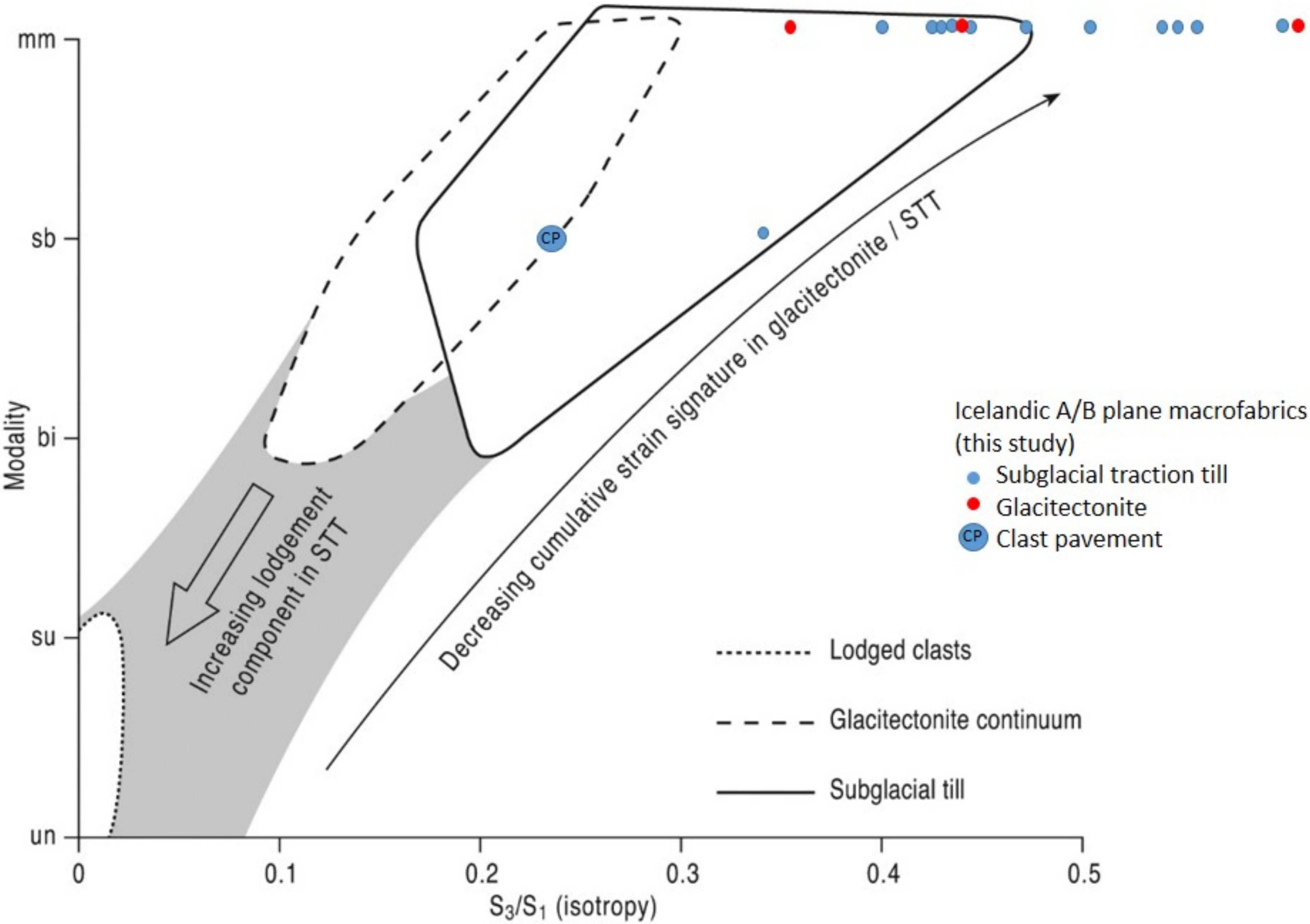
mm
sb
bi
su
un
Modality
0
0.1
0.2
0.3
0.4
0.5
S3/S1 (isotropy)
CP
Increasing lodgement component in STT
Decreasing cumulative strain signature in glacitectonite / STT
Icelandic A/B plane macrofabrics (this study)
Subglacial traction till
Glacitectonite
Clast pavement
Lodged clasts
Glacitectonite continuum
Subglacial till

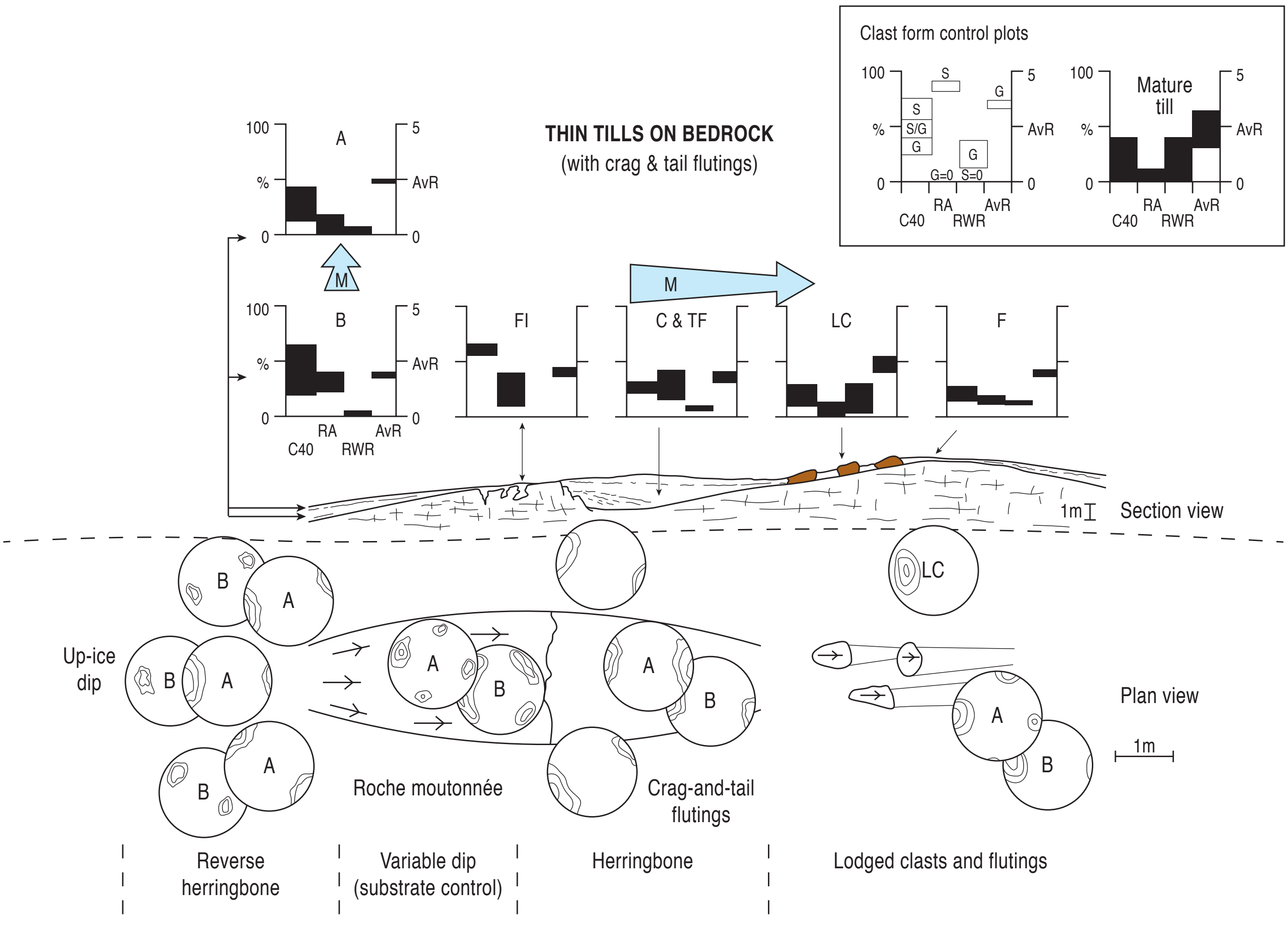

THIN TILLS ON BEDROCK
(with crag & tail flutings)
Clast form control plots
100
%
0
S
S/G
G
G=0
S=0
C40
RA
RWR
AvR
5
0
Mature
till
A
B
FI
C & TF
LC
F
M
1m
Section view
Up-ice
dip
Roche moutonnée
Crag-and-tail
flutings
Plan view
Reverse
herringbone
Variable dip
(substrate control)
Herringbone
Lodged clasts and flutings

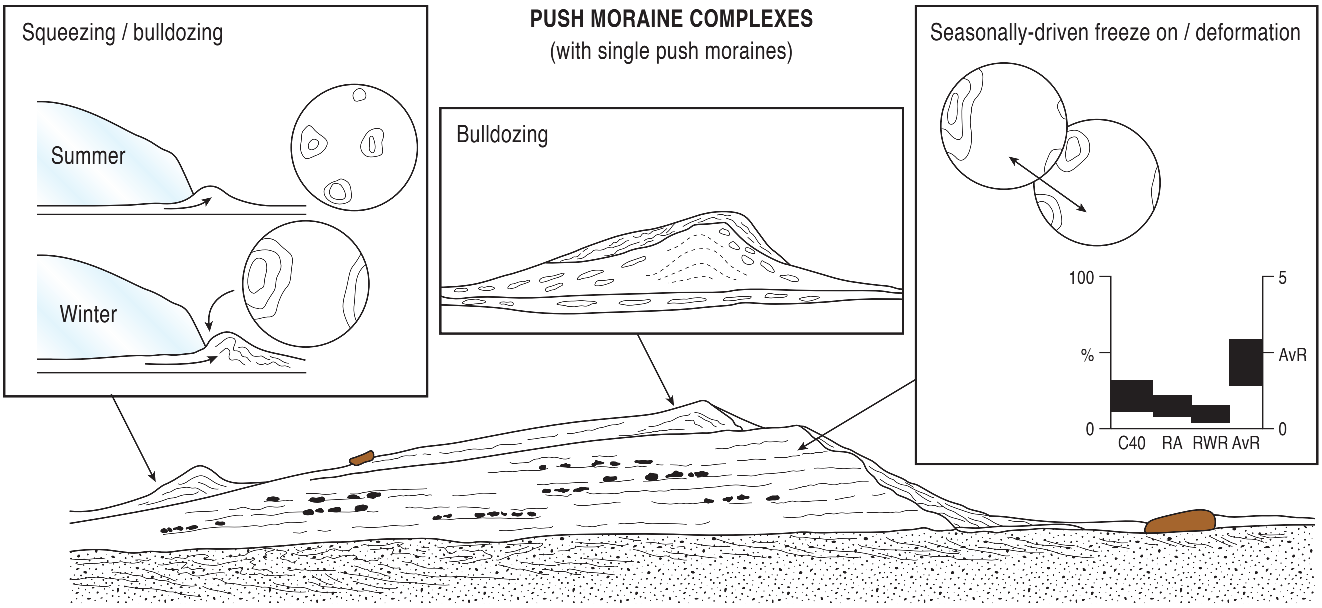
PUSH MORAINE COMPLEXES
(with single push moraines)
Squeezing / bulldozing
Summer
Winter
Bulldozing
Seasonally-driven freeze on / deformation
100
%
0
5
AvR
0
C40
RA
RWR
AvR

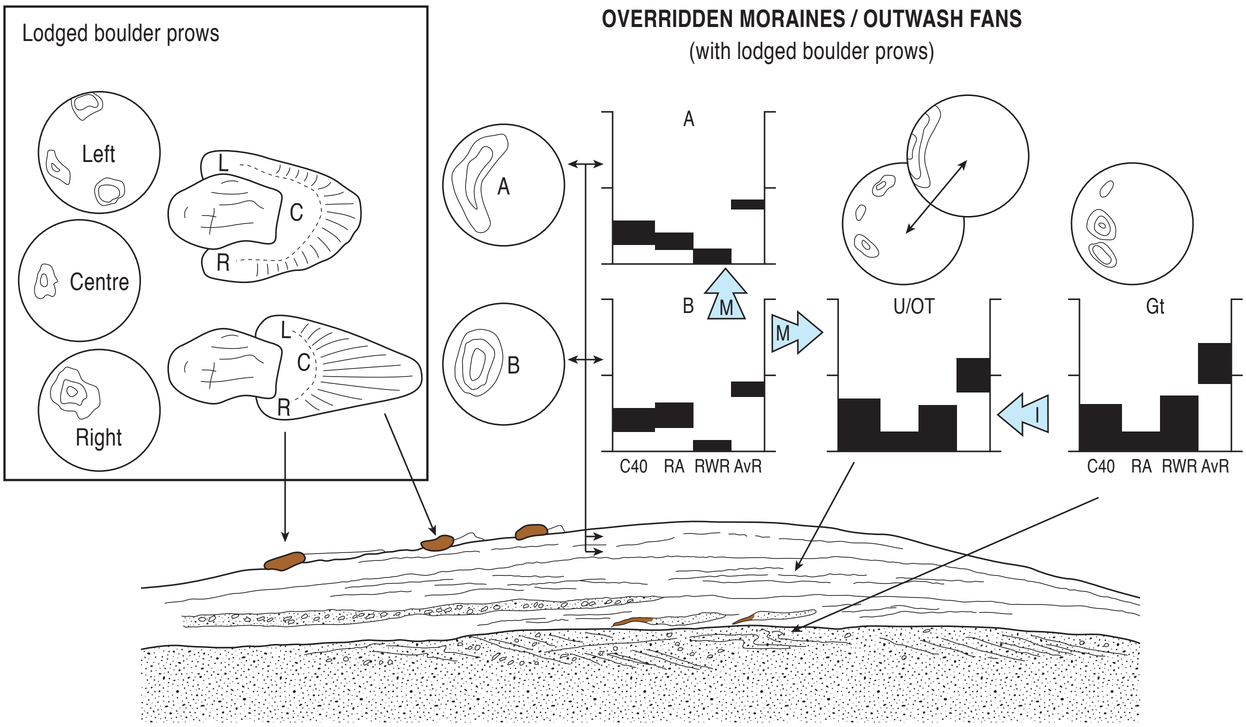

Lodged boulder prows
Left
Centre
Right
L
C
R
L
C
R
OVERRIDDEN MORAINES / OUTWASH FANS
(with lodged boulder prows)
A
A
B
B
M
M
U/OT
Gt
I
C40
RA
RWR
AvR
C40
RA
RWR
AvR